BILINGUAL PUBLISHING CO.
Pioneer of Global Academics Since 1984

Journal of Atmospheric Science Research

Volume 5 • Issue 2 • April 2022 ISSN 2630-5119(Online)

Volume 5 Issue 2 • April 2022 • ISSN 2630-5119 (Online)

Journal of Atmospheric Science Research

BILINGUAL PUBLISHING CO.
Pioneer of Global Academics Since 1984

BILINGUAL PUBLISHING CO.
Pioneer of Global Academics Since 1984

Volume 5 | Issue 2 | April 2022 | Page1-66
Journal of Atmospheric Science Research

Contents

Editorial

Articles

BILINGUAL PUBLISHING CO.
Pioneer of Global Academics Since 1984

Journal of Atmospheric Science Research
https://ojs.bilpublishing.com/index.php/jasr

ARTICLE

Spatio-temporal Changes in the Regime of Rivers in the Pripyat River Catchment and Climate Change

Budnik Svetlana Vasilivna*

The central geophysical observatory of a name of B.Sreznevskogo the State Emergency Service of Ukraine, Kyiv, Ukraine

ARTICLE INFO

Article history
Received: 24 January 2022
Revised: 1 March 2022
Accepted: 7 March 2022
Published: 21 March 2022

Keywords:
Runoff
Silt discharge
Precipitation
Climate
Temperature of water
Agro-forest-melioration

ABSTRACT

In work features of a hydrological regime of catchments of the river of the Pripyat in climate change are considered. Researches of meteorological characteristics of the given territory show the tendency to growth, both temperatures of air, and precipitation, evaporation from a surface of water and ground also show the tendency to increase. That is not unequivocally reflected in change of a course of hydrological characteristics waters objects of territory. On a part of pools of the rivers the mid-annual runoff of water in the rivers in time tends to growth, and Change of levels of subsoil waters decreases for parts - on a turn - here, as a rule, tends a course in time opposite to a mid-annual runoff of water in the rivers. Change of the maximal temperature of water in the rivers in time repeats the tendency of a course of a runoff of water in them, i.e. at increase in a runoff of water in the rivers - the maximal temperature increases, and at reduction - decreases. The increase in temperature of a superficial component of a runoff of the rivers occurs because of the general increase in temperature of air in considered territory. Silt charge waters in all territory decreases, despite of increase in quantity of atmospheric precipitation and increases or reduction of a runoff of water in the rivers. The relationship between the water runoff layer and precipitation and soil moisture has a certain time delay. The average annual water temperature over time shows a tendency to increase at almost all stations, while the change in the maximum water temperature in rivers over time has a multidirectional tendency and to a greater extent depends on the change in water depth in the river, a decrease in high water maximums and frequent thaws, etc. The studies carried out show that the preservation of moisture in thick layers of soil (0 cm-100 cm) contributes to an increase in water flow in rivers and in the modern conditions of Polesie of Ukraine this will solve a number of problems with the provision of high-quality water resources for various industries and the population.

*Corresponding Author:
Budnik Svetlana Vasilivna,
The central geophysical observatory of a name of B.Sreznevskogo the State Emergency Service of Ukraine, Kyiv, Ukraine;
Email: svetlana_budnik@ukr.net

DOI: https://doi.org/10.30564/jasr.v5i2.4396

1. Introduction

The hydrological mode of the rivers is characterized by set of parameters, including a runoff of water, precipitation, a temperature mode, etc. Changes of a climate of last decades are reflected in all components of a hydrological mode that causes in their constant research and forecasting of directions of their possible changes for stable work of branches of a national economy, sewn up from flooding, droughts, etc. [1,2]. In work the river basin Pripyat (a wood and forest-steppe natural zone) is investigated located in northwest of Ukraine. Territory of pool of Pripyat also it is constantly investigated for changes of components of a hydrological mode [3-9]. On catchments of Pripyat settles down two states, scientific both pay to its research significant attention. So, the analysis of dynamics of a runoff of water of the rivers Belarusskoj of a part of catchments of Pripyat has shown [3], that since the middle of 60th years of the last century, mid-annual, minimal years and winter charges have the steady tendency to increase, during too time, the runoff of a spring high water decreases.

As a result of climatic changes there was a displacement of dates of approach of the maximal charges of water of a spring high water for earlier terms (71.5% of cases peak of high waters fall to the third decade of March) in a direction from a southwest on northeast of Belarus [4]. Reduction of the maximal charges of water of a spring high water of the large rivers Belarusii, caused is established by winter thawing weather therefore the part of a spring runoff passes in the minimal winter runoff [4]. Also it is revealed, that in connection with non-uniform spatial distribution of trends of precipitation on territory of Belarus and in adjoining regions it is observed different directed change of conditions of formation of a river runoff, especially during the open channel [5].

Owing to prevalence of a flat relief, a high arrangement of subsoil waters and significant marshiness of a reservoir, the mode of the river Pripyat is characterized by smooth change of charges of water in time, more inert fluctuations water content and the stretched high waters. The rivers water content in considered pool in each of phases of a hydrological cycle it is caused water content a previous season. The prolonged influence of meteorological factors on formation of a runoff is marked. Calculations of trends of the monthly sums of precipitation for the period 1948-2018 have shown increase in the monthly sums of precipitations, reduction of duration of loss of precipitations and growth of the maximal sums of precipitations that can testify to increase in duration of the periods without precipitations and more frequent formation of droughty conditions. The increase in precipitations was expressed in small increase in a share of an aestivo-autumnal runoff and positive trends of the least charges of water of the period of the open channel [5].

Modern warming of a climate has affected not only the maximal charges of a spring high water, but also on a level [6]. Practically on all rivers downturn of average values of maximum levels of water of a spring high water for the period c1988 for 2014 in comparison with the period with 1946 for 1987 as a whole is observed, for the period (1946-2014) for the rivers of catchments of Pripyat the tendency to decrease in a water level is observed. Local decrease in water levels during with 80th for 90th years of the last century, caused by meliorative influences, and the period of some growth caused by modern climatic changes, and its stabilization in current century takes place [7].

The anthropogenic impact on the study area, one way or another, affects the hydrological regime of the rivers. Reclamation work in Polesie could not but affect the water regime of the river. Pripyat and its floodplains [8,9]. After the draining of bogs and wetlands on the catchments of rivers, swampy up to 30%, according to studies [9], there is a decrease in spring runoff by 0%-20%, an increase in low-water runoff by 10%-50% and annual runoff by 0%-15%. The decrease in the maximum levels of spring floods cannot be attributed only to the influence of land reclamation, but it has a significant effect [8].

Agriculture also influences the components of the hydrological regime of the rivers in the study area [12], since the plowing of the basins here is 10%-80% (on average 40%-50%).

Based on assessments of possible climate change, it was found that with the most unfavorable development of climate changes, the flow of individual rivers of the Pripyat basin can decrease to 45%, which is equivalent to a change in supply (from 50% to 85%), and the variation coefficient from 0.47 to 0.54. When the anthropogenic component influences the runoff, the decrease in the average annual runoff can reach 50%-70% [5].

2. Materials and Methods

To study the features of the hydrological regime of the rivers of the Pripyat River basin on the territory of Ukraine over a long-term period, we used standard observation materials at stationary observation posts of the Hydrometeorological Service of Ukraine for the entire observation period. These are materials of the state water cadastre (basic hydrological characteristics, hydrological yearbooks) and climatic cadastre (climate reference books, meteorological monthly books, etc.).

The list of observation points for water runoff, which, in one way or another, were used in the studies is

presented in the Table 1. In Figure 1 the arrangement of a river basin Pripyat in Ukraine and an arrangement of items of supervision over a runoff of water on it are presented. Some of the observation points are currently closed, which shortens the observation series and allows the use of this information in the ranges of observation periods as addi-

Table 1. Characteristics of observation posts for water flow in the Pripyat river basin

River - observation point for discharge	Distance from the source, km	Catchment area, km^2	Note
Pripyat - Rechitsa	84	2210	
Pripyat - Lyubyaz	157	6100	
Vyzhevka - Ruda	10	141	
Vyzhevka- Staraya Vyzhevka	44	722	
Tur'ya - Yagodnoye	57	459	
Turya - Kovel	102	1480	
Turya - Buzaki	164	2630	Closed 1988
Stokhod - Malinovka	48	692	
Stokhod - Gulevka	99	1420	Closed 1988
Stokhod - Lyubeshov	173	2970	
Styr - Shchurovtsy	57	2020	
Styr - Lutsk	194	7200	
Styr - Kolki	335	9050	observation point for water level
Styr - Polonnoe	345	10400	Closed 1940
Styr - Mlynok	400	10900	
Radostavka-Troitza	19	316	
Ikva - Velikiye Mlynovtsy	59	632	
Goryn - Yampol	71	1400	
Goryn - Ozhenin	223	5860	
Goryn - Derazhno	379	9160	
Goryn - Stepan	456	10300	
Goryn - Dubrovitsa	488	12000	Closed 1990
Vyrka - Svaryny	21	231	
Sluch - Bolshaya Klitna	30	232	Closed 1983
Sluch -Gromada	139	2480	
Sluch - Novograd-Volynsky	252	7460	Open 1974 г.
Sluch - Sarny	409	13300	
Homora - Poninka	105	1410	Closed 1988
Tnya - Bronniki	68	982	
Smolka - Susly	65	632	
L'va - Osnitsk	24	276	
Ubort' - Rudnya - Ivanovskaya	45	510	
Ubort' - Perga	136	2880	
Uzh - Korosten'	84	1450	
Uzh - Polesskoye	169	5690	Closed 1995
Zherev-Vyazovka	78	1360	Closed 1988
Noreen - Lukishki	40	531	Closed 1943
Noreen - Slavenshina	79	804	
Grezlya - Ur.Brod	28	616	Open 1967 - Closed 1982
Ilya - Lubyanka	32	300	Closed 1986

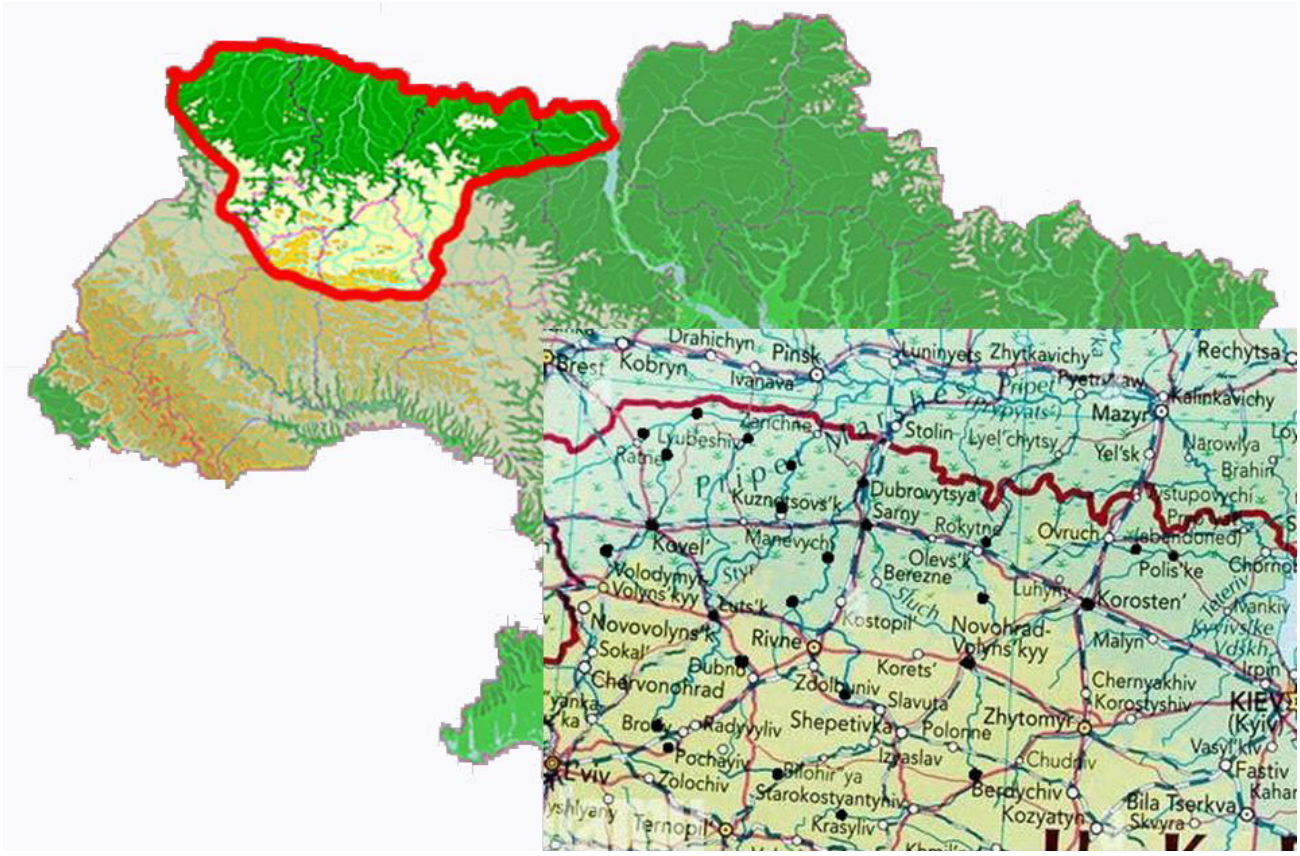

Figure 1. Position of a river basin Pripyat and an arrangement of items of supervision over a runoff of water on it.

tional. Among the research methods, the methods of water balance and graphical analysis were mainly used. Sizes of a runoff, precipitations, evaporations were compared, a soil moisture in identical units (in mm), that allows to compare with them among themselves. The graphs of the course of the characteristics of the hydrological regime and the characteristics of the climate in time were plotted for observation posts and stations, and the directions of the trends and the tangents of their inclination angles were revealed. Based on the analysis of the direction and slope of the trend lines, schematic maps of the spatial-temporal direction of changes in the indicators of the hydrological regime of the territory were built.

3. Results

The study of changes over time in climate characteristics such as precipitation and temperature showed that they tend to increase in the study area (Figures 2-3). However, over the basin area, this trend is uneven [11]. Thus, the maximum increase in atmospheric precipitation falls on the northern part of the study area, and the minimum on the middle course of the Pripyat tributaries. In the southern part of the territory (the headwaters of the Pripyat tributaries, the spurs of the Podolsk Upland), there is also a small maximum increase in precipitation.

Analysis of the course of water runoff over time for most rivers in the Pripyat River basin shows that surface runoff tends to increase (Figures 4a, 5b). However, in part of the catchments of the study area, the opposite tendency is observed: the surface runoff decreases (Figures 4b, 5a), while the groundwater runoff increases. Some researchers also argue that an increase in the water content of rivers is observed in the upper reaches of the Dnieper [11,12], while others [13] argue that the water content decreases in the middle and lower reaches of the Dnieper.

It is important that if we consider the observation series for the Tur'ya River not for the entire observation period, but in the range of 1962 -2018, then the direction of the trend changes, at the Tur'ya-Yagodnoye post the runoff decreases, and at the Tur'ya-Kovel it increases.

This is shown by the manifestation of the cyclicity of hydrological processes in the directions of trends with longer observation periods. The longer the observation series, the more information about the cyclicity of hydrological processes they carry and the more important the information at these posts. I would like to emphasize that the more observation posts cover secular observation periods, the more informative the observation materials

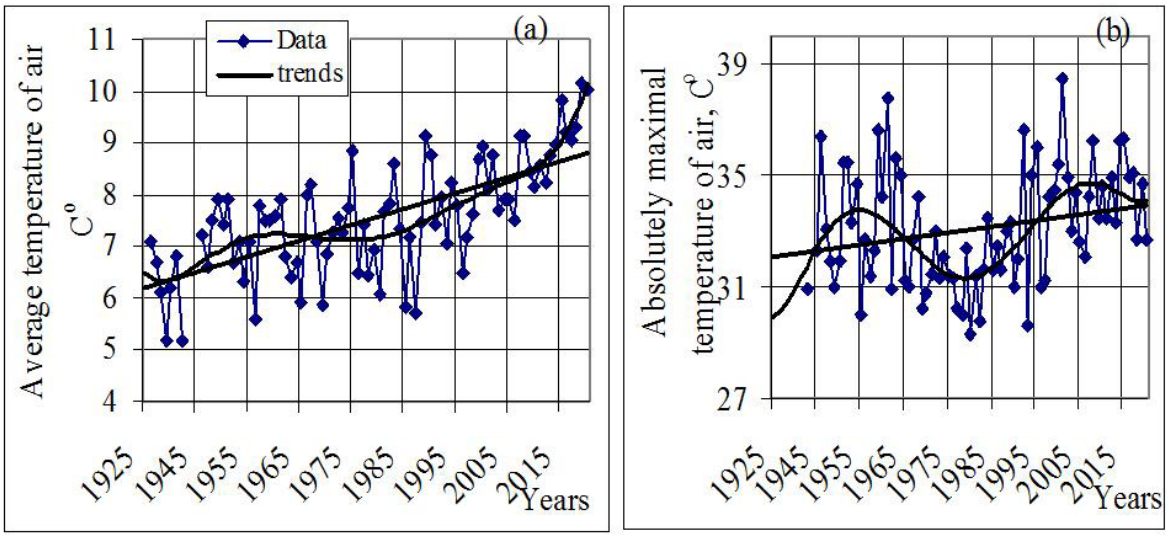

Figure 2. Change in time of Average (a) and maximal (absolutely) (b) temperature of a on meteorological station Sarny

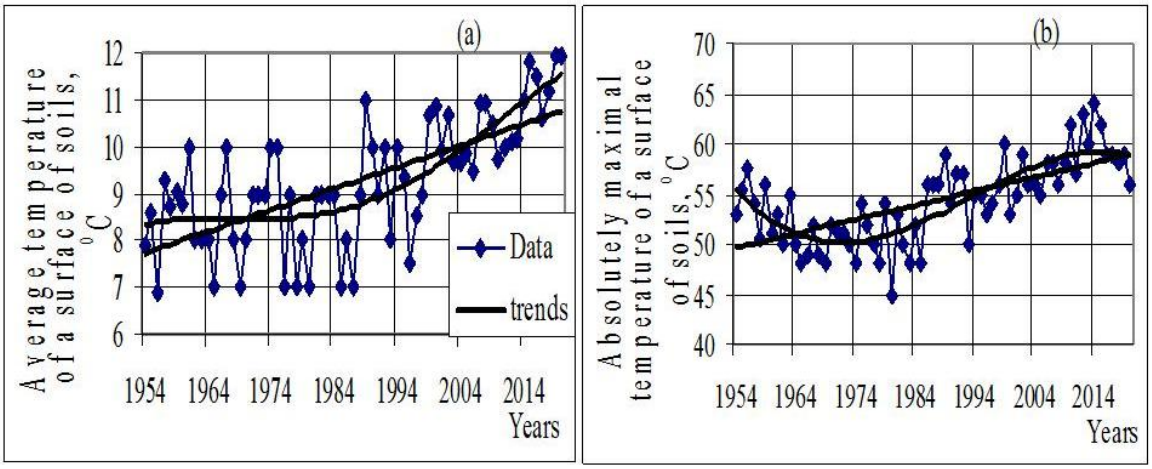

Figure 3. Change in time of average (a) and maximal (absolutely) (b) temperature of a surface of soils on meteorological station Sarny

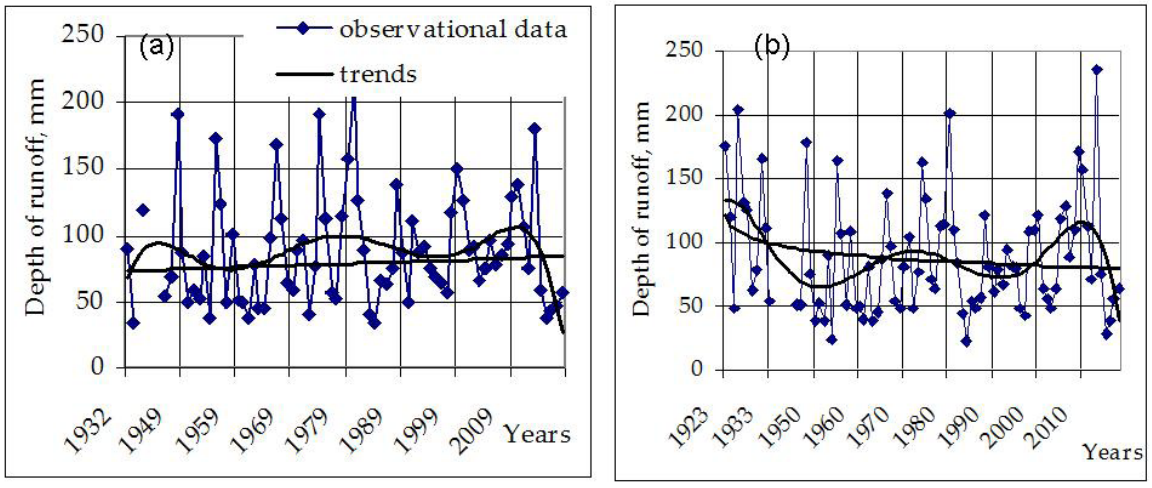

Figure 4. Changes in the depth of runoff in the time of the Tur'ya river observation point (a) - post Yagodnoe, (b) -post Kovel

and, accordingly, the conclusions about the hydrological regime of the territory, the more substantiated the conclusions.

The study of the relationship between the direction of the trend in the course of water runoff in time with the hydrographic characteristics of the catchments showed that the trend of a decrease in runoff is traced in the entire range of changes in the areas and heights of catchments, their plowing, forest cover, swampiness, etc. no quantitative regularity was found (the territory is flat and swampy in places). A change in water content and air temperature also affects a change in the temperature regime of rivers (Figures 6-8), Namely, a change in water depth and ratios in the components of river feeding (an increase or decrease in the ground component of river feeding) is reflected in a change in water temperature along the length of the river. Thus, in the upper reaches of the Pripyat at the Pripyat-Rechitsa post, an increase in the average and maximum water temperature is observed, and 73 km lower at the Pripyat-Lyubyaz post, the maximum water temperature in the river shows a tendency to decrease (Figures 6-8).

The analysis of observational materials showed that the average water temperature for the year in the river changes to a greater extent with time than along the length of the river. Moreover, over time, it mainly increases. The lowest temperature is observed closer to the source of the river and to its mouth. The temperature of the sources is influenced by the outflow of groundwater (from which, in fact, the rivers originate), and the lower temperature of

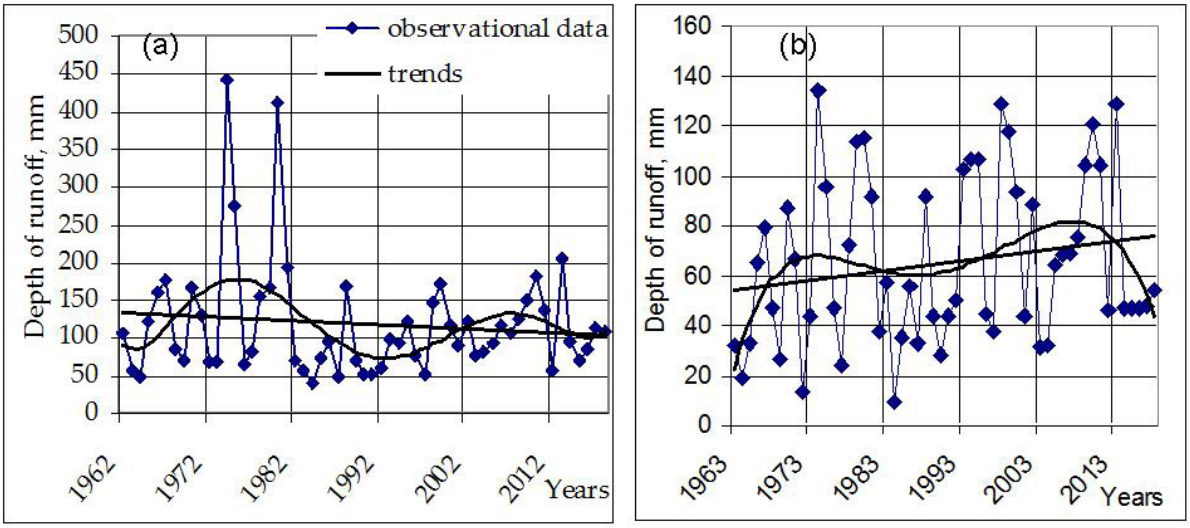

Figure 5. Changes in the depth of runoff in the time of the Pripyat river observation point (a) - post Rechitsa, (b) - post Lyubyaz

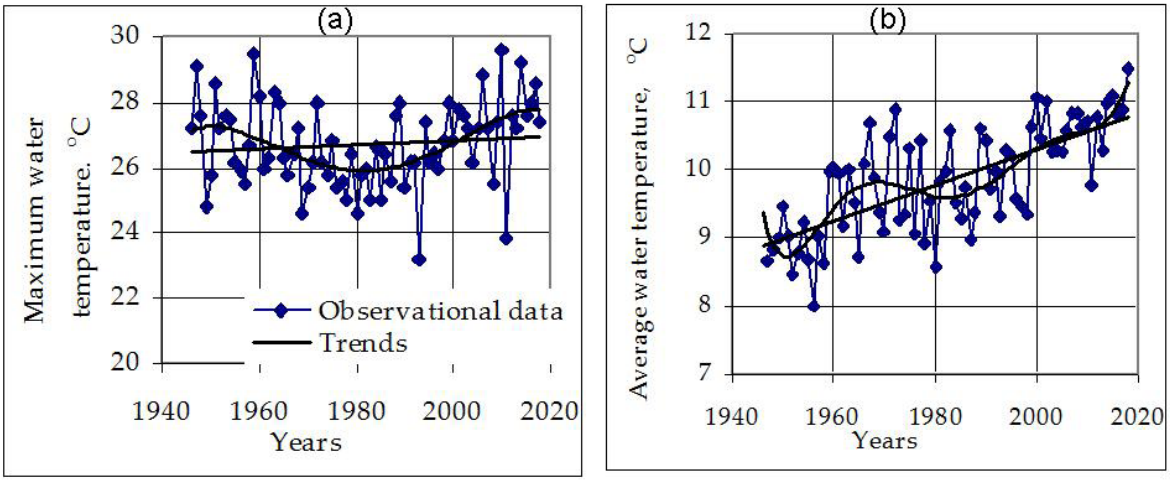

Figure 6. Change in time of the maximum (a) and average (b) water temperatures in the river Pripyat - post Rechitsa

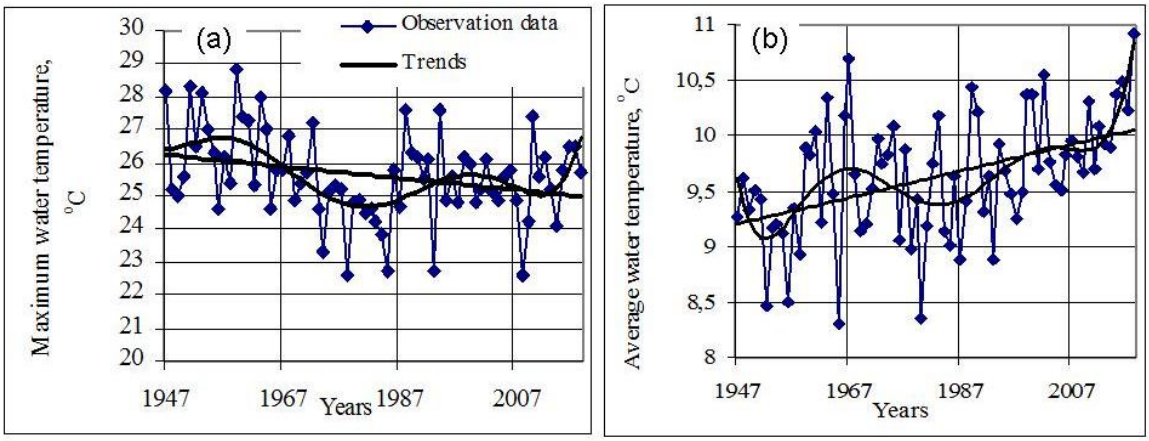

Figure 7. Change in time of the maximum (a) and average (b) water temperatures in the river Pripyat - post Lyubyaz

the estuaries is most likely explained by an increase in the water depth in the river and, accordingly, a decrease in the heating of the water column.

The temperature of groundwater water, which can be taken as average with a minimum runoff and a predominance of groundwater supply, within Pripyat is 8 °C-9 °C [16-18]. The change in the maximum water temperature in the Goryn River in time and along the length of the river has minima almost along the entire length of the river in the 70s-80s of the last century, it seems, this is due to the presence of some long-term cycles (Figure 8). However, in recent years it has also shown an upward trend over time. The change in the overgrowth of the river channel [19] is also consistent with the change in water temperature and the change in the water depth in the river.

While the surface runoff in the study area has different directions of its course in time, the course of water silt charge in time along all the rivers of the region shows a tendency to decrease, starting from the 60s-70s of the XX century (Figure 9). The reasons for the decrease in silt charge are high regulation of the flow of water bodies, agroforestry in the catchments area, and a decrease in high water maximums [10]. A good dependence of the maximum silt charge of water on the reserves of productive moisture in the soil was revealed. With an increase in soil moisture, the maximum silt charge increases, since the total moisture supply to the catchments increases.

The study of the relationship between the annual layer of river runoff with the annual precipitation and the average annual air temperature showed a weak dependence, probably due to the presence of a shift in the

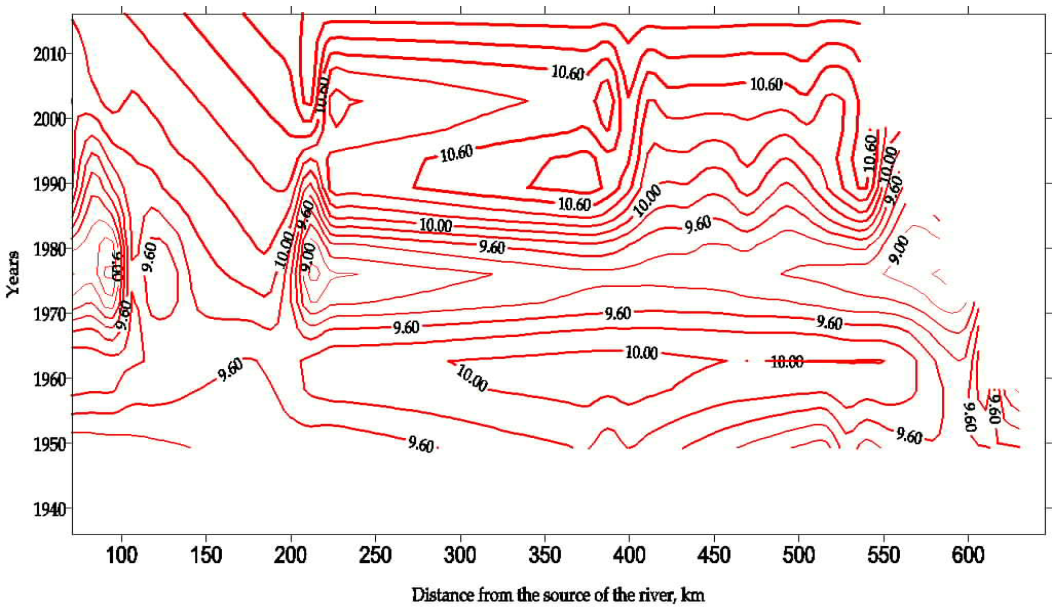

Figure 8. Change in the average water temperature in the Goryn River along the length of the river and in time

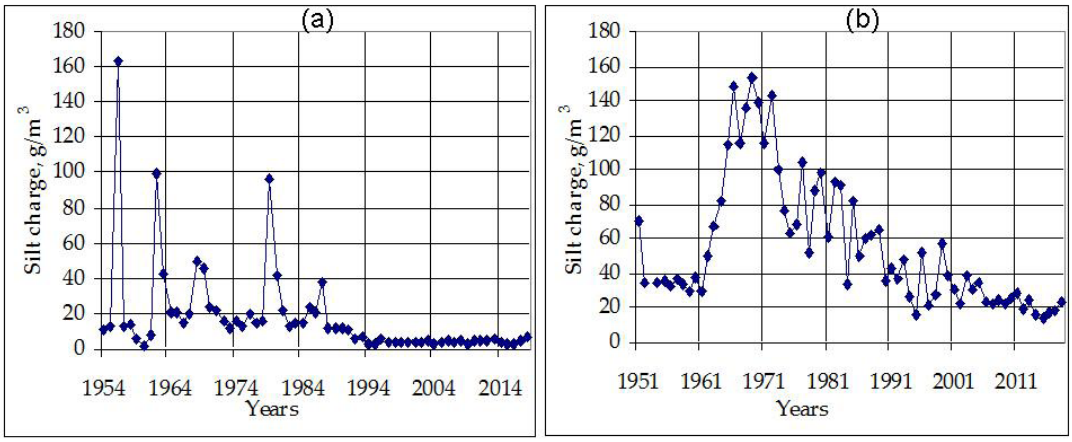

Figure 9. Change silt charge waters in time in the river Sluch posts the Gromada (a) and Sarny (b)

response time of the basin to precipitation (flat, in places swampy territory). Moistening of the catchments surface has a more significant effect on the course of the average annual water runoff layer, which is determined by the presence of a significant amount of wetlands and marshes. With an increase in moisture reserves in the soil, the minimum water runoff per year increases (Figure 10).

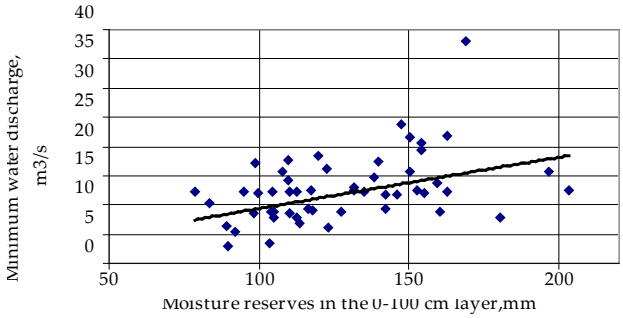

Figure 10. Dependence of the minimal discharges of water for a year in river Sluch - post Sarny from stocks of a moisture in 0-100 sm a layer of soils.

4. Conclusions

It has been established that the surface runoff of the rivers in the humid zone tends to increase predominantly, while the groundwater runoff tends to decrease. However, in part of the catchments of the study area, the opposite tendency is observed that the surface runoff decreases, while the groundwater runoff increases. The directions of the trend of the course of water runoff in time are not consistent with the hydrographic characteristics and the geological and geomorphological structure of the territory. The main climatic indicators (precipitation and air temperature) under conditions of the humid zone do not have a direct effect on the course of the average annual water flow layer; flow rationing for these indicators practically does not change the flow trend. Among the components of the water balance, humidification of the catchments surface plays a significant role in the flow of water in the rivers of the humid zone. The relationship between the water runoff layer and precipitation and soil moisture has a certain time delay. The average annual water temperature over time shows a tendency to increase at almost all stations, while the change in the maximum water temperature in rivers over time has a multidirectional tendency and to a greater extent depends on the change in water depth in the river, a decrease in high water maximums and frequent thaws, etc. The silt charge of water in all rivers of the study area decreases with time.

The studies carried out show that the preservation of moisture in thick layers of soil (0-100 cm) contributes to an increase in water flow in rivers and in the modern conditions of Polesie of Ukraine this will solve a number of problems with the provision of high-quality water resources for various industries and the population.

Preservation of moisture in thick layers of soil and soil can be achieved 1) restoration of bog massifs, 2) construction of small dams in the upper reaches of gullies and hollows with a seasonal delay in the runoff of rain and melt water (for example, the Unitsky reserve - the experiments of V. Dokuchaev) with 3) mandatory forest reclamation work to create a favorable microclimate (reduce wind speed, temperature, evaporation, etc.). It should also be borne in mind that an increase in evaporation ultimately contributes to an increase in air humidity, cloudiness and precipitation.

A decrease in the surface component of the river runoff of small rivers due to dams should not ultimately negatively affect the runoff of larger rivers. Part of the runoff will go into subsurface and groundwater, which will reduce the water temperature in the rivers and thus remove a number of environmental problems caused by

the rise in water temperature in them. The use of fully anti-erosion methods for protecting the territory of river catchments (hydrotechnical, agro and forest reclamation) will reduce the negative manifestations of climate change, including reducing the dehydration of the territory, overheating of the earth's surface.

Declaration of Conflict of Interest

The author declares that they have no individual relationships that could have performed to affected the work reported in this study and have no known conflict of financial interests.

References

[1] Musau, J., Sang, J., Gathenya, J., et al., 2015. Hydrological responses to climate change in Mt. Elgon watersheds. Journal of Hydrology: Regional Studies. 3, 233-246.

[2] Tadic, L., Dadic, T., 2016. Leko-Kos Marija Variability of Hydrological Parameters and Water Balance Components in Small Catchment in Croatia. Advances in Meteorology. Article ID 1393241, pp. 1-9. DOI: http://dx.doi.org/10.1155/2016/1393241.

[3] Volchek, A.A., 2015. Water resources of the Belarusian Polesie and their use. PolesGU. pp. 65-69. (In Russian)

[4] Volchek, An.A., 2017. Flooding on the territory of Belarus. Bulletin of the Brest State Technical University. 2, 39-53. (In Russian)

[5] Danilovich, I.S., Kvach, E.G., Zhuravovich, L.N., et al., 2021. Modern changes in the humidification regime in the warm period of the year and the conditions for the formation of the runoff of the summer-autumn dry season on the rivers of Belarus. Natural resources. 1, 22-33. (In Russian)

[6] Rusetsky, A.P., Lukyanova, E.A., Trukhan, L.A., 2010. State and hydrological regime of the Pripyat river floodplain after reclamation in Polesie. PolesGU. pp. 42-49. (In Russian)

[7] Volchek, A.A., Shpoka, I.N., Shpoka, D.A., 2020. Assessment of fluctuations in the maximum water levels of the rivers of the Pripyat basin on the territory of Belarus. Bulletin of the Brest State Technical University. 2, 27-30. (In Russian)

[8] Pokumeiko, Yu.M., 1980. Changes in the water regime of the rivers of Belarus under the influence of drainage reclamation. Collection of works of Minsk and Vilnius hydrometeorological observatories. issue 1. Research on the hydrometeorological regime of the Byelorussian SSR and the Lithuanian SSR. pp. 107-114. (In Russian)

[9] Shebeko, V.F., Zakrzhevsky, P.I., 1975. Influence of drainage on river runoff and evaporation. Hydrotechnics and melioration. No.8, 49-55. (In Russian)

[10] Budnik, S.V., 2018. Anthropogenic influence on the silt charge of the Western Bug and Pripyat rivers. Scientific bulletin of Belgorod State University. Series: Natural Sciences. 42(4), 532-539. DOI: https://doi.org/10.18413 / 2075-4671-2018-42-4-532-539. (In Russian)

[11] Kalinin, M.Yu., Obodovsky, A.G., 2003. Monitoring, use and management of water resources in the Pripyat river basin. Under the general ed. Minsk: Balsens. pp. 293. (In Russian)

[12] Budnik, S.V., 2019. Spatio-Temporal Change of Atmospheric Precipitation on Territory of North-West of Ukraine. Journal of Atmospheric Science Research. 2(4), 1-4 DOI: https://doi.org/10.30564/jasr.v2i4.1564.

[13] Jamalov, R.G., Frolova, N.L., Krichevets, G.N., et al., 2012. Formation of modern surface and groundwater resources in the European part of Russia. Water resources. 39(6), 571-589. (In Russian)

[14] Kukharuk, N.S., Smirnova, L.G., Narozhnyaya, A.G., et al., 2017. Dynamics of soil moisture in protected areas of the forest-steppe against the background of intrasecular climatic variability. Scientific statements of the Belgorod state. un-that, Ser. Natural Sciences. 25(41), 79-90. (In Russian)

[15] Shtogrin, I., 23 April 2020. "Znevodnennya": in Ukraine, the lowest level of water is being promoted at the riverside for the rest of 100 years. Radio freedom. https://www.radiosvoboda.org/a/voda-vidstnist-opadiv-posuha-harchi/30572821. html? fbclid = IwAR0ar4ldSOQfVc6kRVfOxg0DD96R1FyiazNzTsKpmU2RrVo6zbXgLg54C0Y

[16] Kuzmin, S.I., 2009. National environmental monitoring system of the Republic of Belarus: observation results for 2008. Minsk: "Bel SRC Ecology". pp. 335. (In Ukrainian)

[17] Voskresenskiy K.P. 1951 Runoff of the rivers and time water-currents in territory of forest-steppe and steppe zones of the European part of the USSR. Works SHI. 29 (83), 1146 p. (In Russian)

[18] Sokolova E.M. 1951 Thermal mode of the rivers USSR. Works SHI. 30 (84), 116 p. (In Russian)

[19] Budnik, S.V., 2020. Long-term changes in the hydraulic characteristics of the rivers of the Pripyat basin and modern problems of small rivers. Regional Geosystems. 44(1), 104-112. (In Russian)

BILINGUAL PUBLISHING CO.
Pioneer of Global Academics Since 1984

Journal of Atmospheric Science Research
https://ojs.bilpublishing.com/index.php/jasr

EDITORIAL

Gathering Data, Providing Theoretical Foundations and Proposing Practical Pollution Reducing Measures to Strengthen the Global Fight against a Warming Atmosphere

Service Opare*

Faculty Member (Physical Geography), University Canada West, Vancouver, Canada

ARTICLE INFO

Article history
Received: 10 April 2022
Revised: 15 April 2022
Accepted: 18 April 2022
Published: 21 April 2022

An extensive and accurate knowledge of atmospheric disturbances such as turbulence, wind veering and other unexpected weather changes that are becoming frequent, violent and unpredictable, and which generate tropical cyclones and other intense weather situations is essential. Such unstable atmospheric happenings are occurring with increasing frequency [1]. They include periodic collusion of unstable air parcels, uncertain wind trajectories some of which tend to veer and assume violent tendencies, precipitation events that are becoming more erratic and rising temperatures. These atmospheric disturbances not only lead to catastrophic events, but they hamper our ability to predict with accuracy and certainty upcoming weather and climate events as well as their, magnitudes and intensities. Low predictive abilities tend to render inaccurate various simulation models that should guide aircraft dynamics, farming practices and other human endeavors upon which our survival as a society depends.

Rising atmospheric concentrations of greenhouse gas (GHGs) that trap returned solar radiation and prevent it from reaching the upper layers of the atmosphere have led to warming of the atmosphere. Carbon dioxide (CO_2), water vapour, methane, nitrous oxide and chlorofluorocarbons (CFC) are being generated through human activity and emitted into the atmosphere in higher quantities [2]. In addition, higher concentrations of airborne particles (aerosols) that eat up and thereby reduce ozone layer content in the stratosphere are being produced. Increased deforest-

*Corresponding Author:
Service Opare,
Faculty Member (Physical Geography), University Canada West, Vancouver, Canada;
Email: service.opare@ucanwest.ca

DOI: https://doi.org/10.30564/jasr.v5i2.4618

ation leads to the release of stored carbon content into the atmosphere. Frequent draining of peatland, and poor waste disposal and management systems being practised worsen these enfolding trends [2].

These harmful situations contributed to violent atmospheric weather and warming of the climate that have been highlighted in various articles presented in this journal. The reading public should therefore be awakened to the disturbing trends which if unchecked could have dire consequences for the society. Diverse harmful impacts on humanity, animals and plants in the ecosystem have been predicted. And the effects are obvious. Temperatures are rising, glacial ice is melting, and sea levels are rising as the oceans become warmer leading to floods and infrastructure damages. Precipitation is becoming unpredictable and violent with destructive power as evidenced by buildings collapsing, farms being inundated with floods, infrastructural facilities being damaged and settlements being abandoned [1,2]. Concerted and collective action is both critical and urgent. The global community is well positioned to act in a coordinated manner based on tools developed from scientific and tested measurements to avert catastrophic consequences.

An effective thrust toward drafting effective policies, designing long-lasting programs and undertaking actions that could eventually, effectively and in a sustainable manner tackle these is critical for successful resolution of these daunting atmospheric disturbances. Warming climatic situations continue to wreck destruction, damage and decimation of prized lives and precious properties. Humanity's ability to respond timely to these challenges hinges on scientific studies and publication of hard facts garnered from experiments and field measurements.

This issue of the Journal of Atmospheric Science Research contributes to the challenge by presenting a range of quality articles that broadly set out key findings of research and analytical works on a set of topics in the field of atmospheric sciences. The articles are presented logically and systematically with adequate attention to atmospheric sciences. They highlight both conceptual issues and practical insights that demonstrate the quality and breadth of scientific vigor and analytical breadth that the authors demonstrated in their publications.

Authors' presented papers provide broad insights into current global concerns but also outline critical priority areas for further research and potential development schemes that could spur industry-level ventures. In addition to the potential of an accelerated highlighting of effective solutions into environmental preservation challenges that confront the global community, these can also provide remedies for value chain downstream and upstream ventures that can be promoted at scale by innovative entrepreneurs.

Improved research in environmental conservation, climate change mitigation and adaptation strategies, waste reduction and management measures in addition to acid rain prevention approaches could also impact positively on health through improve air quality [3]. The positive health impacts would occur through minimized asthmatic conditions as well as better control of lung-impairments and heat-related illness such as exhaustion and heat stroke. Possible exposure to ultraviolet rays that lead to skin damage, skin cancer and cataracts will be minimized. Better air quality will result in lessened respiratory, eye and nasal diseases, chronic obstructive pulmonary disease (COPD), chronic bronchitis and emphysema or lung cancer. Thus in addition to environmental conservation and habitat preservation, stabilized atmospheric conditions could improve human health [3].

Research papers presented in this current journal provide renewed focus on efforts at generating evidence, factual knowledge grounded in scientific processes and refined data that enable or yield practical, innovative measures which address both short-term and long-term challenges confronting the global community. Most importantly, a broad understanding of diverse physical environment systems that influence the way we live and operate, the interlocking interactions between different populations as well as between them and the environment will be on offer. Additionally, the availability of ready and effective the scientific tools and skillset gleaned from journal articles and research papers would equip the society with the capacity to examine the suitability as well as outcomes of our mitigation and adaptations efforts. Failure to adopt and adapt will obviously imperil our existence as a global technologically capable society.

Impacts of human actions that lead to atmospheric concentrations of poisonous gases do not only threaten human health when inhaled but adversely affect society indirectly through various ways. A better assessment and understanding of the workings of atmospheric will empower the global society with the ability, skills and technology to design remedial measures that could limit global warming on a sustainable level.

In summary, it can be argued that finding long lasting solutions for the warming atmospheric conditions that imperil the global community's very existence is essential. This is particularly critical for developing countries and countries with transition economies that have fragile socio-economic systems and which can slide into deteriorating living conditions [4]. However, it must be stressed that these challenges can also threaten the fabric of developed

countries as well if not tackled effectively. Unpalatable atmospheric disturbances caused largely by atmospheric and climate warming could ultimately collapse the global economy, lead to regional conflicts over access to declining energy sources, generate public unrest due to revolts over dwindling resource supplies as well as power struggles and wars between nations over not only diminishing resource availability but access to, ownership of, and control over their use.

Conflict of Interest

There is no conflict of interest.

References

[1] Mendelsohn, R., Emanuel, K., Chonabayashi, S., et al., 2012. The Impact of Climate Change on Global Tropical Cyclone Damage. Nature Climate Change. DOI: https://doi.org/10.1038/NCLIMATE1357

[2] Warren, F.J., Lemmen, D.S., 2014. Canada in a Changing Climate: Sector Perspectives on Impacts and Adaptation; Government of Canada, Ottawa. www.nrcan.gc.ca/files/earthsciences/pdf/assess/2014/pdf/Full-Report_Eng.pdf (Accessed November 5 2021)

[3] Paavola, J., 2017. Health Impacts of Climate Change and Health and Social Inequalities in the UK. Environment Health. 16, 113. DOI: https://doi.org/10.1186/s12940-017-0328-z

[4] Wijaya, A.S., 2014. Climate Change, Global Warming and Global Inequity in Developed and Developing Countries (Analytical Perspective, Issue, Problem and Solution). IOP Conference Series: Earth and Environmental Science. 19. DOI: https://doi.org/10.1088/1755-1315/19/1/01200

BILINGUAL PUBLISHING CO.
Pioneer of Global Academics Since 1984

Journal of Atmospheric Science Research
https://ojs.bilpublishing.com/index.php/jasr

ARTICLE

Pollution of Airborne Fungi in Naturally Ventilated Repositories of the Provincial Historical Archive of Santiago de Cuba (Cuba)

Sofía Borrego[1*] Alian Molina[1] Yuneisis Bonne[2] Anyilena González[2] Lidiersy Méndez[2]

1. Conservation Preventive laboratory, National Archive of the Republic of Cuba, Havana city, Cuba
2. Conservation Department, Provincial Historic Archive of Santiago de Cuba, Santiago de Cuba city, Cuba

ARTICLE INFO

Article history
Received: 16 March 2022
Revised: 20 April 2022
Accepted: 24 April 2022
Published: 19 May 2022

Keywords:
Archive environments
Fungal pollution
Indoor air
Environmental quality
Ventilated repositories
Toxigenic species

ABSTRACT

Environmental fungi can damage the documentary heritage conserved in archives and affect the personnel's health if their concentrations, thermo-hygrometric parameters and ventilation conditions are not adequate, problems that can be accentuated by Climate Change. The aims of this work were to identify and to characterize the airborne fungal pollution of naturally ventilated repositories in the Provincial Historical Archive of Santiago de Cuba and predict the risk that these fungi pose to the staff's health. Indoor air of three repositories of this archive and the outdoor air were sampled in an occasion every time in 2015, 2016 and 2017 using a SAS sampler. The obtained fungal concentrations varied from 135.6 CFU/m^3 to 421.1 CFU/m^3 and the indoor/outdoor ratios fluctuated from 0.7 to 4.2, evidencing a variable environmental quality over time, but in the third sampling the repositories environments showed good quality. *Aspergillus* and *Cladosporium* were the predominant genera in these environments. *A. flavus* was a prevailed species in indoor air, while *A. niger* and *Cl. cladosporioides* were the species that showed the greatest similarities with the outdoor air. *Coremiella* and *Talaromyces* genera as well as the species *Aspergillus uvarum*, *Alternaria ricini* and *Cladosporium staurophorum* were the first findings for environments of Cuban archives. Xerophilic species (*A. flavus, A. niger, A. ochraceus, A. ustus*) indicators of moisture problems in the repositories were detected; they are also opportunistic pathogens and toxigenic species but their concentrations were higher than the recommended, demonstrating the potential risk to which the archive personnel is exposed in a circumstantial way.

1. Introduction

Among the actions that are usually performed in the archives, libraries and museums of the world to conserve the Documentary Heritage, are the monitoring of temperature (T) and relative humidity (RH), environmental parameters of great importance since are involved in the chemical processes that occur during the aging of substrates, inks

*Corresponding Author:
Sofia Borrego,
Conservation Preventive laboratory, National Archive of the Republic of Cuba, Havana city, Cuba;
Email: sofy.borrego@gmail.com; sofy.borrego@rediffmail.com

DOI: https://doi.org/10.30564/jasr.v5i2.4536

and pigments. The luminous intensity and in particular the UV radiation intensity, the chemical pollution levels in the repositories air, etc. are also measured. However, in relation to environmental microbial contamination in Heritage Institutions, there is no established internationally standard for the collections conservation, only the Italian Ministry of Cultural Heritage proposed limit values of ≤ 150 CFU/m^3 for fungi and between 100 CFU/m^3-120 CFU/m^3 for bacteria or the collections should be subjected to disinfection [1]. For this reason, there are groups of scientists that perform specific studies to assess the environmental microbial diversity and distribution, particularly of fungi, and have established some regulations in their countries.

The Cuba geographical location and the existence of high values of T and RH favor the increase of dust and the fungal propagules (spores, hyphae and fragments of spores and hyphae) concentration in the air, as well as their settlement over different materials, facilitating the fungal development and proliferation. On the other hand, it is known that papers and other documentary supports (microforms, films, audiovisuals, etc.) are infected during the manufacturing process [2] and that these microorganisms, particularly fungi, can trigger the materials biodeterioration when environmental conditions are optimal for their growth and propagation since they use all the components of the documentary supports as nutrients. They have powerful, versatile and adaptable metabolic machinery, which allows them to degrade a great diversity of substrates, both of organic and inorganic origin, favoring the biodeterioration of the different materials stored in archives repositories, libraries and museums [3-5].

Fungi are characterized by having different structures and pathogenicity mechanisms, which cause specific diseases in humans [6]. They behave as allergens triggering numerous allergenic and respiratory diseases [7], some of them can even lyse the blood erythrocytes to obtain the iron necessary for growth during infectious processes [8], they also facilitate tissue damage and affect the immune system mechanisms in human [9]. In addition, they have a high degradation capacity of the organic matter existing in documents of heritage interest and in other substrates such as wood, textile, leather, etc. [10-12]. They can also excrete organic acids, which, when reacting with the paper, acidify and deteriorate it, accelerating the degradation processes caused by the fungi themselves [10,13], as well as excrete pigments that irreversibly and aesthetically affect the documents [5]. These effects are greater in countries with a tropical climate, such as Cuba, due to the influence of high T and RH values that favor the proliferation of fungi, sometimes triggering pests that are difficult to control and eliminate.

Likewise, these effects can be enhanced by Climate Change (CC), since environmental conditions are suitable for increasing the fungal load in the air due to the increase in air transport of fungal propagules from long distances in the planet [14,15]; this will also accelerate the proliferation of fungi and their metabolic recrudescence, which will further facilitate the increase in the environmental fungal load, the efficient degradation of natural materials cellulosic (due to damage to plants and soils that constitute their natural reservoirs), as well as exacerbation of its virulence and pathogenicity causing emerging diseases, all as adaptation and survival mechanisms to adverse environmental conditions [16]. In fact, it has been reported that CC will increase the chronic phenomena of allergies and invasive mycoses because the human immune system will also be affected by climatic stress [17]. Therefore, the possibility of acquiring these diseases will be exacerbated in indoor environments where people spends more than 90% of his time, be it at home, work, school or even doing recreational and social activities [16]. Although studies are being made to monitor a group of factors that will vary with the CC and that will affect the Cultural Heritage of Humanity preserved indoors environments [18], these investigations are still insufficient.

Several authors have established a close relationship among environmental conditions, the presence of airborne fungal propagules and in the settled dustborne, as well as the existence of viable fungi over the stored artworks and documents with the possibility of triggering the biodeterioration of these materials [4,19], respiratory disorders in humans [7,20], and other symptoms belonging to different types of pathologies [6,21]. Hence, multiple research groups recommend the need to increase the frequency of systematic studies in the indoor premises to assess the quality of the environments, in order to guarantee an environmental characterization of the same that allow the early solution of problems associated with the fungal pest development and their effects on the human health.

The indoor environments of archives and libraries are a reservoir of airborne fungal propagules mainly due to the abundance of dust, the heterogeneity of the substrates with a predominance of those of an organic nature and the conditions of document overcrowding in the repositories, which is why they constitute complex ecosystems. The National Archive of the Republic of Cuba (NARC), as the governing entity of the Network of Historical Archives in the country, has been conducting research on the environmental mycobiota in several Cuban Historical Archives, among which is the Provincial Historical Archive of Santiago de Cuba (PHA SC). Hence the aims of this work were to identify and to characterize the airborne fungal pollution of the naturally ventilated repositories of the

PHA SC and predict the risk that these fungi pose to the staff's health.

2. Materials and Methods

2.1 Characteristics of the Archive Building and the Studied Repositories

The PHA SC is located in one of the eastern provinces of Cuba (20°1'19.524" N and 75°49'52.823" W), at 877.6 km (by road) from Havana city, country capital (Figure 1A). The archive is located in a centric area of the Santiago de Cuba city surrounded by avenues with high vehicular and pedestrian traffic.

The building that occupies the archive fulfilled different functions in the past. Firstly, it was the church of Santa Catalina, which in 1515 was built with mud walls and a guano roof. It was in that humble church that Diego Velásquez celebrated the first mass during the founding ceremony of the Villa. On April 15, 1522, by the bull of Pope Adriano VI, the church assumed the rank of cathedral, when the headquarters of the diocese of Baracoa was transferred to Santiago de Cuba. Later, at the beginning of the 19th century, the Provincial Prison of Oriente was built there. The building is characterized by having a symmetrical neoclassical architecture made up of two floors, built with materials of the time based on earth, limestone, clay and masonry. Given the function for which the property was built, the walls are excessively thick with small and very high windows. On the other hand, the roof is funnel-shaped, with creole tiles and has a system of channels and downspouts for collecting rainwater that accumulates in the cistern located in the central courtyard (Figure 1B). It has wide interior corridors and seven galleries that have been transformed into repositories for documents.

In 1997 - 1998, the Historian Office of the Santiago de Cuba city undertook the restoration work of the property and, among other repairs that were performed, covered the walls with cement. As this material is not compatible with the wall stone and as a result of the humidity existing in them, the cement began to detach from the walls in mid-2014, leaving part of the stone exposed and increasing the dust level in the repositories that falls on the documents constantly (Figures 1C and 1D).

For the study, three of the five repositories of the PHA SC were selected; especially, three located on the ground floor of the building and around the central courtyard that has the cistern. All these repositories are naturally ventilated. Repository 1 (R-1) coincides with the current repository 3 of the archive, it has two small and very tall windows (located close to 4 m high), it is located in the northwest side of the building and it measures (length × width × height) 8.2 m × 5.5 m × 6 m. Repository 2 (R-2) coincides with repository 4, it has only one window (installed at the same height), it is located on the north side and it measures 2 m × 5 m × 6 m, while repository 3 (R-3) coincides with repository 5, it has two windows similar to R-1, it is located on the northeast side and its dimensions are 11.2 m × 5.2 m × 6 m (Figure 1E).

2.2 Indoor Microclimate Monitoring

T and RH were recorded continuously from the first days of 2015 and until the end of 2017 using a thermo-hygrograph per repository that was placed in the center of each one of them. Weekly the recorded data was taken to an Excel page to determine the average values and the standard deviations by day, week, month and year.

2.3 Sampling of Airborne Fungal Propagules

The samplings were performed in different months of three years. The first two samplings were performed in months belonging to the rainy season in Cuba, and specifically they were made on September 1, 2015 and June 9, 2016. The third isolation was carried out on February 22, 2017, month corresponding to the season of little rain. The number of points to be sampled was determined according to Sánchis [22], which indicate a simple method based on the cube root of the premises volume. According to this criterion, a total of 8 points were sampled, 3 in R-1 and R-3 as well as 2 points in R-2 (Figure 1F). Also, a point outdoor in the courtyard center was sampled.

The samples were taken between approximately 10:00 am and 1:30 pm, considering the working hours. Each selected point (indoor and outdoor) was sampled by triplicate with a SAS biocollector (Super 100^{TM}, Italy) in vertical position at intervals of one hour between replicates. Airflow of 100 L of air in 1 min was used and the biocollector was located at 1.5 m of height approximately. Two variants of the culture medium were used to guarantee the greatest possible fungal diversity and were Malt Extract Agar (MEA) (Biocen, Cuba) at pH 5 [23] and MEA supplemented with NaCl (7.5%) [12,19]. Later, the dishes were transported sealed and invert to the laboratory in NARC (Havana), where they were incubated at 30 ºC for 7 days after removing the seal. The colonies were counted to calculate the fungal concentration per m^3 of air expressed in colony forming units (CFU/m^3) according to air sampler's manual. Then the colonies were isolated, purified and conserved in slants of MEA at 4 ºC.

Along with taking microbiological samples, T and RH were measured in the same points with a Pen TH 8709 digital thermo-hygrometer (China).

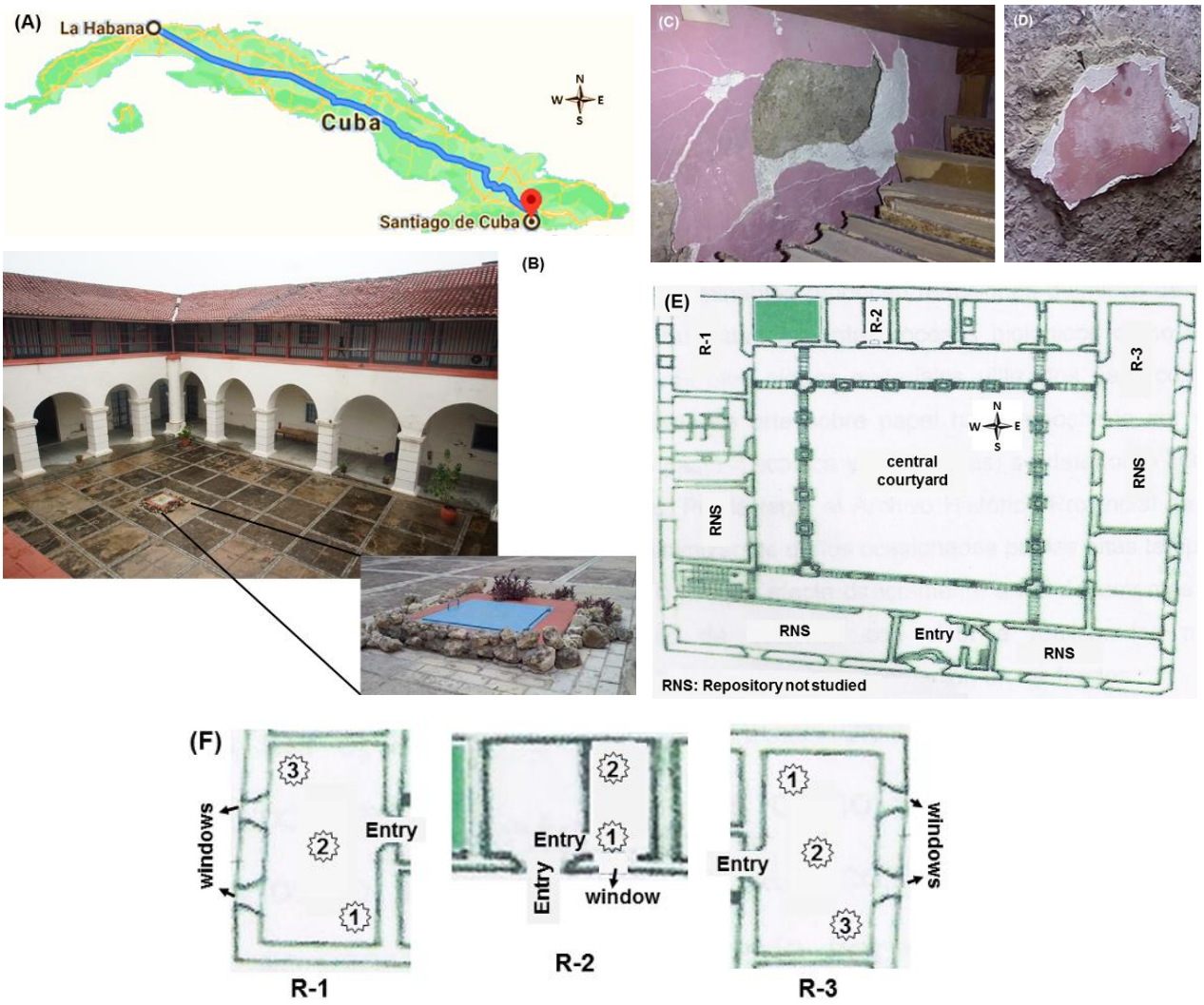

Figure 1. (A) Location of the Provincial Historic Archive of Santiago de Cuba (PHA SC) in Cuba map (20°1'19.524" N and 75°49'52.823" W). (B) General view of the building indoor with the central courtyard and the cistern. (C) Mortar layer with which the repositories walls were covered during the last building restoration (1997-1998) that by not allowing the water to escape from the wall, favors the presence of efflorescence and the detachment of the concrete plaster, generating dust in the environments and over the documents. (D) Walls particular characteristics in R-1. (E) Building ground floor sketch where the analyzed repositories are located. (F) Sampling points in each of the studied repositories.

2.4 Identification of the Fungal Isolates

Macroscopic observations of morphological characteristics of each colony, both front and back were made with the naked eye and using a stereomicroscope (14X). Through a clear field trinocular microscope (Olympus, Japan) at 40X (dry) and 100X (with oil immersion) connected to a digital camera (Samsung, Korea), conidia, conidiophores and other fungal structures of taxonomic value were observed from preparations made with lactophenol or lactophenol with cotton blue (for hyaline structures) or microcultures. For taxonomic identification some manuals and keys were consulted. To locate the isolates in genera the criteria of Barnett and Hunter [24] and Domsch *et al.* [25] were followed.

For the identification of *Aspergillus* and *Penicillium* species different procedures were followed [26-31]. In the identification of *Cladosporium* species other keys were used [32-35]. The MycoBank website was also consulted.

2.5 Ecological Criteria of the Taxa Isolated in the Environments

The Relative density (RD) analysis was performed according to Smith [36], where:

RD = (number of colonies of a specific taxa/total number of colonies of all taxa counted) × 100.

Relative frequency (RF) was calculated according to

Esquivel *et al*. [37], where:

RF = (number of times a genus or species is detected/ total number of samplings realized) × 100

According to RF five ecological categories were established: Abundant taxa (A) were those that had a RF = 100% - 81%, Common taxa (C) had a RF = 80% - 61%, Frequent taxa (F) had a RF = 60% - 41%, Occasional taxa (O) had a RF = 40% - 21% and Rare taxa (R) had a RF = 20% - 0.1% [19].

Sørensen's coefficient of similarity (QS) was used to compare the taxa obtained in the indoor air of each repository with those obtained in the outdoor air [23].

$$QS = 2a/b + c$$

where *a* is the number of common genera detected in the two environments that are comparing, *b* the number of detected genera only in a sample and *c* the number of detected genera only in the other sample.

The QS values ranged between 0 - 1. A value equal to 0 indicates that the obtained taxa in both compared environments were completely different and a value equal to 1 indicates that taxa were identical [38].

2.6 Statistical Analysis

The data obtained were analyzed using the statistical program the Statgraphics Centurion XV. Normal distribution of data was analyzed for 95% confidence interval ($p \leq 0.05$). Pearson's correlation was used to determine the relationship between fungal concentration and thermo-hygrometric parameters. To compare the averages of T and RH obtained in 2015, 2016 and 2017, as well as the fungal concentrations averages obtained per year and per repository, a simple classification analysis of variance (ANOVA) was used followed by the Fisher LSD test (Least Significant Difference). Also a Duncan test was used to determine the differences among fungal concentrations obtained in the repositories per each sampling.

3. Results

3.1 Thermo-hygrometric Parameters Behavior and Concentration of Airborne Fungi in the Repositories

The average values of T and RH obtained in the three studied repositories during the year 2015 were 30 ºC and 75%, respectively, in 2016 they were 28 ºC and 80% and in 2017 they were 29 ºC and 72%; this made the general average values of T and RH during the three years of study were 29.6 ºC and 77%, respectively. However, the T showed great stability in 2015 with values close to 30 ºC, a behavior that was not similar in 2016 and 2017. In these years values lower than 29.6 ºC were detected during the months of March to May 2016 and from January to April 2017, the remaining months showed fluctuations in T that were in the order of approximately 29.6 ± 1 ºC (Figure 2). Regarding RH, the behavior was less stable and the variations were more marked. In 2015, although the values remained above 70%, the oscillations were between 72% and 75%. In 2016 the values were more unstable and higher, since most of the year the values oscillated between 77% and 87%. In 2017, the RH trend was lower than the previous year and the values fluctuated between 71% and 73%, even in March an average of 69% was obtained (the lowest).

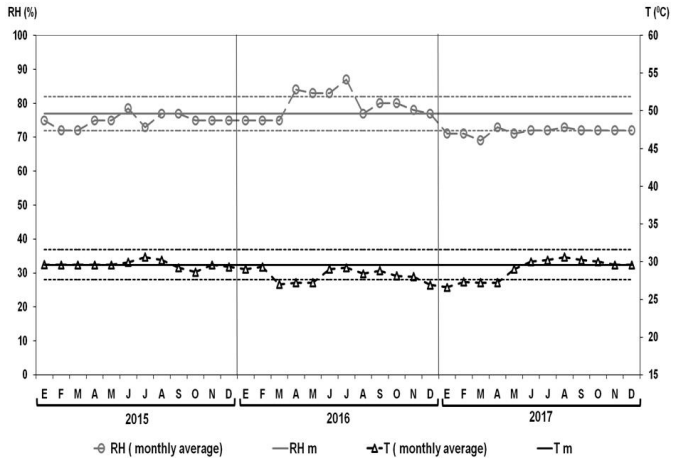

Figure 2. T and RH behavior during the 3 years of study in the analyzed three repositories of the AHP SC. The recorded T and RH values comprise average of all the readings made in the three repositories per month. The first microbiological sampling was performed on September 1, 2015 (month included in the rainy season), the second sampling was carried out on June 9, 2016 (another month belonging to the rainy season) and the third isolation was made on February 22, 2017 (month belonging to the season of little rainy). General averages of T and RH for the 3 years were 29.6 ± 2.5 ºC and 77.3 ± 5.2%, respectively.

In the statistical analysis of the obtained thermo-hygrometric parameters during the studied years, no statistically significant differences were found for both T and RH within each year, which indicates stability of these parameters. However, there were significant differences of these variables between the years, with a decrease in T and an increase in RH over time (negative linear correlation, p = –0.3595) (Figures 3A and 3B).

At the time of each sampling, the T average values oscillated between 33.1 ºC and 27.8 ºC, while those of RH fluctuated between 80.7% and 48.6%. The first two sampling were performed in months that corresponded to the rainy season in Cuba (June to November) and the RH values were higher than 64%, even in the first sampling (2015) they were higher than 74%. R-1 showed slightly higher RH values (79.7% to 80.7%) than the other two repositories (74.4% to 78.3%), possibly due not only to the existing environmental humidity on those days but also to marked moisture problems in the building that was evidenced in the deterioration of some repositories walls, with a higher incidence in R-1 (Figures 1C and 1D).

About the obtained fungal concentrations, it could be seen that in 2015 the highest concentrations were detected (Figure 3C) and that R-1 in the first sampling was the most contaminated repository of the three sampling (Figure 3D). There were also statistically significant differences in the fungal concentrations obtained in 2015 compared to 2016 (p = 0.0356) and between the R-1 and R-3 repositories (p = 0.0248).

Table 1 shows the average values of the fungal concentrations obtained in each repository and in each sampling. As can be seen, R-1 showed the highest concentration (421.1 CFU/m^3) in the first sampling (2015) followed by R-2 (229.1 CFU/m^3) and R-3 (147.8 CFU/m^3). In the second isolation (2016) the values were more homogeneous with each other. Contrary to what happened in the previous isolation, R-1 was the repository that showed the lowest concentration (135.6 CFU/m^3), followed by R-3 (153.7 CFU/m^3) and R-2 (176.7 CFU/m^3). In the third isolation (2017), R-2 again showed the highest concentration (298.9 CFU/m^3) followed by R-1 (268.9 CFU/m^3) and R-3 (162.2 CFU/m^3). Also, there were statistically significant differences of R-1 among the three samplings, while R-2 and R-3 did not show significant differences between the samplings. Fungal concentrations obtained in these years did not show any correlation with T and RH for $p \leq 0.05$ (RH, p = 0.5270; T, p = 0.1862).

The environmental mycological quality of the repositories in 2015 was very bad in general (Table 1). R-1 with an I/O ratio of 4.2 and R-2 with an I/O ratio of 2.3 stood out for having poor environmental quality and for being poorly ventilated environments with little air circulation, only R-3 showed a regular environmental quality (I/O = 1.5). Though, the environmental quality improved in the following isolates because in the second isolation (2016) the repositories showed a regular quality (I/O = 1.5 - 2), while already in the third isolation (2017) the environmental quality was good (I/O < 1.5).

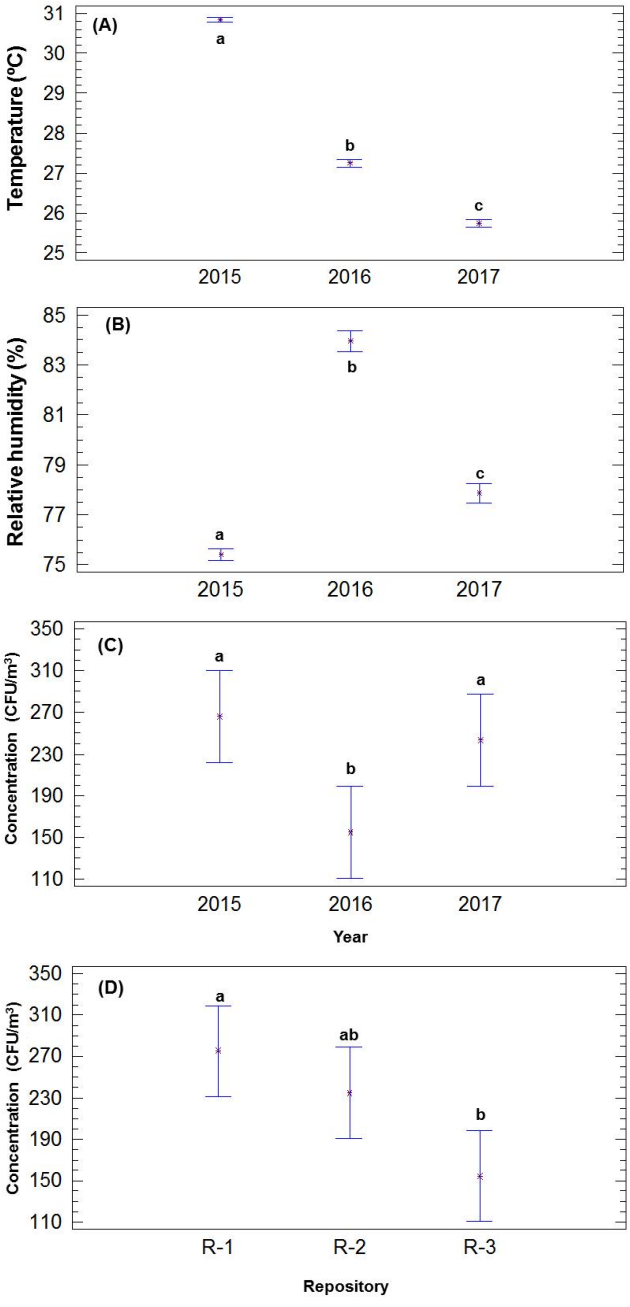

Figure 3. Statistical behavior (LSD) of the recorded T (A) and RH (B) in the analyzed repositories during the three years of study as well as the fungal concentrations per year (C) and per studied repository (D). a, b, c: Indicates statistically significant differences ($p \leq 0.05$). Similar letters designate that there are no significant differences.

Table 1. Fungal concentrations in the studied repositories and the indoor/outdoor ratio (I/O) obtained in each of them.

Isolation	R-1		R-2		R-3		Outdoor
	(CFU/m^3) ± SD	I = I/O	(CFU/m^3) ± SD	I = I/O	(CFU/m^3) ± SD	I = I/O	(CFU/m^3)
First (2015)	421.1 ± 328.2 a	4.2	229.1 ± 197.4 d	2.3	147.8 ± 36.7 e	1.5	100.0
Second (2016)	135.6 ± 27.9 b	1.5	176.7 ± 97.8 d	1.9	153.7 ± 30.3 e	1.7	90.0
Third (2017)	268.9 ± 132.7 c	1.2	298.9 ± 124.9 d	1.4	162.2 ± 95.5 e	0.7	220.0

SD: Standard deviation. a, b, c, d, e: Indicates statistically significant differences ($p \leq 0.05$) of the fungal concentrations among the samples according to Duncan's test. Similar letters signpost that there are no significant differences. I ≤ 1.5: Non-contaminated environment with good ventilation. I = 1.5 – 2: Environment of regular quality. I > 2: Contaminated environment and with poor ventilation [59].

3.2 Diversity and Distribution of the Airborne Fungi

According to the culture method used, the anamorphic genera of the phylum Ascomycota (including yeasts) predominated in the air of the PHA SC repositories. Mytosporic fungi prevailed among them, evidencing the hyphomycetes *Alternaria*, *Aspergillus*, *Candida*, *Chrysonilia*, *Cladosporium*, *Coremiella*, *Curvularia*, *Fusarium*, *Penicillium*, *Talaromyces*, *Torula*, *Tritiriachium* and *Zygosporium*. A genus belonging to coelomycetes (*Pestalotia*), one corresponding to ascomycetes (*Eurotium*) and two types of non-sporulating mycelia (WNSM: white non-sporulating mycelium and PNSM: pigmented non-sporulating mycelium) were also detected in minority (Table 2).

In the first and third sampling 8 taxa were isolated, while in the second isolation 12 taxa were obtained. The predominant genera both in outdoor and indoor environments were *Aspergillus* and *Cladosporium*, which were obtained in all the samplings hence they turned out to be

Table 2. Ecological behavior of the fungal taxa detected in the analyzed environments in the different samplings.

Taxa	R-1			R-2			R-3			RF (%)	EC	Outdoor		
	1st	2nd	3rd	1st	2nd	3rd	1st	2nd	3rd			1st	2nd	3rd
	RD (%)											RD (%)		
Alternaria Nees	-	-	8.6	6.3	4.0	-	-	-	-	33.3	O	-	-	-
Aspergillus P. Micheli ex Link	27.7	71.4	37.0	56.2	40.0	8.4	56.3	66.6	58.8	100	A	30.0	11.1	4.5
Candida Berkhout	2.2	-	-	-	-	-	-	-	-	11.1	R	-	-	-
Chrysonilia Arx.	-	-	8.6	-	-	-	-	-	-	11.1	R	5.0	-	-
Chrysosporium Corda	-	-	-	-	-	-	-	-	-	0	-	-	55.6	-
Cladosporium Link	29.7	17.9	17.2	18.7	44.0	20.7	12.7	2.4	26.4	100	A	40.0	11.1	32.7
Coremiella Bubák & Krieg.	19.1	-	-	-	-	-	-	-	-	11.1	R	5.0	-	-
Curvularia Boedijn	-	-	-	-	4.0	-	-	-	-	11.1	R	-	-	-
Eupenicillium F. Ludw.	-	-	-	-	-	-	-	-	-	0	-	-	11.1	-
Eurotium Link	-	-	-	-	-	-	-	-	2.9	11.1	R	-	-	-
Fusarium Link	3.2	-	8.6	9.4	8.0	4.2	-	-	-	55.6	F	15.0	11.1	13.6
Neurospora Shear & B.O. Dodge	-	-	-	-	-	-	-	-	-	0	-	-	-	9.1
Penicillium Link	18.1	10.7	20.0	-	-	8.3	14.1	26.2	8.8	77.8	C	-	-	31.0
Pestalotia De Not.	-	-	-	-	-	8.3	-	-	-	11.1	R	-	-	-
Talaromyces C.R. Benj.	-	-	-	-	-	29.2	2.8	4.8	-	33.3	O	-	-	-
Tritiriachium Limber	-	-	-	-	-	4.2	-	-	-	11.1	R	-	-	-
Torula Pers.	-	-	-	-	-	-	1.4	-	-	11.1	R	-	-	-
Zygosporium Mont.	-	-	-	-	-	-	2.8	-	-	11.1	R	5.0	-	9.1
Other Yeasts	-	-	-	9.4	-	-	-	-	-	11.1	R	-	-	-
WNSM	-	-	-	-	-	12.5	9.9	-	3.1	33.3	O	-	-	-
PNSM	-	-	-	-	-	4.2	-	-	-	11.1	R	-	-	-

RD: Relative density. RF: Relative frequency. The ecological categories (EC) are classified as: Abundant (A) with RF = 100%-81%, Common (C) with RF = 80%-61%, Frequent (F) with RF = 60%-41%, Occasional (O) with RF = 40%-21%, Rare (R) with RF = 20%-0%. WNSM: white non-sporulating mycelium and PNSM: pigmented non-sporulating mycelium.

ecologically abundant (Table 2). *Penicillium* genus was also isolated, which due to being detected in the three samplings (but not in all the repositories) was classified as common, *Fusarium* that was isolated in the first and second sampling (although not in all the repositories) turned out to be a frequent genus; *Alternaria*, *Talaromyces* and a non-sporulating mycelium (WNSM) which, due to having been detected in two samplings, were classified as occasional. Likewise, *Candida*, *Chrysonilia*, and *Coremiella* were isolated in the first sampling, *Curvularia*, *Pestalotia*, *Tritiriachium* and other non-sporulating mycelium (PNSM) in the second sampling, *Eurotium*, *Torula* and *Zygosporium* in the third sampling and all of them were classified as rare. The yeasts that were isolated in 2016 from air of R-1 were classified as rare.

Sørensen similarity coefficient was used to analyze the similarity of detected genera in the indoor air of the repositories as well as between these and those isolated from the outdoor air. This coefficient showed values that varied between 0.3 to 0.5, i.e., the values were not high, and rather they were low to medium, indicating that there was a certain exchange of taxa between the environments during the years of study (Table 3).

Regarding the isolated species, 2 corresponded to the *Alternaria* genus, 17 belonged to *Aspergillus*, 5 were from the *Cladosporium*, 5 from *Penicillium* and only 1 species was obtained from the remaining genera. The analysis of all taxa detected in the indoor of R-1, R-2 and R-3 as well as the outdoor air during the three samplings showed the exchange of species among these environments manifesting with certain similarities within the wide diversity (Figure 4). The *Alternaria* species isolated were *Al. alternata* (Fr.) Keissl (R-3) and *Al. ricini* (Joshi) Hansford (R-1 and R-2), but as this last species was detected on two occasions was categorized as an occasional (RF = 22.2%), and constitutes the first record for Cuban archives environments. Of the *Fusarium* genus, the species *F. xylaroides* Steyaert was the predominant one (detected in R-1, 1st sampling and in R-3, 1st and 2nd samplings with FR = 33.3%) and also constituted the first report for Cuban archive environments.

Within *Aspergillus* species, *A. flavus* Link dominated (RF = 77.8%), which due to having been isolated on seven occasions (three times on R-1 and twice on both R-2 and R-3), was considered as common from these environments, while *A. niger* Tiegh. and *A. parasiticus* Speare were detected in second place (four times, equivalent to RF = 44.4%) and hence were classified as frequent species. In third place were *A. oryzae* (Ahlburg) Cohn and *A. versicolor* (Vuill.) Tirab, which turned out to be occasional (RF = 33.3%). Two other species were detected with lower frequencies (RF = 22.2%) and they also turned out to be occasional (*A. chevaliery* (L. Mangin) Thom & Church and *A. ochraceus* K. Wilh.), while another 10 were classified as rare species: *A. auricomus* (Guegen) Saito, *A. cervinus* Massee, *A. glaucus* Link, *A. japonicus* Saito, *A. nidulans* (Eidam) G. Winter, *A. penicilloides* Speg., *A. tamarii* Kita, *A. terreus* Thom, *A. ustus* (Bainier) Thom & Church and *A. uvarum* G. Perrone, Varga & Kozak. From *Cladosporium* genus, *Cl. sphaerospermum* Penz prevailed followed by *Cl. cladosporioides* (Fresen.) G.A. de Vries that were classified as common (RF = 77.8%) and frequent (RF = 44.4%), respectively; the other species (*Cl. oxysporum* Berk. & Curt., *Cl. staurophorum* Kendrick and *Cl. tenuissimum* Cooke) were obtained in minority hence turned out to be rare (RF = 11.1%). Although *Cl. staurophorum* was only isolated in R-2 in 2015, this species constitutes the first record for Cuban archives environments. From *Penicillium* genus, *P. citrinum* Thom dominated followed by *P. brevicompactum* Dierckx, hence they were

Table 3. Sørensen similarity coefficient (QS) values obtained by comparing the common genera detected in the repositories environments as well as between these and those isolated in the outdoor environment.

	R-1			R-2			R-3		
	QS_1	**QS_2**	**QS_3**	**QS_4**	**QS_5**	**QS_6**	**QS_7**	**QS_8**	**QS_9**
Outdoor	0.4	0.4	0.4	0.3	0.4	0.4	0.3	0.3	0.4
	QS_{10}	**QS_{11}**	**QS_{12}**	-	-	-	**QS_{13}**	**QS_{14}**	**QS_{15}**
R-2	0.4	0.5	0.4	-	-	-	0.3	0.3	0.4
	-	-	-	-	-	-	**QS_{16}**	**QS_{17}**	**QS_{18}**
R-1	-	-	-	-	-	-	0.4	0.3	0.4

QS_1, QS_2, QS_3: Indicate the similarities between R-1 and Outdoor in the three samplings (2015, 2016, 2017). QS_4, QS_5, QS_6: Indicate the similarities between R-2 and Outdoor in the three samplings. QS_7, QS_8, QS_9: Indicate the similarities between R-3 and Outdoor in the three samplings. QS_{10}, QS_{11}, QS_{12}: Indicate the similarities between R-1 and R-2 in the three samplings. QS_{13}, QS_{14}, QS_{15}: Indicate the similarities between R-2 and R-3 in the three samplings. QS_{16}, QS_{17}, QS_{18}: Indicate the similarities between R-1 and R-3 in the three samplings.

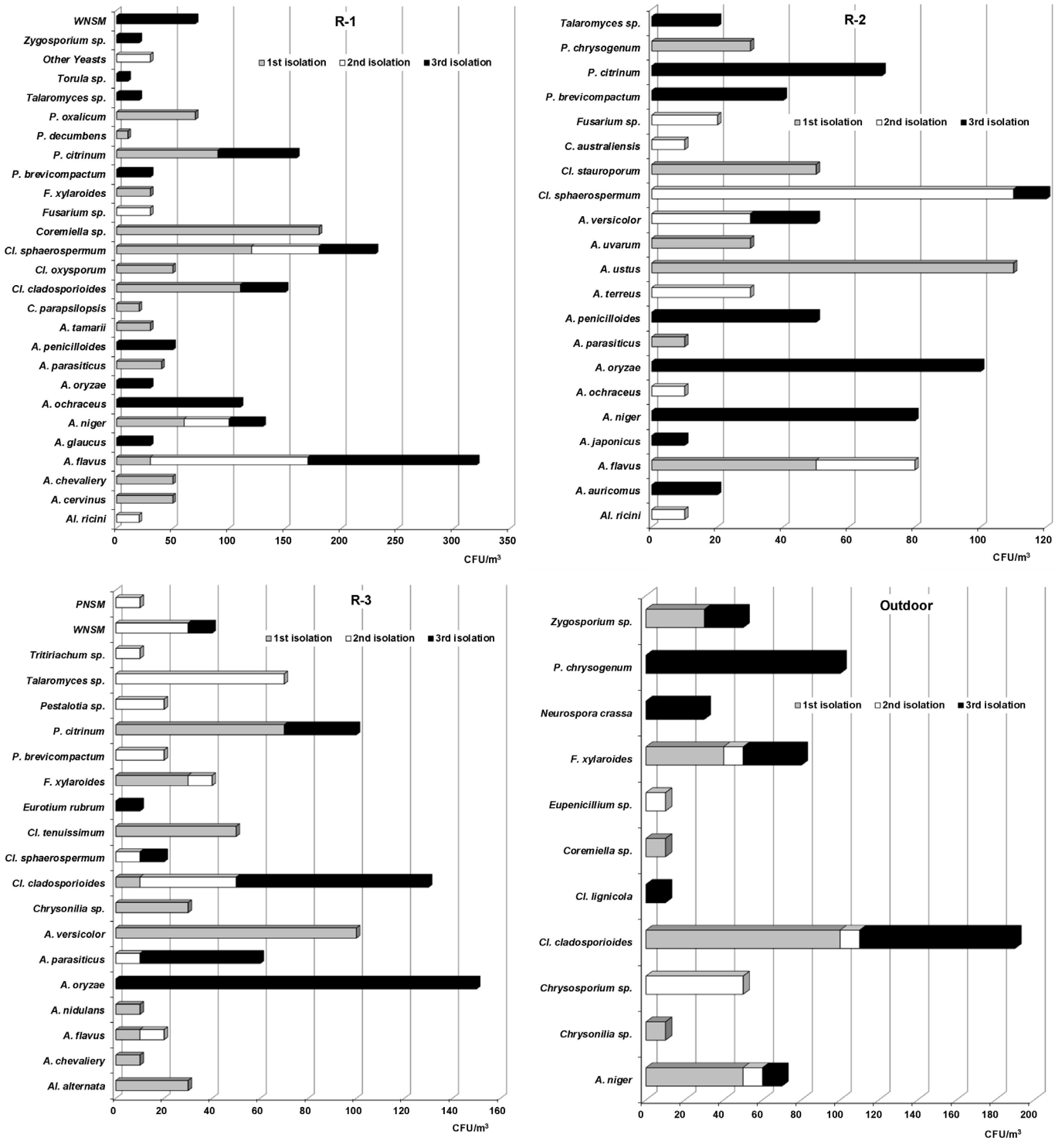

Figure 4. Species concentrations (CFU/m^3) detected in the indoor air of studied repositories by sampling and in the outdoor air.

classified as frequent (RF = 55.6%) and occasional (RF = 22.2%), respectively. The other three detected species were classified as rare (Table 4).

As *Aspergillus* has toxigenic species, the concentrations of all the detected species in the studied indoor environments were taken into account, and in the same way the concentrations of all *Cladosporium* and *Penicillium* species were also analyzed (Table 4). Some species of *Aspergillus* were detected with concentrations ≥ 50 CFU/m^3, distinguishing *A. flavus*, *A. niger*, *A. oryzae* and *A. versicolor*, while the other species were detected at concentrations between 10 CFU/m^3 and 40 CFU/m^3. *Aspergillus flavus* dominated with concentrations that ranged between 10 CFU/m^3 to 150 CFU/m^3, being R-1 in the second and third sampling where the highest concentrations were obtained (140 CFU/m^3 and 150 CFU/m^3, respectively); *Aspergillus ochraceus* was also detected in R-1 in the third isolation with a high concentration (110 CFU/m^3). In R-2, *A. ustus* were isolated in the first sampling and *A. oryzae* in the third isolation with high concentrations (110 CFU/m^3 and 100 CFU/m^3, respectively).

In general, the obtained concentrations sum from the different *Cladosporium* and *Penicillium* species together by isolation were markedly less than 500 CFU/m^3. R-1, which was the most contaminated repository in the first sampling, showed only 342 CFU/m^3 of the total species belonging to these two genera, in the other repositories the concentrations ranged between 60 CFU/m^3 and 150 CFU/m^3.

Table 4. Concentrations (CFU/m^3) and ecological behavior of the different species of *Aspergillus* spp., *Cladosporium* spp. and *Penicillium* spp. isolated in the repositories' air per sampling.

Specie	1st isolation			2nd isolation			3rd isolation			RF (%)	EC
	R-1	R-2	R-3	R-1	R-2	R-3	R-1	R-2	R-3		
A. auricomus (Guegen) Saito	-	-	-	-	-	-	-	20	-	11.1	R
A. cervinus Massee	50	-	-	-	-	-	-	-	-	11.1	R
A. chevaliery (L. Mangin) Thom & Church *	50	-	10	-	-	-	-	-	-	22.2	O
A. flavus Link *	30	50	10	140	30	10	150	-	-	77.8	C
A. glaucus Link *	-	-	30	-	-	-	-	-	-	11.1	R
A. japonicus Saito *	-	-	-	-	-	-	-	10	-	11.1	R
A. niger Tiegh. *	60	-	-	40	-	-	30	80	-	44.4	F
A. nidulans (Eidam) G. Winter *	-	-	10	-	-	-	-	-	-	11.1	R
A. ochraceus K. Wilh. *	-	-	-	-	10	-	110	-	-	22.2	O
A. oryzae (Ahlb.) Cohn *	-	-	-	-	-	-	30	100	150	33.3	O
A. parasiticus Speare	40	10	-	-	-	10	-	-	50	44.4	F
A. penicilloides Speg.	-	-	-	-	-	-	-	50	-	11.1	R
A. tamarii Kita *	30	-	-	-	-	-	-	-	-	11.1	R
A. terreus Thom *	-	-	-	-	30	-	-	-	-	11.1	R
A. ustus (Bainier) Thom & Church *	-	110	-	-	-	-	-	-	-	11.1	R
A. uvarum G. Perrone, Varga & Kozak.*	-	30	-	-	-	-	-	-	-	11.1	R
A. versicolor (Vuill.) Tirab. *	-	-	100	-	30	-	-	20	-	33.3	O
Cl. cladosporioides (Fresen.) G.A. de Vries*	110	40	10	-	-	40	-	-	80	44.4	F
Cl. oxysporum Berk. & Curt. *	50	-	-	-	-	-	-	-	-	11.1	R
Cl. sphaerospermum Penz. *	120	-	-	60	110	10	50	10	10	77.8	C
Cl. staurophorum Kendrick	-	50	-	-	-	-	-	-	-	11.1	R
Cl. tenuissimum Cooke, Grevillea	-	-	50	-	-	-	-	-	-	11.1	R
P. brevicompactum Dierckx *	-	-	-	-	-	20	30	40	-	22.2	O
P. citrinum Thom *	90	-	70	-	-	-	70	70	30	55.6	F
P. chrysogenum Thom *	-	30	-	-	-	-	-	-	-	11.1	R
P. decumbens Thom *	10	-	-	-	-	-	-	-	-	11.1	R
P. oxalicum Currie & Thom	70	-	-	-	-	-	-	-	-	11.1	R

*: Species reported as pathogens according to de Hoog *et al.* [75]. RF: Relative frequency. The ecological categories (EC) are classified as: Abundant (A) with RF = 100%-81%, Common (C) with RF = 80%-61%, Frequent (F) with RF = 60%-41%, Occasional (O) with RF = 40%-21%, Rare (R) with RF = 20%-0%.

The indoor/outdoor ratios (I/O) of the 6 species that were common in both environments (*A. niger*, *Chrysonilia* sp., *Cl. cladosporioides*, *Coremiella* sp., *F. xylaroides*, *Zygosporium* sp.) showed in general that, there was a low contamination level in the repositories indoor environments by them (I/O ≤ 1.5), with the exception of *A. niger* (R-2, 3rd isolate), *Chrysonilia* sp. (R-3, 1st isolation) and *Coremiella* sp. (R-1, 1st isolation), which presented I/O ratios of 4.2, 1.7 and 3.8, respectively, indicating the presence of an internal source of contamination of these species in the air (Table 5). R-1 in the first isolation was the repository that presented the largest number of common species (4) and within them *Coremiella* sp. which turned out to be predominant in that environment (RD = 19.1%), although in later isolates this species was never detected again. The remaining repositories showed one to three common species with a low degree of contamination by them. Only *A. niger* and *Cl. cladosporioides* were the species that showed the greatest similarities with the outdoor air. In fact, *A. niger* was detected in R-1 in all isolates, indicating that it is a typical species of this environment. *Cladosporium cladosporioides* was a species that turned out to be common in R-1 and R-3, but with ratios that did not indicate environmental contamination.

Table 5. Indoor/outdoor (I/O) ratios of the common species detected in each repository and in the outdoor environment by isolation performed.

Taxa	First isolation			Second isolation			Third isolation		
	R-1	R-2	R-3	R-1	R-2	R-3	R-1	R-2	R-3
A. niger	0.2	-	-	1.1	-	-	0.9	4.2	-
Chrysonilia sp.	-	-	1.7	-	-	-	-	-	-
Cl. cladosporioides	0.3	-	0.1	-	-	1.5	0.2	-	0.3
Coremiella sp.	3.8	-	-	-	-	-	-	-	-
F. xylaroides	0.2	-	0.6	-	-	0.4	-	-	-
Zygosporium sp.	-	-	-	-	-	-	0.3	-	-

I = I/O ratio. I ≤ 1.5: Non-contaminated environment with good ventilation. I = 1.5 - 2: Environment of regular quality. I > 2: Contaminated environment and poor ventilation [59].

4. Discussion

Although some research has been performed in Cuba on the environmental mycobiota of archives, libraries and museums, these have focused on the western region of the country, mainly in the Capital (Havana) because the largest number of these institutions are located in this region, hence this is the first investigation to be carried out in an archive of country eastern region.

To have a representativeness of the fungal concentrations and diversity in the environments of the repositories of this archive, the samplings were performed in different seasons and years. Cuba is characterized by having only two annual seasons that are a season of little rains or winter (December - April) and the rainy season or summer (May - November) that coincides with the period in which hurricanes occur in the Caribbean region (June 1 to 30 November) and that Cuba is affected by at least one of them every year. Although the eastern region of the country is the least affected by these meteorological phenomena, it is the most disturbed by earthquakes and in particular the province of Santiago de Cuba. Earthquakes occur almost constantly there, which in most cases are imperceptible by man, but are perceived by the sensors that the National Center for Seismological Research has located throughout the province. It was precisely intended to perform a sampling at the beginning of 2016 (rainy season) and it had to be postponed several months because on January 17, 2016, an earthquake was recorded south of the Santiago de Cuba bay that had 1500 aftershocks in 50 days, 37 of them perceptible not only in the Santiago de Cuba province but also in neighboring provinces [39]. Hence, the sampling for that year was performed on June 9.

In addition, the location of the province between the sea to the south and the high mountains of the Sierra Maestra to the north, provide it with high T and RH throughout the year [40], for that reason the thermo-hygrometric parameters were taken into account in the investigation.

Microclimatic conditions are known to play an important role in microbial proliferation [41,42]. The thermo-hygrometric parameters favor the microbial colonization of the substrates that make up the artworks [15]. Environmental RH directly determines the moisture content in materials, promotes sedimentation of suspended airborne fungal propagules, as well as proliferation and growth of fungi on surfaces [1,16]. The interactions of existing microorganisms in the bioaerosols, in particular fungal propagules, with microclimatic conditions and environmental chemical pollutants create alterations in the structures of the Cultural Heritage, including the documentary heritage, favoring the fungal attack of the substrates [3]. Therefore, T and RH behavior was evaluated in the repositories studied.

The T and RH in the repositories showed a normal distribution during the three years of study. Those thermo-hygrometric parameters can be considered high (29.6 ± 2.5 °C and 77.3 ± 5.2%, respectively), since the RH must be ≤ 65% to reduce the deposition of fungal propagules and the T must be ≤ 25 °C to minimize the microbial growth [43]. However, high RH values can negatively influence sporulation and

the growth of fungal spores that settle on materials [44]. So, the microclimatic conditions of the studied repositories in the PHA SC were not suitable for the development of fungi. Although natural ventilation does not achieve to lower the T and RH in the repositories to those recommended values, it does manage to keep them stable. For this reason, this type of ventilation is recommended in Cuba to guarantee thermo-hygrometric stability in archival repositories that do not store special materials, since it allows dealing with the daily variations of these parameters and the disasters that involve water, such as intense rains and hurricanes, as well as to face the climatic variations that CC is causing in the country [45].

Although the studied archive building has a cistern under the central courtyard that favors the considerable increase in humidity in the land that rises to the repositories by capillarity through the walls, no values higher than 85% or statistically significant differences were found of the RH in the repositories within each year, indicative of the stability of this parameter, possibly due to the beneficial role played by natural ventilation [1]. The detected differences in the thermo-hygrometric parameters among the years, with a decrease in T and an increase in RH with respect to time could be due to the raininess levels or drought of each season analyzed and to the construction conditions of the building that led to high moisture in the walls and floors of the repositories. This construction, like the majority of the buildings destined to conserve documentary collections in Cuba, was not conceived for this purpose, so there is a whole group of aspects related to the construction materials, the conception and distribution of the premises that are not they meet some of the most elementary construction standards required for an archive building. This corroborates the fact that the structure type of a building will determine the risk, the deterioration kind and the problems associated with the management of the indoor environment [15].

The quantification of the airborne mycobiota in the archive repositories constitutes, without a doubt, an indicator of the environmental microbiological quality that has a direct influence on the conservation of the documentary heritage and on the quality of life of the personnel. Air pollution in these places, mainly by filamentous fungi (aeromycobiota), is considered one of the greatest threats to health [7,46]. Because of this, many specialists dedicated to the cultural heritage conservation suggest systematic aerobiological sampling in archive and library environments. With them, an environmental reference of the risk to which the heritage value documents and the personnel who work with them are exposed is guaranteed [4,47].

Although the fungal concentrations detected in the repositories air did not exceed 500 CFU/m^3, they considered intermediate [48] or moderate [49], R-1 being the most contaminated repository during the three years studied. However, the concentrations obtained in this research were similar to those reported in previous studies performed in archives and libraries in other countries [41,47,50] and in Cuba both in naturally ventilated and air-conditioned environments [12,51-53]. Likewise, these concentrations turned out to be low in relation to others obtained in foreign archives [48,54,55].

It was evidenced that there was no correlation of the fungal concentration with the T and RH, indicative of the thermo-hygrometric stability in the repositories that favored the fungal load steadiness, demonstrating once again the importance of natural ventilation. Contrary behaviors were previously reported [3,41,51,52,54,55].

Although it is suggested that the fungal concentration of the outdoor environment is generally higher than that of the indoor environment, being a modulator of the fungal concentration in indoor environments [56,57] because it levels the quality of these environments, it has been reported that the I/O ratio is indicator of the emission of microorganisms and, therefore, defines the environmental microbiological quality. If this I/O ratio is ≤ 1, the outdoor environment is the main source of bioparticles emission to the indoor environments [3,58], if it oscillates between 1.5 and 2 the environment has a regular quality, while if it is ≥ 2, the indoor sources are responsible for environmental pollution, in addition to indicating poor ventilation or poor air circulation indoors [59]. According to these criteria, variations were observed from one sampling to another. In the first sampling R-1 and R-2 revealed I/O ratios typical of a poor environmental quality suggesting the existence of internal sources of fungal contamination that could induce or accelerate the degradative activity and the documents deterioration; in the second sampling all the repositories showed a regular environmental quality, while in the third sampling all repositories showed values lower than 1.5 indicative of a correct ventilation and air circulation in the repositories and consequently a normal exchange with the outdoor air [59], which prevented the formation of amplification zones of the fungal load in the indoors. A similar result was obtained in the PHA of Pinar del Rio (PHA PR) [52].

These behaviors in the environmental quality indicated that the conservators were not carrying out a correct management of the natural cross ventilation in the repositories at the beginning of the study and that after the first results and the suggestions offered to them, was possible to improve the environmental quality in repositories, demonstrating that the natural cross ventilation system turned out to be efficient to control the of fungal propagules load

within the monitored spaces despite the walls moisture. However, the high ratios obtained in R-1 and R-2 in the first isolation as well as in R-2 and R-3 in the second sampling could also be due to the fact that the external fungal loads were very low at those moments. It should be noted that the first two samplings were performed days after it had rained a lot in Santiago de Cuba city and is very likely that the outdoor environment was little polluted as a result of the washing that the rain causes into the atmosphere, since by dragging the suspended bioparticles in the air, their concentrations decrease [60]. Similar results were obtained in previous studies in the NARC and the PHA PR, respectively [52,60].

Regarding the taxa detected a preponderance of anamorphs of the phylum Ascomycota was evidenced, a question that had been previously reported [50-53,55-57] and this may be due to the fact that in the Caribbean region, representatives of this phylum have been detected in high concentrations in the outdoor air [14] and particularly in Cuba [62]. A total of 18 taxa were identified in the archive environments with a prevalence of the genera *Aspergillus*, *Cladosporium* and *Penicillium*, a result that was expected and agrees with others previously obtained in Cuba [11,12,19,51-53]. In earlier studies with similarity of culture methods, comparable amounts of taxa were referred [19,44,50,51,63].

In relation to the prevalence of *Aspergillus*, *Cladosporium* and *Penicillium*, everything seems to indicate that they were among the genera existing in the outdoor environment and penetrated to the indoor environments of the repositories at some time; although these genera are considered part of the indoor environments mycobiota [42,64] and particularly of archives and libraries due to the large amount of materials of an organic nature that are conserved in these institutions that serve as nutrients [1]. It has also been reported that humidity in indoor spaces, whether in the air or in walls and ceilings, is a factor that promotes the germination of spores and the harboring of fungal propagules belonging to *Penicillium* and *Aspergillus* genera [65]. Perhaps the fact that there was moisture on the studied repositories walls has contributed to the fact that these genera have remained viable and have also been detected of majority.

The three predominant genera are characterized by having a cosmopolitan distribution and include a large number of species that form small and dry spores (dry walled spores) that can be easily dispersed by the effect of air [21]. These spores can be quite numerous in indoor air that they can be easily inhaled [21,42,54]. They can also deposit on materials if the RH is high [15] and grow on paper, leather, textiles and other substrates, forming extensive biofilms. The fungal biofilms on documents compromise the structural cohesion of paper and book binding, irreversibly deteriorating them [57]. These fungi can degrade the substrates due to the excretion of hydrolytic enzymes, cause staining on the documentary materials due to the excretion of secondary metabolites and acidify the substrates causing irrevocable damages [5,49,51,56].

It should be noted that for the first time the genus *Coremiella* is detected in the indoor environment of a Cuban archive repository. This genus characterized by growing on submerged and terrestrial plant remains and by having species that have been isolated from the outdoor environment of several countries with different climates types [66]. It is probable that this fungal genus entered the of R-1 air from the outside, and was possibly isolated due to the high concentration that existed at the time of sampling in the repository air, since it was not detected in any of the other studied repositories or in any other sampling.

It is also important to note that for the first time the *Talaromyces* genus (teleomorph of *Penicillium*) was detected in the environment of a Cuban archive repository. It had previously been isolated from documents preserved in the NARC [11,20,66], but never from the air of an archive repository. However, it was isolated from the air in a Turkish archive [63] and several Brazilian libraries [54] as well as of Greek documents [68], Italians [69], Czechs and Poles [70]. It is suspected that the presence of *Talaromyces* in indoor environment of repositories could be influenced by the existence of species of this genus over documents, or their propagules could have entered the indoor air at some time from the outside, since *Eupenicillium* F. Ludw was detected in outdoor air of PHA SC, and is also a teleomorph of *Penicillium*. In relation to the genus *Tritiriachum*, it is not very common to find it in the environment of archives, libraries and museums, although it was previously isolated in the environment of a Cuban museum [71] and on artworks surface in two Cuban museums [70,71].

Zygosporium genus has been isolated in repositories environments of the NARC [20], which is located in the western region of the country, where there are also reports of being isolated from outdoor air [73]. This genus was isolated of the outdoor air in the first and third sampling performed in PHA SC, indicating that this genus is part of the country's aerial mycobiota and that it penetrated at some time into the indoor environment of the documents' repositories analyzed.

The species number detected in the studied indoor environments was slightly higher than those discovered in the outdoor environment, suggesting the existence of an internal source of contamination that could be risky for the documents kept in these repositories. However, contrary behaviors were obtained in previous studies [4,57]. The

exchange between the studied environments was low to moderate. Sørensen's coefficient of similarity showed that most of the values were less than 0.5, indicative of a low to moderate interchange between environments. Likewise, the I/O ratio for most of the common species were equal to or less than 1.5, showing that these species came from outdoor air and did not represent important pollutants in premises indoor. Only *A. niger* showed an I/O ratio of 4.8 (in R-2, third isolation) and *Coremiella* sp. (in R-1, first sampling) yielded a I/O ratio of 3.8, that were, very high, but since they were detected only once (even *Coremiella* sp. was never isolated again), it could be indicative of specific events.

Fungi, not yet viable, can be harmful to the personnel's health that work in archives, libraries and museums, since their propagules and mycotoxins can be inhaled as well as the volatile organic compounds that they excrete [6,7,14,42,46], it has been suggested that to define the mycological quality of an indoor environment not only must take into account the total fungal concentration but also the concentration of the isolated species [1,74]. In addition, analyzing the existence of "indicator species" and their concentrations are of great value for indoor environmental quality studies, hence the selection of those species that can be used as markers of improper indoor conditions should be performed by studying the ecology of the microbial communities in indoor environments [1].

Yang and Li [64] reported that persistently high RH in places with poor ventilation allows hygroscopic materials to increase water activity (a_w) to a level that favors the growth of xerophilic fungi. They also stated that xerophilic species limit their growth if the RH is less than 75% or greater than 98%. Although the genera *Chaetomium*, *Stachybotrys* and *Ulocladium* are indicators of high humidity or water damage in buildings [1,42,64], some *Aspergillus* species, such as *A. versicolor*, are also indicators of humidity in buildings. Likewise, species considered xerophilic can also be indicators of moisture problems in the premises; such is the case of *A. flavus, A. niger, A. nidulans, A. ochraceus, A. terreus* and *A. ustus* [64]. According to these criteria, it could be affirmed that the *Aspergillus* species mentioned above and that were detected in the studied environments, were indicators of moisture problems in the building of PHA SC despite their xerophilic condition.

It should be noted that the *Aspergillus uvarum* pathogenic species according to de Hoog *et al*. [75], constitutes the first record for the environment of a Cuban archive. Although its ecological impact was low, is a species that was recently isolated in the outdoor environment of Havana [23] indicating its existence and dispersion in the outdoor air of the all country.

It has been mentioned in some countries that an indoor environment of acceptable quality should have concentrations between 100 CFU/m^3 and 500 CFU/m^3 of various non-pathogenic fungal species and that for toxigenic species (*Stachybotrys chartarum*, various species of *Aspergillus*, *Fusarium* and *Penicillium*) the concentrations should be less than 12 CFU/m^3 [43], while for other countries these concentrations must be up to 50 CFU/m^3 [47]. However, among the *Aspergillus* species isolated in the repositories, *A. flavus* stood out first, as it had been detected on five occasions at concentrations between 30 CFU/m^3 and 150 CFU/m^3 followed by *A. niger*, which was isolated on four occasions at concentrations that ranged from 30 CFU/m^3 and 80 CFU/m^3. The other isolated species showed concentrations $\geq$ 100 CFU/m^3 in some repository, such was the case of *A. ochraceus, A. oryzae, A. ustus* and *A. versicolor*. Although these findings were specific, they could be signs that in the repositories there were conditions for a significant amplification of dangerous species both for documents and for the personnel's health; hence, if adequate conservation measures are not taken and the correct management of natural ventilation is maintained in the repositories, there is a risk that the documentation begins to be damaged quickly and progressively. These conditions could affect the staff health, but the fact that employees do not work constantly in the repositories and that when they have to take out or save documents in them they use personal protective equipment, avoids negative effects on their health.

The two aforementioned behaviors are justified by the existing moisture problems in the building, and in particular in the repositories wall, that favors the detachment of concrete from the stone walls and increases the dust level within these premises, a situation that can contribute to a significant increase in environmental fungal diversity. Therefore, it was proposed to perform further studies that allow comparing the behaviors of the airborne mycobiota, that of dust and that of documents surface.

The *Aspergillus* genus is characterized by having toxigenic (*A. flavus, A. ochraceus, A. terreus, A. versicolor*) and pathogenic species (examples: *A. chevaliery, A. flavus, A. japonicus, A. niger*, etc.) [6,9,75-77]; however, a large number of them were isolated from the air of the studied repositories to a greater or lesser extent, evidencing the risk they cause to the staff's health. There are species that can grow on materials with low a_w because they are xerophilic or xerotolerant [78], it should be noted that a xerophilic species are capable of growing at $a_w \leq 0.85$. Though xerotolerance is not related to the species pathogenicity, these two conditions have coincided in some of them [75].

Of these species, some are considered within Biosafety Level (BSL or BL) 1 such is the case of some *Cladosporium* species that rarely cause infections in humans [78], so they are considered opportunistic pathogens [79], while others can be included in BSL-2 or BSL-3 [78].

Among the species detected in the studied repositories environment, 15 were found to be xerotolerant and were *A. flavus, A. niger, A. ochraceus, A. oryzae, A. penicillioides, A. tamarii, A. terreus, A. ustus, A. versicolor, Cl. cladosporioides, Cl. sphaerospermum, P. chrysogenum, P. citrinum, P. oxalicum*, and *Talaromyces* sp. Of these, only *A. flavus* is cataloged with BSL-2 for being a pathogenic species [76-78], while remaining of the 14 species were categorized with BSL-1 [78] despite being opportunistic pathogens [9,75,78]; but the frequency of health damage by *A. flavus* is higher than the rest of the species detected [76]. Although *A. niger* was isolated to a lesser extent and at lower concentrations than *A. flavus*, it should be noted that this species in addition to being xerotolerant is also thermotolerant [80], which could have a significant impact on health in situations of important of the environmental temperature increases as can happen in the case of CC. This evidences the risk to which personnel are exposed in a circumstantial way, since *A. flavus* was the dominant species within the *Aspergillus* genus.

If one takes into account that with CC many characteristics of environmental fungi will be modified or enhanced [17] then it is important to take these aspects into account to establish mitigation and resilience strategies in Cuban archives with a view to preserving both their documentary heritage such as the staff's health.

It should be noted that these results allowed the administration of the PHA SC to make efforts in the search for another more adequate building that allows it to better preserve its documentary collections.

At present, this process has already been resolved with the help of the provincial government and they are focused on the culmination of the constructive adjustments to soon start the movement of documents. This will not only improve the conservation conditions of the collections but also the environmental quality of the staff work areas.

5. Conclusions

This paper summarizes four key aspects obtained from the study of the naturally ventilated repositories in the PHA SC related to 1) the diversity of airborne fungi isolated from the indoor of these environments, 2) the environmental mycological quality of the repositories studied, 3) the isolated species behavior and 4) the potential risk that these environments represent for the personnel´s health. The conclusions are potted below:

- This first study performed in environments of different repositories of the PHA SC showed that the mycological quality of these environments varied over time as a consequence of the lack of systematicity in the correct management of the natural ventilation by conservators. Despite this, it was evidenced that the species number detected was slightly higher than those discovered in the outdoor environment, suggesting the existence of an internal source of contamination that could be risky for the documents kept in these repositories. Sørensen's coefficient of similarity indicated a moderate interchange between the indoor and outdoor environments. In addition, the I/O ratios for most of the common species proved that these species came from outdoor air and did not represent important pollutants from premise indoor.
- *Aspergillus* and *Cladosporium* were found to be predominant genera and ecologically abundant, while *Penicillium* was found to be a common genus.
- The *Coremiella* and *Talaromyces* genera, as well as the species *Aspergillus uvarum*, *Alternaria ricini*, *Cladosporium staurophorum* and *Fusarium xylaroides*, turned out to be new findings for the Cuban archives, despite the fact that most of these taxa did not show a significant ecological impact.
- Xerophilic species such as *A. flavus, A. niger, A. nidulans, A. ochraceus, A. terreus* and *A. ustus* were indicators of moisture problems in the repositories, evidencing the potential risk that this situation represents for the conservation of the documentary heritage that this archive treasures.
- Some species that have been reported as opportunistic and toxigenic pathogens (*A. flavus, A. niger, A. ochraceus, A. oryzae, A. ustus, A. versicolor*) were detected in concentrations higher than those recommended. It was also shown that most of the isolated environmental species correspond to the Biosafety Level (BSL) 1, and that only *A. flavus* is cataloged with BSL-2 for being a pathogenic species. These aspects, together with the exposure level of the personnel during the working day to the studied environments, showing that there is a potential risk to health and that the personnel is circumstantially exposed to biological risk.

Author Contributions

Sofia Borrego directed the project, conceptualized the research and the methodology to be used, participated in the analysis of results and data, in the writing, review and

editing of the manuscript, as well as in the final version approval of the manuscript to submit.

Alian Molina contributed to the experiments design, performed all the mycological experiments, participated in the data analysis, wrote the first version of the manuscript, and gave final approval of the version to be submitted.

Yuneisis Bonne participated in the experiments design, calibrated and weekly placed the continuous measurement instruments of T and RH in the analyzed repositories, weekly extracted the data of T and RH from the instruments and placed them in the database created for this purpose, facilitated the sketch of the PHA SC, participated in the realization of some figures and in the reviewed of the written manuscript.

Anyilena González participated in the experiments design, performed the statistical processing of the T and RH data and their graphing, participated in the revision of the written manuscript.

Lidiersy Méndez participated in the experiments design, monitored the building constructive conditions and performed the daily management of the repositories, participated in the creation of some tables and figures and in the critical review of the significant intellectual content, and gave the final approval of the version to submit.

Conflict of Interest

The authors declare that they have no competing financial interests or personal relationships that could have negatively influenced the work reported in this document. They also declare that they have no conflict of interest.

Funding

This research project was financially supported by the Ministry of Science, Technology and Environment (CITMA) of Cuba (Grant number I-2118025001).

Acknowledgements

The authors want to thank to Dr. Matilde Anaya for the help provided in the statistical processing of data.

References

[1] Pinzari, F., 2011. Microbial ecology of indoor environments: The ecological and applied aspects of microbial contamination in archives, libraries and conservation environments. In Sick building syndrome in public buildings and workplaces; Abdul-Wahab, SA., Ed.; Springer-Verlag Heidelberg: Berlin, Germany. pp. 153-178.
DOI: https://doi.org/10.1007/978-3-642-17919-8_9

[2] Michaelsen, A., Pinzari, F., Ripka, K., et al., 2006. Application of molecular techniques for identification of fungal communities colonising paper material. International Biodeterioration and Biodegradation. 58, 133-141.
DOI: https://doi.org/10.1016/j.ibiod.2006.06.019

[3] Awad, A.H.A., Saeed, Y., Shakour, A.A., et al., 2020. Indoor air fungal pollution of a historical museum, Egypt: A case study. Aerobiologia. 36, 197-209.
DOI: https://doi.org/10.1007/s10453-019-09623-w

[4] Pinheiro, A.C., Sequeira, S.O., Macedo, M.F., 2019. Fungi in archives, libraries, and museums: A review on paper conservation and human health. Critical Reviews in Microbiology. 45(5-6), 686-700.
DOI: https://doi.org/10.1080/1040841X.2019.1690420

[5] Sequeira, S.O., Paiva de Carvalho, H., Mesquita, N., et al., 2019. Fungal stains on paper: is what you see what you get? Conservar Património. 32, 8-27.
DOI: https://doi.org/10.14568/cp2018007

[6] Haleem-Khan, A.A., Mohan-Karuppayil, S., 2012. Fungal pollution of indoor environments and its management. Saudi Journal of Biological Sciences. 19, 405-426.
DOI: http://dx.doi.org/10.1016/j.sjbs.2012.06.002

[7] Twaroch, T.E., Curin, M., Valenta, R., et al., 2015. Mold allergens in respiratory allergy: From structure to therapy. Allergy, Asthma and Immunology Research. 7(3), 205-220.
DOI: http://dx.doi.org/10.4168/aair.2015.7.3.205

[8] Nayak, A.P., Green, B.J., Beezhold, D.H., 2013. Fungal hemolysins. Medical Mycology. 51, 1-16.
DOI: https://doi.org/10.3109/13693786.2012.698025

[9] Aboul-Nasr, M.B., Zohri, A.N.A., Amer, E.M., 2013. Enzymatic and toxigenic ability of opportunistic fungi contaminating intensive care units and operation rooms at Assiut University Hospitals, Egypt. Springer Plus. 2, 347.
DOI: https://doi.org/10.1186/2193-1801-2-347

[10] Oetari, A., Susetyo-Salim, T., Sjamsuridzal, W., et al. 2016. Occurrence of fungi on deteriorated old dluwang manuscripts from Indonesia. International Biodeterioration and Biodegradation. 114, 94-103.
DOI: http://dx.doi.org/10.1016/j.ibiod.2016.05.025

[11] Borrego S, Molina A, Santana A. 2017. Fungi in archive repositories environments and the deterioration of the graphics documents. EC Microbiology, 11(5), 205-226. https://www.researchgate.net/publication/319713307_Fungi_in_Archive_Repositories_Environments_and_the_Deterioration_of_the_Graphics_Documents.

[12] Borrego, S., Molina, A., 2020. Behavior of the cultivable airborne mycobiota in air-conditioned environ-

ments of three Havanan archives, Cuba. Journal of Atmospheric Science Research. 3(1), 16-28. DOI: https://doi.org/10.30564/jasr.v3i1.1910

[13] Mallo AC, Nitiu DS, Elíades LA, Saparrat MCN. 2017. Fungal degradation of cellulosic materials used as support for cultural heritage. International Journal of Conservation Science, 8(4), 619-632. http://www.ijcs.uaic.ro/public/IJCS-17-59_Mallo.pdf.

[14] Fröhlich-Nowoisky, J., Kampf, C.J., Weber, B., et al., 2016. Bioaerosols in the Earth system: Climate, health, and ecosystem interactions. Atmospheric Research. 182, 346-376. DOI: https://doi.org/10.1016/j.atmosres.2016.07.018

[15] De Nuntiis, P., Palla, F., 2017. Bioaerosols. In Biotechnology and conservation of cultural heritage; Palla, F., Barresi, G., Eds.; Springer International Publishing: Switzerland. pp. 31-48. DOI: https://doi.org/10.1007/978-3-319-46168-7_2

[16] Vardoulakis, S., Dimitroulopoulou, C., Thornes, J., et al., 2015. Impact of climate change on the domestic indoor environment and associated health risks in the UK. Environment International. 85, 299-313. DOI: https://doi.org/10.1016/j.envint.2015.09.010

[17] Panackal, A.A., 2011. Global climate change and infectious diseases: Invasive mycoses. Journal of Earth Science & Climatic Change. 1, 108. DOI: https://doi.org/10.4172/2157-7617.1000108

[18] Anaf, W., Leyva, D., Schalm, O., 2018. Standardized indoor air quality assessments as a tool to prepare heritage guardians for changing preservation conditions due to Climate Change. Geosciences. 8, 276. DOI: https://doi.org/10.3390/geosciences8080276

[19] Borrego, S., Perdomo, I., 2016. Airborne microorganisms cultivable on naturally ventilated document repositories of the National Archive of Cuba. Environmental Science and Pollution Research. 23(4), 3747-3757. DOI: https://doi.org/10.1007/s11356-015-5585-1

[20] Borrego S, Molina A. 2018. Determination of viable allergenic fungi in the documents repository environment of the National Archive of Cuba. Austin Journal of Public Health and Epidemiology, 5(3), 1077. https://austinpublishinggroup.com/public-health-epidemiology/fulltext/ajphe-v5-id1077.php.

[21] Viegas, C., Pinheiro, A.C., Sabino, R., et al., 2015. Environmental mycology in public health: Fungi and mycotoxins risk assessment and management, 1st ed.; Academic Press: Cambridge, Massachusetts, UK.

[22] Sánchis, J., 2002. Los nueve parámetros más críticos en el muestreo microbiológico del aire. Revista Técnicas de Laboratorio, 24(276), 858-862. https://www.microkit.es/publicaciones/12-publi%20parametros%20criticos%20en%20control%20ambiental.pdf.

[23] Sánchez, K.C., Almaguer, M., Pérez, I., et al., 2019. Diversidad fúngica en la atmósfera de La Habana (Cuba) durante tres períodos poco lluviosos. Revista Internacional de Contaminación Ambiental. 35, 137-150. DOI: http://dx.doi.org/10.20937/RICA.2019.35.01.10

[24] Barnett, H.L., Hunter, B.B., 1998. Illustrated genera of imperfect fungi, 4th ed.; APS Press: Minneapolis, USA.

[25] Domsch, K.H., Gams, W., Anders, T.H., (Eds.), 1980. Compendium of soil fungi. Academic Press LTD: London, UK.

[26] Klich, M.A., Pitt, J.I., 1994. A laboratory guide to common *Aspergillus* species and their teleomorphs. CSIRO, Division of Food Processing: Australia.

[27] Pitt, J.I., 2000. A laboratory guide to common *Penicillium* species, 3rd ed.; Food Science Australia: Australia.

[28] Simões, M.F., Santos, C., Lima, N., 2013. Structural diversity of *Aspergillus* (section *Nigri*) spores. Microscopy and Microanalysis. 19(5), 1151-1158. DOI: https://doi.org/10.1017/S1431927613001712

[29] Samson, R.A., Noonim, P., Meijer, M., et al., 2007. Diagnostic tools to identify black aspergilla. Study in Mycology. 59, 129-145. DOI: https://doi.org/10.3114/sim.2007.59.13

[30] Visagie, C.M., Houbraken, J., Frisvad, J.C., et al., 2014. Identification and nomenclature of the genus *Penicillium*. Study in Mycology. 78, 343-371. DOI: https://doi.org/10.1016/j.simyco.2014.09.001

[31] Chen, A.J., Hubka, V., Frisvad, J.C., et al., 2017. Polyphasic taxonomy of *Aspergillus* section *Aspergillus* (formerly *Eurotium*), and its occurrence in indoor environments and food. Studies in Mycology. 88, 37-135. DOI: https://doi.org/10.1016/j.simyco.2017.07.001

[32] Ellis, M.B., 1971. Dematiaceous hyphomycetes. Commonwealth Mycological Institute: England.

[33] Ellis, M.B., 1976. More Dematiaceous hyphomycetes. Commonwealth Mycological Institute: England.

[34] Bensch, K., Groenewald, J.Z., Dijksterhuis, J., et al., 2010. Species and ecological diversity within the *Cladosporium cladosporioides* complex (Davidiellaceae, Capnodiales). Studies in Mycology. 67, 1-94. DOI: https://doi.org/10.3114/sim.2010.67.01

[35] Bensch, K., Groenewald, J.Z., Meijer, M., et al.,

2018. *Cladosporium* species in indoor environments. Studies in Mycology. 89, 177-301.
DOI: https://doi.org/10.1016/j.simyco.2018.03.002

[36] Smith, G., 1980. Ecology and field biology. 2nd ed.; Harper & Row: New York, USA.

[37] Esquivel, P.P., Mangiaterra, M., Giusiano, G., et al., 2003. Microhongos anemófilos en ambientes abiertos de dos ciudades del nordeste argentino. Boletín Micológico. 18, 21-28.
DOI: https://doi.org/10.22370/bolmicol.2003.18.0.376

[38] Moreno, C.E., 2001. Métodos para medir la biodiversidad. M&T-Manuales y Tesis SEA: Zaragoza, España.

[39] González OF, Arango ED, Moreno B, Leyva M, Berenguer Y. (2021). Comportamiento de la actividad sísmica anómala iniciada el 17 de enero de 2016 al sur de Santiago de Cuba. Minería y Geología, 37(2), 130-145. https://www.redalyc.org/journal/2235/223568255001/html/.

[40] Weather Atlas, 2021. Previsión meteorológica y clima mensual Santiago de Cuba, Cuba. https://www.weather-atlas.com/es/cuba/santiago-de-cuba-clima.

[41] Karbowska-Berent, J., Górny, R.L., Strzelczyk, A.B., et al., 2011. Airborne and dust borne microorganisms in selected Polish libraries and archives. Building and Environment. 46, 1872-1879.
DOI: https://doi.org/10.1016/j.buildenv.2011.03.007

[42] Yang, C., Pakpour, S., Klironomos, J., et al., 2016. Microfungi in indoor environments: What is known and what is not. In Biology of microfungi, fungal biology; Li, D-W., Ed.; Springer International Publishing: Switzerland. pp. 373-412.
DOI: https://doi.org/10.1007/978-3-319-29137-6_15

[43] Pinheiro, A.C., 2014. Fungal communities in archives: Assessment strategies and impact on paper conservation and human health. PhD Thesis. Universidad de Nova de Lisboa: Portugal. https://run.unl.pt/bitstream/10362/14890/1/Pinheiro_2014.pdf.

[44] Kalyoncu, F., 2010. Relationship between airborne fungal allergens and meteorological factors in Manisa City, Turkey. Environmental Monitoring and Assessment. 165, 553-558.
DOI: https://doi.org/10.1007/s10661-009-0966-x

[45] Resolución No. 201. Lineamientos generales para la conservación de las fuentes documentales de la República de Cuba. Ministerio de Ciencia, Tecnología y Medio Ambiente (CITMA). Gaceta Oficial no. 55, Ordinaria de 2020, Cuba. https://www.gacetaoficial.gob.cu/es/gaceta-oficial-no-55-ordinaria-de-2020.

[46] Novohradská, S., Ferling, I., Hillmann, F., 2017. Exploring virulence determinants of filamentous fungal pathogens through interactions with soil amoebae. Frontiers in Cellular and Infection Microbiology. 7, 497.
DOI: https://doi.org/10.3389/fcimb.2017.00497

[47] Díaz MJ, Gutiérrez A, González MC, Vidal G, Zaragoza RM, Calderón C. (2010). Caracterización aerobiológica de ambientes intramuro en presencia de cubiertas vegetales. Revista Internacional de Contaminación Ambiental, 26(4), 279-289. https://www.redalyc.org/pdf/370/37015993003.pdf.

[48] Elenjikamalil, S.M.R., Kelkar-Mane, V., 2019. Seasonal variations in the aerobiological parameters of a state archival repository in India. World Journal of Pharmaceutical Research. 8(5), 1459-1474.
DOI: https://doi.org/10.20959/wjpr20195-14734

[49] Fekadu, S., Melaku, A., 2014. Microbiological quality of indoor air in university libraries. Asian Pacific Journal of Tropical Biomedicine. 4(Suppl 1), S312-S317.
DOI: https://doi.org/10.12980/APJTB.4.2014C807

[50] Osman ME, Abdel Hameed AA, Ibrahim HY, Yousef F, Abo Elnasr AA, Saeed Y. (2017). Air microbial contamination and factors affecting its occurrence in certain book libraries in Egypt. Egyptian Journal of Botany, 57, 93-118. https://journals.ekb.eg/article_3328_c2a38d2c1a72028eee89d3fe9ae159cf.pdf.

[51] Rodríguez JC, Rodríguez B, Borrego SF. (2014). Evaluación de la calidad micológica ambiental del depósito de fondos documentales del Museo Nacional de la Música de Cuba en época de lluvia. AUGMDOMUS, 6, 123-146. https://revistas.unlp.edu.ar/domus/article/view/867/1277.

[52] Borrego, S., Molina, A., Abrante, T., 2020. Sampling and characterization of the environmental fungi in the Provincial Historic Archive of Pinar del Río, Cuba. Journal of Biomedical Research & Environmental Sciences. 1(8), 404-420.
DOI: https://dx.doi.org/10.37871/jbres1172

[53] Borrego S, Molina A, Castro M. (2021). Assessment of the airborne fungal communities in repositories of the Cuban Office of the Industrial Property: Their influence in the documentary heritage conservation and the personnel's health. Revista Cubana de Ciencias Biológicas, 9(1), 1-18. http://www.rccb.uh.cu/index.php/RCCB/article/view/312/388.

[54] Leite-Jr, D.P., Pereira, R.S., Almeida, W.S., et al., 2018. Indoor air mycological survey and occupational exposure in libraries in Mato Grosso-Central Region-Brazil. Advances in Microbiology. 8, 324-353.
DOI: https://doi.org/10.4236/aim.2018.84022

[55] Savković, Ž., Stupar, M., Unković, N., et al., 2021. Diversity and seasonal dynamics of culturable airborne fungi in a cultural heritage conservation facility. International Biodeterioration and Biodegradation. 157, 105-163.
DOI: https://doi.org/10.1016/j.ibiod.2020.105163

[56] Mallo AC, Nitiu DS, Elíades LA, García M, Saparrat MCN. (2020). Análisis de la carga fúngica en el aire de la sala "Fragmentos de Historia a Orillas del Nilo" y del exterior del Museo de La Plata, Argentina. Ge-conservación, 17, 33-46.
https://www.ge-iic.com/ojs/index.php/revista/article/view/680/933.

[57] Pyrri, I., Tripyla, E., Zalachori, A., et al., 2020. Fungal contaminants of indoor air in the National Library of Greece. Aerobiologia. 36, 387-400.
DOI: https://doi.org/10.1007/s10453-020-09640-0

[58] Stryjakowska-Sekulska M, Piotraszewska-Pająk A, Szyszka A, Nowicki M, Filipiak M. (2007). Microbiological quality of indoor air in University rooms. Polish Journal of Environmental Studies, 16(4), 623-632. http://www.pjoes.com/Microbiological-Quality-of-Indoor-Air-r-nin-University-Rooms,88030,0,2.html.

[59] de Aquino Neto, F.R., de Goes Siqueira, L.F., 2000. Guidelines for indoor air quality in offices in Brazil. Proceedings of Healthy Buildings. 4, 549-554.

[60] Sabariego S, Díaz de la Guardia C, Sánchez FA. (2004). Estudio aerobiológico de los conidios de Alternaria y Cladosporium en la atmósfera de la ciudad de Almería (SE de España). Revista Iberoamericana de Micología, 21, 121-127. https://1library.co/document/y8pk5w5z-estudio-aerobiologico-de-los-conidios-de-alternaria-y-cladosporium-en-la-atmosfera-de-la-ciudad-de-almeria-se-de-espana.html.

[61] Borrego, S., Lavin, P., Perdomo, I., et al., 2012. Determination of indoor air quality in archives and the biodeterioration of the documentary heritage. ISRN Microbiology.
DOI: https://doi.org/10.5402/2012/680598

[62] Almaguer M, Rojas TI. (2013). Aeromicota viable de la atmósfera de La Habana, Cuba. Nova Acta Científica Compostelana (Bioloxía), 20, 35-45. https://revistas.usc.gal/index.php/nacc/article/view/1404.

[63] Kadaifciler, D.G., 2017. Bioaerosol assessment in the library of Istanbul University and fungal flora associated with paper deterioration. Aerobiologia. 33, 151-166.
DOI: https://doi.org/10.1007/s10453-016-9457-z

[64] Yang, C.S., Li, D.W., 2007. Ecology of fungi in the indoor environment. In Sampling and analysis of indoor microorganisms; Yang, CS., Heinsohn PA., Eds.; Jhon Wiley & Sons, Inc.: New Jersey, USA. pp. 191-214.
DOI: https://doi.org/10.1002/9780470112434.ch10

[65] Cepeda, R., Luque, L., Ramírez, D., et al., 2019. Monitoreo de hongos ambientales en laboratorios y reservas patrimoniales bioarqueológicas. Boletín Micológico. 34(2), 33-49.
DOI: http://dx.doi.org/10.22370/bolmicol.2019.34.2.1909

[66] Heredia, G., Arias-Mota, R.M., Mena-Portales, J., et al., 2018. Saprophytic synnematous microfungi. New records and known species for Mexico. Revista Mexicana de Biodiversidad. 89, 604-618.
DOI: https://doi.org/10.22201/ib.20078706e.2018.3.2352

[67] Borrego S, Guiamet P, Vivar I, Battistoni P. (2018). Fungi involved in biodeterioration of documents in paper and effect on substrate. Acta Microscopica, 27, 37- 44. https://acta-microscopica.org/acta/article/download/112/33.

[68] Karakasidou, K., Nikolouli, K., Amoutzias, G.D., et al., 2018. Microbial diversity in biodeteriorated Greek historical documents dating back to the 19th and 20th century: a case study. Microbiology Open. e596.
DOI: https://doi.org/10.1002/mbo3.596

[69] Adelantado, C., Bello, C., Borrell, A., et al., 2005. Evaluation of the antifungal activity of products used for disinfecting documents on paper in archives. Restaurator. 26, 235-238.
DOI: https://doi.org/10.1515/REST.2005.235

[70] Kraková, L., Šoltys, K., Otlewska, A., et al., 2018. Comparison of methods for identification of microbial communities in book collections: Culture-dependent (sequencing and MALDI-TOF MS) and culture-independent (IlluminaMiSeq). International Biodeterioration and Biodegradation. 131, 51-59.
DOI: https://doi.org/10.1016/j.ibiod.2017.02.015

[71] Rojas, T.I., Aira, M.J., Batista, A., et al., 2012. Fungal biodeterioration in historic buildings of Havana (Cuba). Grana. 51, 44-51.
DOI: https://doi.org/10.1080/00173134.2011.643920

[72] Borrego, S., Molina, A., 2019. Fungal assessment on storerooms indoor environment in the National Museum of Fine Arts, Cuba. Air Quality, Atmosphere & Health. 12, 1373-1385.
DOI: https://doi.org/10.1007/s11869-019-00765-x

[73] Almaguer M, Sánchez KC, Rojas TI. (2017). Dinámica de conidióforos de Zygosporium en la atmósfera de La Habana, Cuba. Revista Cubana de Ciencias Biológicas, 5, 1-7. http://www.rccb.uh.cu/index.php/RCCB/article/view/189/299.

[74] Guild, S., MacDonald, M., 2004. Mould prevention and collection recovery: Guidelines for heritage collections. Technical Bulletin No 26. Canada: Canadian Conservation Institute (CCI). https://www.cci-icc.gc.ca/resources-ressources/publications/downloads/technicalbulletins/eng/TB26-MouldPrevention.pdf.

[75] de Hoog, G.S., Guarro, G., Gene, J., et al., 2000. Atlas of clinical fungi, 2nd ed.; Centraalbureau voor Schimmelcultures (CBS): The Netherlands.

[76] Hedayati, M.T., Pasqualotto, A.C., Warn, P.A., et al., 2007. *Aspergillus flavus*: Human pathogen, allergen and mycotoxin producer. Microbiology. 153, 1677-1692.
DOI: https://doi.org/10.1099/mic.0.2007/007641-0

[77] Rudramurthy, S.M., Paul, R.A., Chakrabarti, A., et al., 2019. Invasive aspergillosis by *Aspergillus flavus*: Epidemiology, diagnosis, antifungal resistance, and management. Journal of Fungi. 5(3), 55.
DOI: https://doi.org/10.3390/jof5030055

[78] de Hoog, G.S., Zalar, P., van den Ende, B.G., et al., 2005. Relation of halotolerance to human-pathogenicity in the fungal tree of life: An overview of ecology and evolution under stress. In Adaptation to life at high salt concentrations in archaea, bacteria, and eukarya; Gunde-Cimerman, N., Oren, A., Plemenitaš A. Eds.; Springer: The Netherlands. pp. 373-395.

[79] Pérez I, Sánchez KC. (2019). Aspectos fisiológicos del género Cladosporium desde la perspectiva de sus atributos patogénicos, fitopatogénicos y biodeteriorantes. Revista Cubana de Ciencias Biológicas, 7, 1-10. http://www.rccb.uh.cu/index.php/RCCB/article/view/255/331.

[80] Krijgsheld, P., Altelaar, A.M., Post, H., et al., 2012. Spatially resolving the secretome within the mycelium of the cell factory *Aspergillus niger*. Journal of Proteome Research. 11(5), 2807-2818.
DOI: https://doi.org/10.1021/pr201157b

BILINGUAL PUBLISHING CO.
Pioneer of Global Academics Since 1984

Journal of Atmospheric Science Research
https://ojs.bilpublishing.com/index.php/jasr

ARTICLE

History and Projection of Hydrological Droughts in the Benin Basin of the Niger River (Benin)

Yarou Halissou[1,4*] Alamou Adéchina Eric[2,4] Biao Iboukoun Eliézer[3,4] Obada Ezéchiel[2,4] Tore Daniel Bio[2,4] Afouda Abel[5,6]

1. International Chair of Mathematical Physics and Applications (ICMPA-UNESCO CHAIRE), University of Abomey-Calavi (UAC), Cotonou, Benin
2. National School of Public Works (ENSTP), National University of Sciences, Technologies, Engineering and Mathematics (UNSTIM), Abomey, Benin
3. National School of Mathematical Engineering and Modeling (ENSGMM), National University of Sciences, Technologies, Engineering and Mathematics (UNSTIM), Abomey, Benin
4. Laboratory of Environmental Geoscience and Application (LaGEA/UNSTIM), Benin
5. Applied Hydrology Laboratory (LHA), University of Abomey-Calavi (UAC), Cotonou, BP, 4521, Benin
6. West African Science Service Center on Climate Change and Adapted Land Use (WASCAL), GRP Climate Change and Water Resources, University of Abomey-Calavi (UAC), Abomey-Calavi, BP, 2008, Benin

ARTICLE INFO

Article history
Received: 2 April 2022
Revised: 5 May 2022
Accepted: 13 May 2022
Published: 20 May 2022

Keywords:
Hydrological
Drought
SDI
Beninese Niger river basin

ABSTRACT

In the context of a changing climate, the Beninese Niger River basin has been the focus of several research studies for the quantification, planning, and modeling of water and related resources for sustainable use. This research aims to characterize the historical (1976-2019) and projected (2021-2050) hydrological drought of the Beninese Niger River basin. The study used daily observations of rainfall, maximum and minimum temperatures, runoff rates and simulations of HIRHAM and REMO RCMs from fifteen (15) rainfall stations installed around the basin. It uses standardized streamflow indices (SDI) at 12-month and 36-month time steps. The results show that the calculated SDI indices show, on average, for all the model scenarios used, chronological trends of increase. These increases are not significant (are of the order of 0.00001 per year). The analysis of the SDI indices shows that, on average, the hydrological droughts in the Beninese basin of the Niger River will increase at 36 months and decrease at 12 months of the SDI. In fact, these small variations of hydrological droughts will be accompanied by the increase of their duration and the decrease of their magnitudes. The droughts detected in the Benin basin of the Niger River during the historical period will continue until 2050 in the same range but with more extended drought lengths. It should be noted that most of the changes observed in the calculated and analyzed indices are not significant.

*Corresponding Author:
Yarou Halissou,
International Chair of Mathematical Physics and Applications (ICMPA-UNESCO CHAIRE), University of Abomey-Calavi (UAC), Cotonou, Benin; Laboratory of Environmental Geoscience and Application (LaGEA/UNSTIM), Benin;
Email: halissou.yarou@gmail.com

DOI: https://doi.org/10.30564/jasr.v5i2.4602

1. Introduction

The impacts of climate change and anthropogenic activities on water resources predicted by climatologists for the rest of the 21st century deserve special attention from mankind. The challenges of monitoring water resources, and in particular the anticipation of scarcity situations, nowadays require the implementation of specific operational hydrological applications, in the same way as those developed in recent years for flood forecasting [1].

Extreme weather events usually have large impacts on society, water resources, health, and the agricultural sector [2]. A small change in average conditions can likely cause large changes for an extreme [2]. A better understanding of the statistical and physical nature of extreme climate events is a necessary step before we can answer questions that are related to these indices. It is important to note that each dry year involves significant socioeconomic losses and ecological damage worldwide [3]. Similarly, a very wet year results in socio-economic losses and damages.

The general problem of climate change is that, under projected climate scenarios, it would result in a higher frequency and intensity of extreme weather events [4]. These phenomena are even more accentuated in Africa where deforestation is very important [5]. The ministerial summit held in South Africa in 2007, which brought together 70 nations, recognized the magnitude of the drought problem and its impacts on food security and the sustainability of water resources, and emphasized the need for early warning systems for drought [6].

The industrial revolution is to promote the impact of human activities on the environment that is becoming increasingly important, altering the climatic balance and thus having effects on precipitation. This phenomenon leads to drought. Drought is a normal and frequent feature of the climate. There are several types of drought [7]. Drought is defined from the meteorological, hydrological, agricultural or socio-economic point of view [8]. Drought does not have a universal definition. There are as many definitions of drought as there are water uses [7,9]. Hydrological drought is a decrease in water supply in streams, surface reservoirs, and groundwater. Hydrological drought is caused by a lack of precipitation accompanied by massive evaporation [10]. However, non-meteorological factors, such as water demand, availability of surface reservoirs, and artesian well drilling, compound the effect.

Since the second half of the 20th century, West Africa has been the region of the world with the largest rainfall deficit [11]. In Nigeria for example, a decreasing trend was observed in 98.2% of the landscape for the moisture index (MI), 96.7% for the SPI and 98.2% for the SPEI, showing drying trends in the country [12]. Similarly in Niger, consecutive dry days have significantly increased and consecutive wet days have decreased. The same is true for rainy days. At the same time, the proportion of daily maximum rainfall in the annual rainfall total has increased over time and the proportion of intense rainfall in the annual rainfall total has significantly increased over the last two decades [13]. For Benin it is indicated for rainfall intensity and frequency indices such as consecutive rainy days and extremely wet day, respectively an increase and decrease [14]. For Kodja [15], over the Oueme basin in Benin, there was a decreasing change in rainfall while the temperature velocity showed increasing changes for the period 1981-2010.

The Niger River has a hydrological regime that has evolved due to climate change and anthropogenic impacts. There are only a few dams on the Niger River, and future planned structures will alter its regime and flooded areas [16]. The Beninese basin of the Niger River, located in the semi-arid zone, is all the more affected as it records a significant demographic increase. This population growth intensifies the anthropic pressures on fragile resources whose degradation is increasingly worrying [17]. In order to highlight the dry sequences that have been little discussed so far in the Beninese basin of the Niger River and to assess their evolution in the near future in the said basin, the present work was interested in the study of standardized flow indices (SDI) at 12-month and 36-month intervals in the basin.

2. Methodology

2.1 Description of the Study Area and Data

The Beninese Niger River basin covers an area of approximately 48,000 km² (42% of the total area of Benin) and is located in the extreme north of Benin (Figure 1). Located between latitudes 10° and 12°30' north and longitudes 1°32' and 3°50' east, it includes the Mékrou, Alibori and Sota sub-basins, and is generally oriented SSW-NNE [18]. The implementation of this research work required the collection of several types of data. These are daily rainfall data observed from 1976 to 2019 at 15 rainfall stations (Figure 1) installed around the basin, which are collected from the Benin Meteorological Agency (Météo-Bénin); flow rate data which are extracted from the database of the Hydrology Department of the DGEau and concern the stations of Couberi and Gbassè on the Sota, Kompongou on the Mékrou and Yakin on the Alibori. These data cover the period from 1953-2017 (Couberi and Yakin), 1953-2014 (Kompongou) and 1953-2006 (Gbassè); daily temperature observations (minimum and maximum) from three (03) synoptic stations (Figure 1) were considered. These data cover the period from 1976 to 2019. These data are com-

plemented by daily observations of radiation, wind speed and humidity for the calculation of daily ETP. It should be noted that data from the regional climate models DMI-HIRHAM5 (Denmark) and MPI- REMO (Germany) that have produced good results in the area [19] are used for the future period. These RCMs (Table 1) have a resolution of 50 km each and have been forced by GCM outputs (ECHAM5 for DMI-HIRHAM5 and MPI for MPI-REMO). These models have, at the daily scale for precipitation, historical simulations over the period 1960-2005 and simulations of RCP4.5 and 8.5 scenarios over the period 2006-2100. The future period selected is 2021-2050. For the observations, the period 1990-2019 was chosen from the historical period as the reference period for assessing changes.

2.2 Method Used

2.2.1 Calculation of SDI Indices

The SDI (Streamflow Drought Index) is a drought index based on streamflow. It is developed by Nalbantis and Tsakiris [22] based on the SPI method and calculations by replacing precipitation with streamflow.

If monthly streamflows $Q_{i,j}$ of a time series are available, where i denotes the hydrological year and j denotes a month of that hydrological year ($j=1$ for October and $j=12$ for September), Vi,k can be obtained based on the equation:

$$V_{i,k} = \sum_{j=1}^{3k} Q_{i,j} \quad i = 1,2,\ldots, j = 1,2,\ldots,12 \quad k = 1,2,3,4 \qquad (1)$$

where $V_{i,k}$ is the cumulative flow rate for the i^{th} water year and k^{th} reference period, $k=1$ for October-December, $k=2$

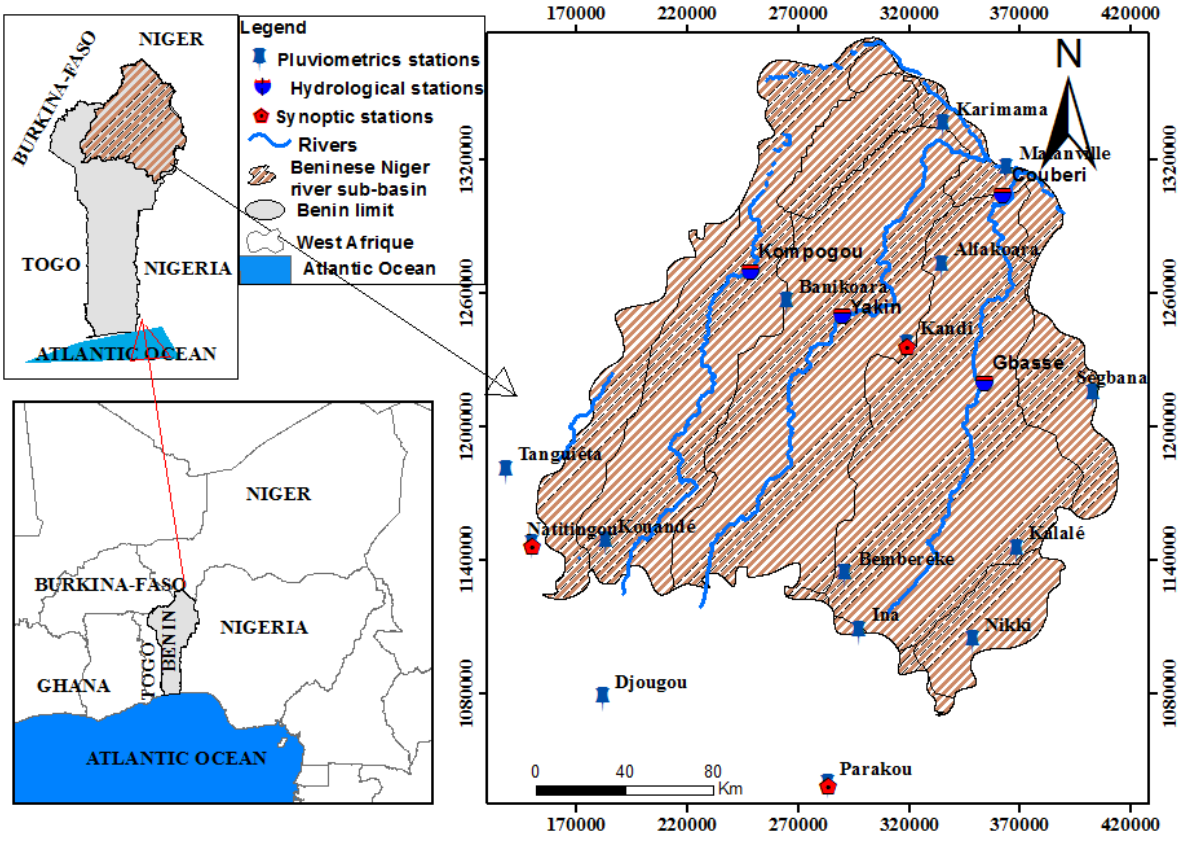

Figure 1. Location of the study stations.

Table 1. Characteristics of the regional climate models.

Model	Institution	Forcing MCG de	Horizontal resolution	Vertical level	Simulations	Reference
HIRHAM5	DMI	EC-EARTH	50 km	31	1951-2100	[20]
REMO	CSC	MPI-ESM-LR	50 km	27	1951-2100	[21]

for October-March, *k=3* for October-June and *k=4* for October-September.

Based on the cumulative flow rate, $V_{i,k}$, the flow drought index is given for each reference period *k* of the hydrological year *i* as follows:

$$SDI_{i,k} = \frac{V_{i,k} - \overline{V_k}}{S_k} \quad i = 1,2, \ldots, \quad k = 1,2,3,4 \tag{2}$$

V_k and S_k are the mean and standard deviation of the cumulative flow rates of the reference period *k* as determined for a long series.

As with the SPI, here too there are classes for the SDI. For this study, four (4) classes are considered (drought class) according to the SDI values. The values range from 1 (normal drought) to 4 (extreme drought) and are defined through the criteria in Table 2.

Table 2. SDI classes [22]

Classes	Description	Intervals
1	near-normal	–0,99≤SDI<0,99
2	Moderate drought	–1,49≤SDI<–1,0
3	Severe drought	–1,99≤SDI<–1,5
4	Extreme drought	SDI<–2,0

Considering these four drought classes, the hydrological drought risk was estimated by the following formula:

$$RS_i = \frac{F_i}{F_T} * F_{ir} \tag{3}$$

RS_i : hydrological drought risk of an event *i*
F_i: its Frequency
F_{ir}: its rank considering the 10^{th} percentile
F_T : the total frequency.

$$RS = SPN + RM + RS + RE \tag{4}$$

RS: the Risk of Hydrological Drought
$SPN = \sum RS_i$ of near-normal Hydrological Drought
$SM = \sum RS_i$ of Moderate Hydrological Drought
$SS = \sum RS_i$ Severe Hydrologic Drought
$SE = \sum RS_i$ Extreme Hydrologic Drought

2.2.2 Bias Correction

A bias correction is generally performed on climate model outputs for the majority of climate change impact studies. This correction is generally univariate and corrects each variable of interest independently of the others. There are a large number of bias correction methods. The bias correction method used in this research is called "Delta Change" (DC).

The DC method is the simplest and most widely used bias correction method [23-25] and consists of scaling the observations to obtain the corrected simulations. This is a modest method in which the parameters are typically corrected with a multiplicative or additive factor. In this method, the factor at the scale of a period is applied to each incorrect daily observation of the same period to generate the corrected daily time series [26]. Equation (5) is used to correct for temperature and Equation (6) is used to correct for precipitation.

$$x_{cor,i} = x_{o,i} + \mu_p - \mu_b \tag{5}$$

$$x_{cor,i} = x_{o,i} \times \frac{\mu_p}{\mu_b} \tag{6}$$

where $x_{cor,i}$ represents the corrected parameters; $x_{o,i}$ represents the observed parameters. μ_b and μ_p are the average of the simulated data from the base period and the average of the data from the projection period, respectively.

In the present study, the Potential Evapotranspiration is calculated by the FAO Penman-Monteith [8] formula. This formula assumes: vegetation is a well-irrigated grass covering at a height of 0.12 m, external resistance of 70 s.m^{-1} and an albedo of 0.23; daily heat flux into the soil is considered negligible in front of the net radiation at this time step (G ≈ 0); required climatic parameters: daily mean, maximum and minimum temperatures; daily mean air velocity at 2 m; daily total net radiation [27]. The formula is given by Equation (7).

$$ETP = \frac{0{,}408.\Delta.R_n.d + \gamma\left(\frac{900}{t+273}\right)v(e_w - e)}{\Delta + \gamma(1 + 0{,}34v)} \tag{7}$$

ETP: potential evapotranspiration (mm.d^{-1}), R_n*:* net radiation (W.m^{-2}), *d:* time step length in k seconds (d=0.0864 ks), *t:* daily mean air temperature at 2m (°C), Δ*:* slope of the saturating vapor pressure curve (kPa.°C^{-1}), *γ:* psychrometric constant (kPa.°C^{-1}), *e:* vapor pressure (kPa), e_w*:* saturation vapor pressure (kPa), *v:* wind speed at 2 m (m.s^{-1}).

The parameters involved in the calculation of the Penman-Monteith daily ETP come from: i) direct field measurements for t_{mean}, R_n and *v*; ii) indirect measurements for e_w and *e* and iii) physical constants: *γ*, Δ.

The use of mean temperature underestimates e_w, the following expression is preferred:

$$e_w = \frac{e_w(t_{max}) + e_w(t_{min})}{2} \tag{8}$$

e_w: saturation vapour pressure of the day (kPa); t_{max}: maximum temperature during the day (°C); t_{min}*:* minimum temperature during the day (°C)

$$e = \frac{e_w(t_{min}).\frac{Hr_{max}}{100} + e_w(t_{max}).\frac{Hr_{min}}{100}}{2} \tag{9}$$

e: actual vapor pressure of the day (kPa); $e_{w(tmax)}$: saturation vapour pressure at the maximum daily temperature (kPa); $e_{w(tmin)}$*:* saturation vapour pressure at the minimum daily temperature (kPa); Hr_{max}: maximum relative humidity (%); Hr_{min}: minimum relative humidity (%).

$$\gamma = 0{,}665.10^{-3}.P \tag{10}$$

γ in kPa.°C^{-1}

$$P = 101{,}3.\left(\frac{293-0{,}0065.z}{293}\right)^{5{,}26} \quad (11)$$

P in kPa, *z* the altitude in m.

$$\Delta = \frac{4098.\left[0{,}6108.exp\left(\frac{17{,}27.t}{t+237{,}3}\right)\right]}{(t+237{,}3)^2} \quad (12)$$

Δ and kPa.°C^{-1}, t and °C.

2.2.3 Assessment of Changes

Quantifying the effects of future changes in the extremes of daily climate variables is of great necessity to enable assessment of the vulnerability of hydrological systems to climate change.

In this study, future changes from the baseline period are evaluated using Equation (13). The 2021-2050 projection period was selected to assess changes in drought under the RCP4.5 and RCP8.5 scenarios of the REMO and HIRHAM climate models. A sub-period (1990-2019) was chosen as the reference period for assessing changes. This is to have the same length of series.

$$Change = \frac{\bar{x}_p - \bar{x}_r}{\bar{x}_r} \quad (13)$$

where $\bar{x}_p$ is the average of the hydroclimatic parameter over the considered projection period and $\bar{x}_r$ is its average over the reference period.

Student's t-test was applied on the hydrological parameters to assess the significance of the quantified changes.

2.2.4 Description of the Model Chosen for the Estimation of Flows (ModHyPMA)

The hydrological model ModHyPMA was used to model the flows of the rivers of the Beninese basin of the Niger River. It is a simple model and less constraining in terms of input data and gives good results. It does not use land use data, which makes it possible to make long-term projections. In addition, this model produces good results used on the Beninese basin of the Niger River by Gaba [28] and on the Mekrou River basin used by Obada [29]. Designed from the Least Action Principle, ModHyPMA (Hydrological Model based on the Least Action Principle) uses the principle of minimum energy expenditure. This principle can be stated as follows: "Nature always follows the simplest paths ... and the simplest paths are those that minimize nature's expenditure of energy" [30,31]. It is a physics-based, two-parameter, global hydrological model.

The ModHyPMA model includes a production function and a transfer function that are described by equations 4.49 and 4.50, respectively [31].

$$\frac{dZ(q,t)}{dt} = \Psi(q,t) \quad (14)$$

$$\frac{d(\lambda Q)}{dt} + vQ^{2v-1} = \Psi(q,t) \quad (15)$$

Equations (14) and (15) are an overall representation of the rainfall-flow transformation process. *Q* is the discharge at the watershed outlet, v is a nonlinearity parameter, λ is the basin drying coefficient, q is equal to the difference between rainfall and PTE all measured during a time *t*, and Ψ is a function. The scheme and main equations of the ModHyPMA are shown in Figure 2.

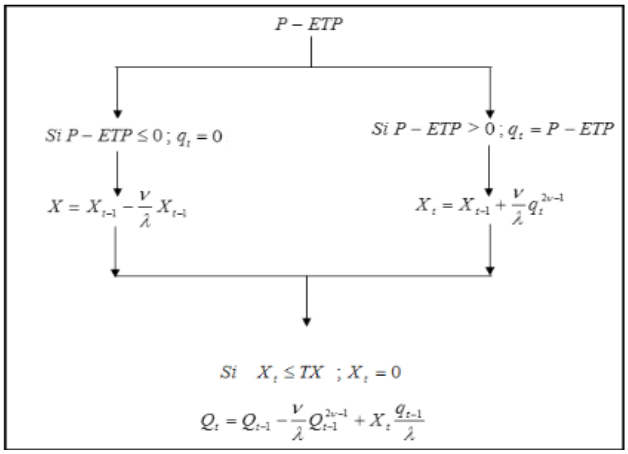

Figure 2. Schematic of the ModHyPMA model and key model equations [32,28,29].

- ✓ *Step 1:* The hydrological model ModHyPMA is calibrated for each watershed using the observed hydrological and climatic series.
- ✓ *Step 2:* The future climate series (2021-2050) are built from the observed series over a reference period of climate scenarios expressing a change in climate parameters.
- ✓ *Step 3:* The hydrological model with the parameters calculated in step 1 simulates the flows using the time series constructed in step 2.

3. Results

3.1 Analysis of the Performance of Bias Corrections on a Monthly Basis

Figures 3, 4 and 5 and Table 3 present the performance of the different results obtained from the method of corrections applied considering the annual averages of temperature and precipitation. On the one hand, these results show that the method (Delta) used to correct the data has been efficient. The table shows a large difference in the mean absolute error (MAE) between the raw data and the corrected data. The corrected data tend towards zero. On the other hand, we note that the method performs better with the temperature parameters than with the precipitation.

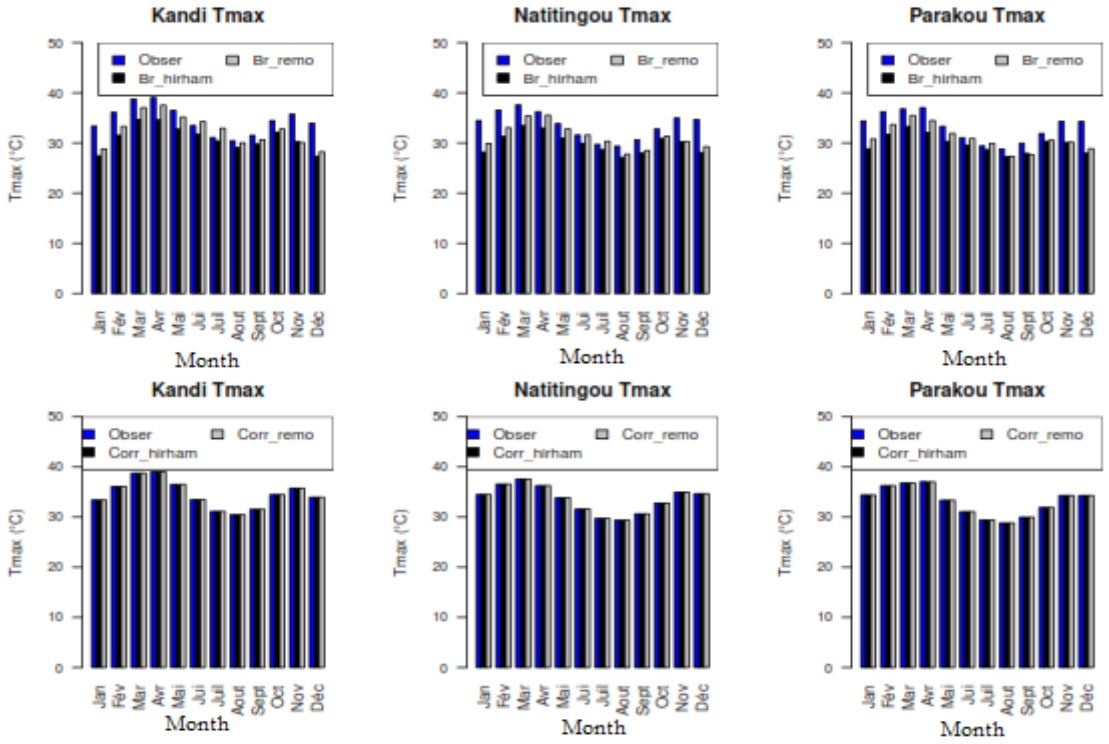

Figure 3. Performance of the correction method on annual temperature maxima (line 1 = raw data, line 2 = corrected data).

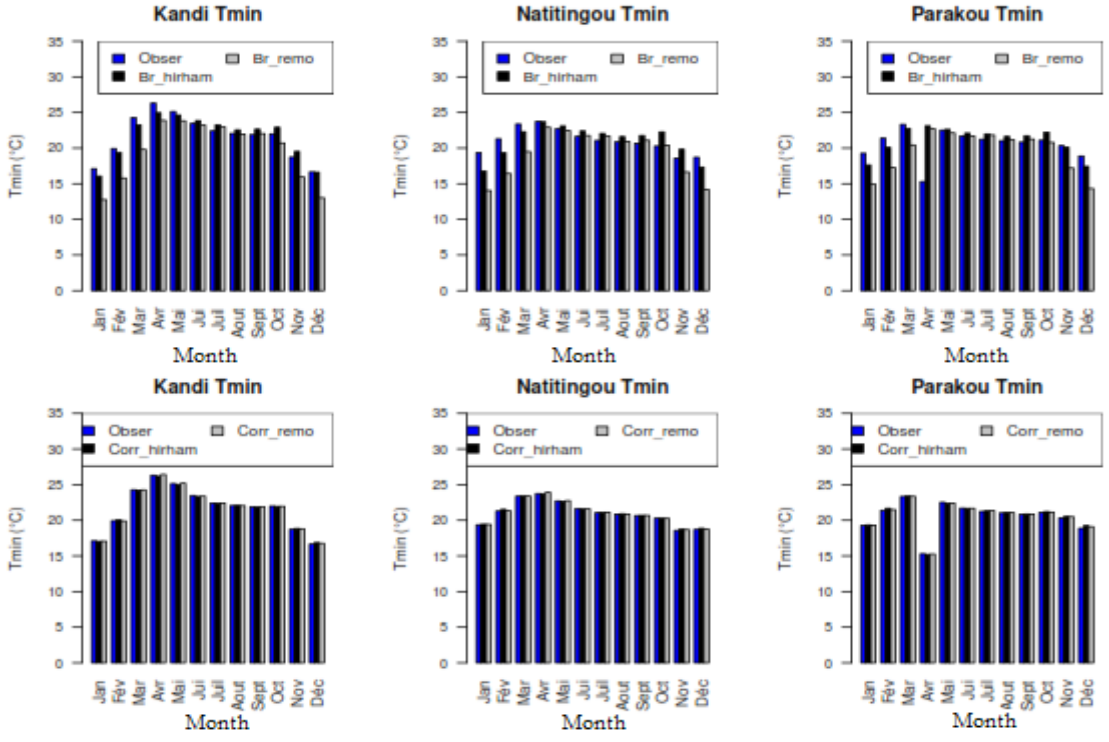

Figure 4. Performance of the correction method on annual temperature minima (line 1 = raw data, line 2 = corrected data).

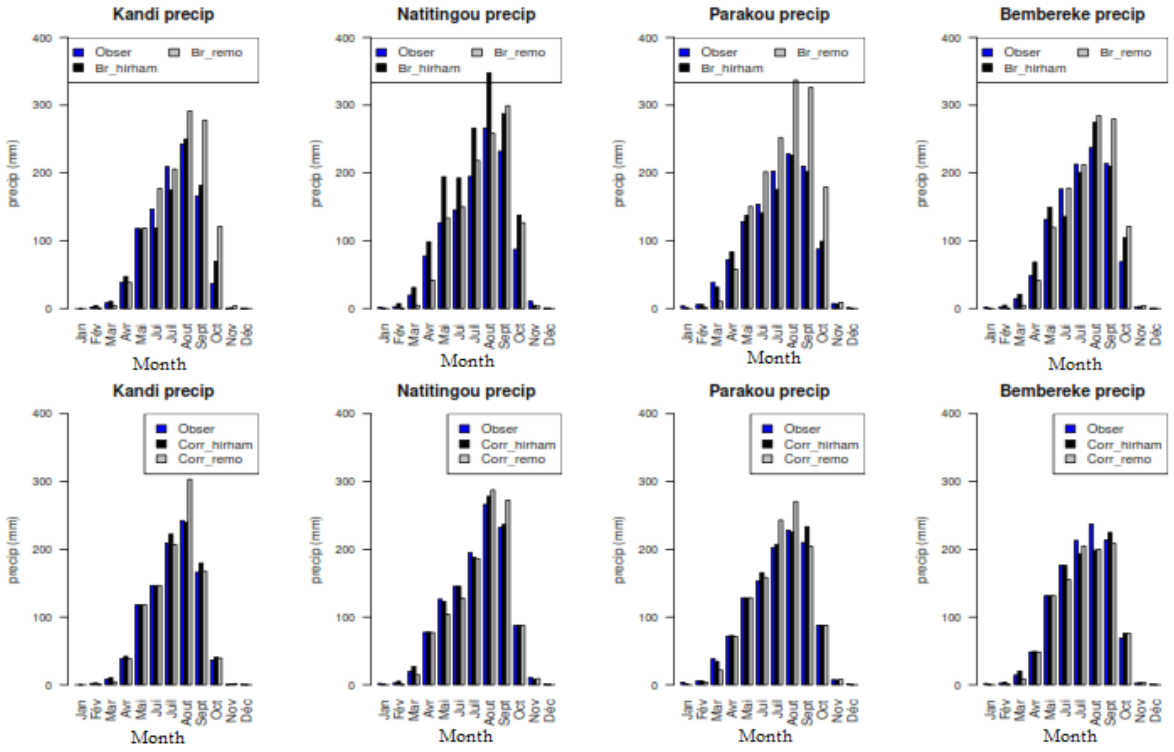

Figure 5. Performance of the correction method on annual rainfall (line 1 = raw data, line 2 = corrected data).

Table 3. Performance of the correction method on climate variables

Variables	Parameters	Station	Observation	Gross hirham	Corrected hirham	Gross remo	Corrected remo
Tmax	Deviation	Kandi	2,81	2,41	2,81	3,08	2,81
		Natitingou	2,74	2,04	2,74	2,50	2,74
		Parakou	2,88	1,85	2,87	2,56	2,87
	MAE	Kandi		3,55	0,00	2,41	0,00
		Natitingou		3,55	0,00	2,32	0,00
		Parakou		3,29	0,01	2,24	0,01
Tmin	Deviation	Kandi	3,05	3,01	2,96	4,17	3,04
		Natitingou	1,68	2,22	1,63	3,17	1,68
		Parakou	2,06	1,91	2,07	2,92	2,05
	MAE	Kandi		0,73	0,09	2,12	0,05
		Natitingou		1,19	0,08	1,91	0,05
		Parakou		1,41	0,13	2,36	0,08
Precipitation	Deviation	Kandi	90,62	86,34	92,62	112,13	101,57
		Natitingou	95,70	125,82	97,24	110,68	104,12
		Parakou	87,15	83,50	91,74	131,00	99,75
		Bembereke	95,44	96,38	89,26	111,79	88,15
	MAE	Kandi		11,06	3,37	24,19	6,26
		Natitingou		34,96	3,54	17,71	10,20
		Parakou		7,79	4,28	40,87	9,88
		Bembereke		14,92	7,19	16,91	7,49

3.2 Flow Simulation and Hydrological Model Performance

The performance of the ModHyPMA model in calibration and validation at each hydrometric station is summarized in Table 4. Figure 6 presents the values of Nash criteria and coefficients of determination (R^2) in calibration and validation for the hydrological stations used. The analysis of the table and the figure shows that during

calibration, the model responded well at all hydrological stations. Indeed, the results show Nash criteria values and coefficients of determination higher than 50% in calibration as in validation. The hydrographs of observed and simulated flows of the ModHyPMA model at each station are shown in Figure 7.

Table 4. Performance of the ModHyPMA model at each station.

		Gbasse	Couberi	Kompongou	Yakin
	Year	**1986-1990**	**1986-1989**	**1971-1974**	**1984-1987**
	X1	1,142	1,0785	1,0114	1,24
Calibration	**X2**	46,313	68,923	35,322	67,883
	R²	0,775	0,701	0,871	0,571
	Nash	0,639	0,684	0,767	0,594
	Year	**2003-2006**	**2003-2007**	**2007-2010**	**2005-2008**
	X1	1,142	1,0785	1,0114	1,24
Validation	**X2**	46,313	68,923	35,322	67,883
	R²	0,635	0,678	0,621	0,557
	Nash	0,59	0,738	0,551	0,534

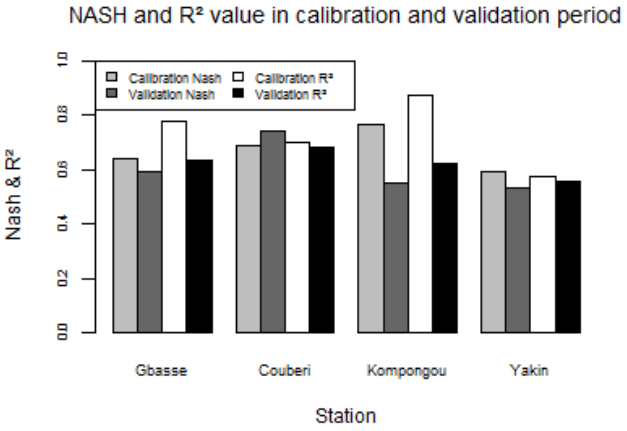

Figure 6. NASH criterion values and coefficient of determination by hydrologic station.

3.3 Analysis of Historical Hydrological Droughts

Figure 8 shows the chronological evolution of the SDI indices at each hydrological station during the period 1976-2019. From this figure, it can be seen that at the

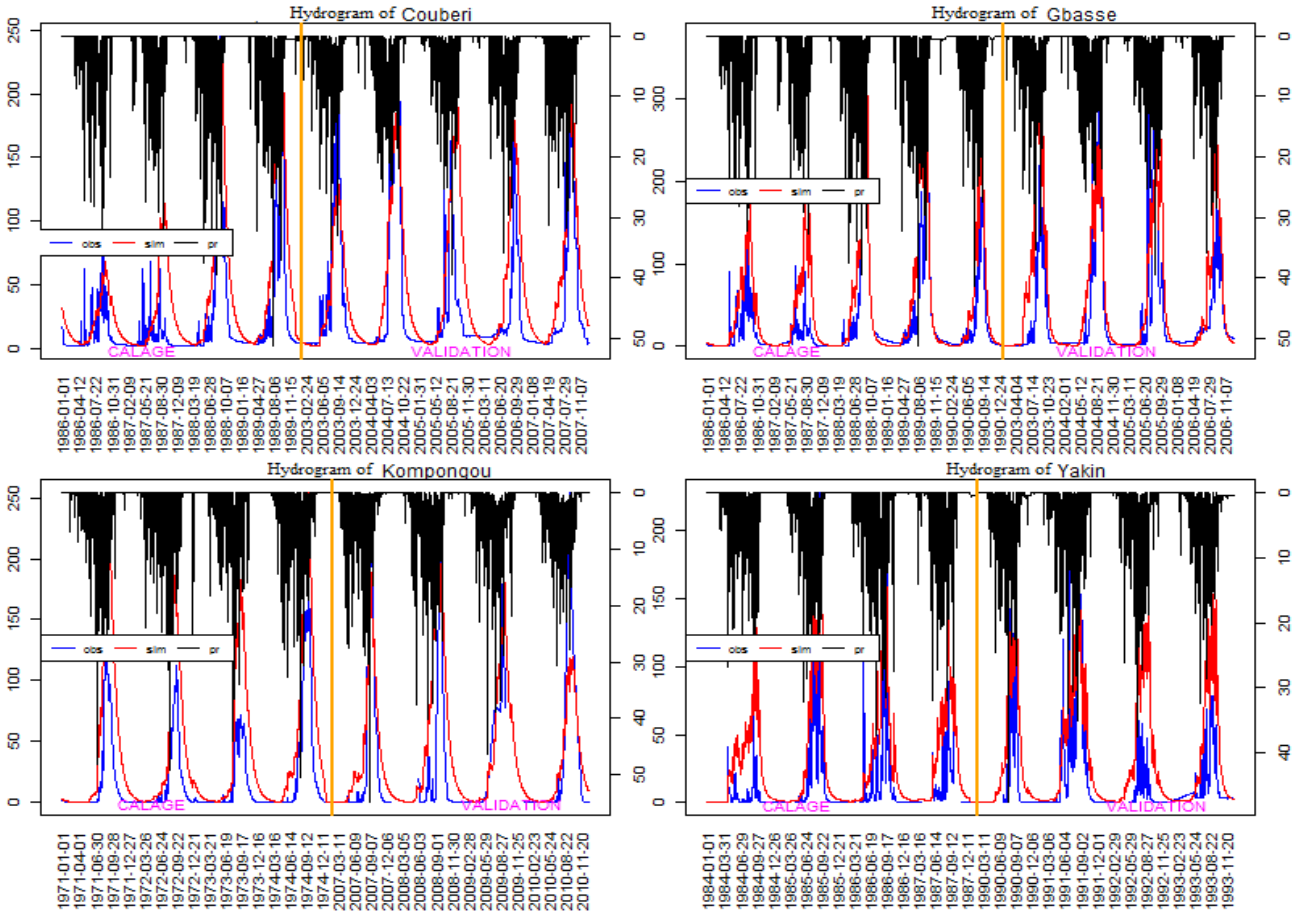

Figure 7. Results of the ModHyPMA model in calibration and validation by hydrological station.

Couberi hydrometric station, the index shows an average increasing trend of 0.0001 per year for the SDI-12 and SDI-36 months. It is also noted that the major dry periods are located between the years 1978-1988. At this station, at the 12-month SDI scale, extreme drought occurred in 1.4% of the cases, severe drought in 12.83% of the cases, moderate drought in 8.72% of the cases, and near-normal conditions 77% of the cases (Figure 9). For the 36-month IDS, we observed 73.87%, 18.67%, 5.07% and 1.4% of near-normal, moderate, severe and extreme conditions respectively (Figure 9). Through Figure 10 we notice that the average duration of drought at this station is 21 months with a peak of –1.68 for the SDI-12 months against 85 months of duration and –2.2 of peak for the SDI-36 months. At Couberi, we also note that at 12 months SDI, there is a greater chance (36%) of hydrological drought than at 36 months SDI (30%) (Figure 11).

In Gbassè, at the 12-month IDS scale, the frequencies of 80.25%, 13.13%, and 6.22% for near-normal, moderate, and severe conditions, respectively, were noted during the reference period (Figure 9). Extreme droughts did not occur. At 36 months IDS, at this station, near-normal, moderate and severe conditions show 76.81%, 17.71% and 5.49% respectively with an absence of extreme droughts (Figure 9). The two calculated SDI windows show very small time series decreases (averaging 1/100000 per year) over the selected historical period (Figure 8). The droughts are localized between 1978-1988 and 2010-2019 (Figure 8). Furthermore, drought duration range up to 47 and 117 months respectively for SDI-12 and SDI-36 months with respective peaks of –1.6 and –1.8 (Figure 10). As in Couberi, here too the risk of drought is higher at 12 months IDS than at 36 months (Figure 11).

At the 12-month and 36-month SDI scale, 80.24% and 81.28% of near-normal droughts; 5.23% and 9.25% of moderate droughts; 9.03% and 5.1% of severe droughts; and 4.51% and 5.57% of extreme droughts are identified at the Kompongou station respectively (Figure 9). These SDI windows (12 months and 36 months) calculated at the Kompongou station all show non-significant increasing time trends (Figure 8). This increase is on average 5/100,000 per year (Figure 8). This station shows its dry periods between 1978-1988 and 2010-2019 (Figure 8). On average, there are 36 months and 117 months of drought duration respectively with SDI-12 and SDI-36 months associated with peaks of –2.12 and –2.75 (Figure 10). Unlike the previous stations, here the risk of drought is higher with SDI-36 (46.11%) months than with SDI-12 (38.38%) months (Figure 11).

At the Yakin hydrometric station, the extreme drought did not occur for all the SDI steps as at Gbassè (Figure 9). For this station, 80.75% of near-normal conditions, 12.5% of moderate drought and 6.25% of severe drought were noted for the SDI-12 months, compared to 79.33% of near-normal drought, 12.927% of moderate drought and 7.75% of severe drought for the SDI-36 months (Figure 9). On average, drought duration is up to 24 months for the SDI-12 months and 48 months for SDI-36 months with respective peaks of –1.64 and –1.6 (Figure 10). The SDI-12 months is increasing over time by 0.007 (very low) per

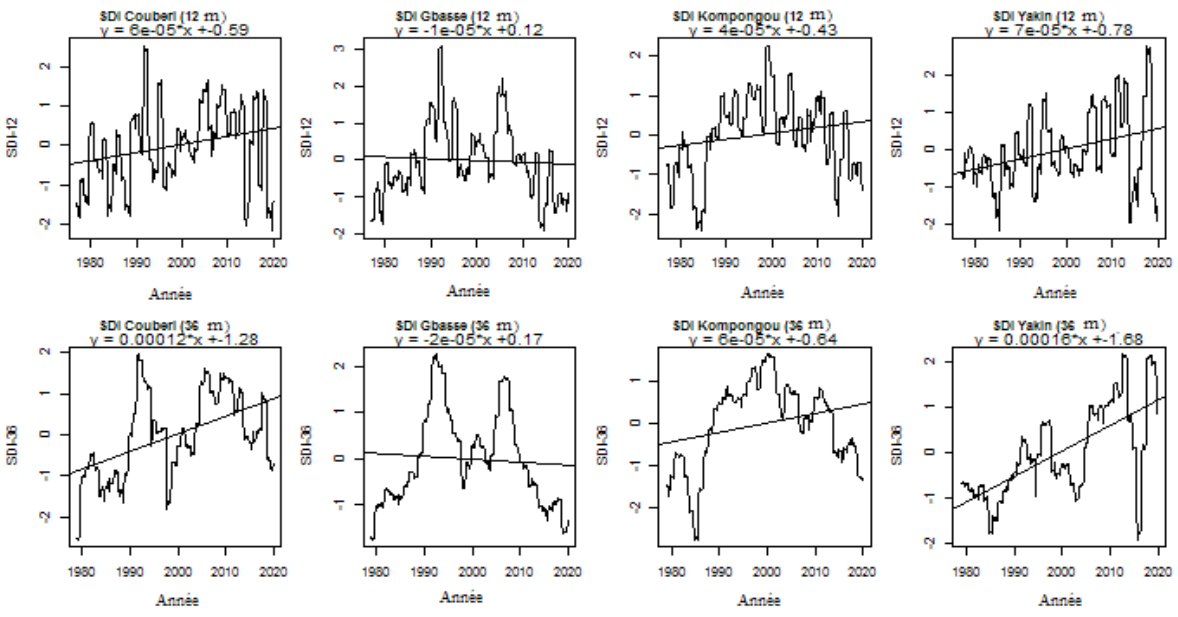

Figure 8. Chronological evolution of SDI indices by hydrological station.

centennial while the SDI-36 months is increasing over time by 0.01 (very low) per centennial (Figure 8). As in Kompongou, in Yakin, we note that at 36 months SDI the risk of drought (which is 29%) is higher than at 12 months SDI (where we have 28%) (Figure 11).

In sum, for all the hydrometric stations considered for the calculation of the SDI, it can be seen that at the 12-month and 36-month scales of the SDI, the frequencies of conditions close to normal drought prevail over the other drought classes (Figure 9). At these IDS scales, extreme droughts always come last while moderate and severe droughts are second and third respectively. The hydrological drought risks calculated at each SDI window (12 months and 36 months) show us that the Kompongou station is the one where the hydrological drought risks are high for all SDI windows. This is followed by Couberi, Yakin and Gbassè stations respectively (Figure 11).

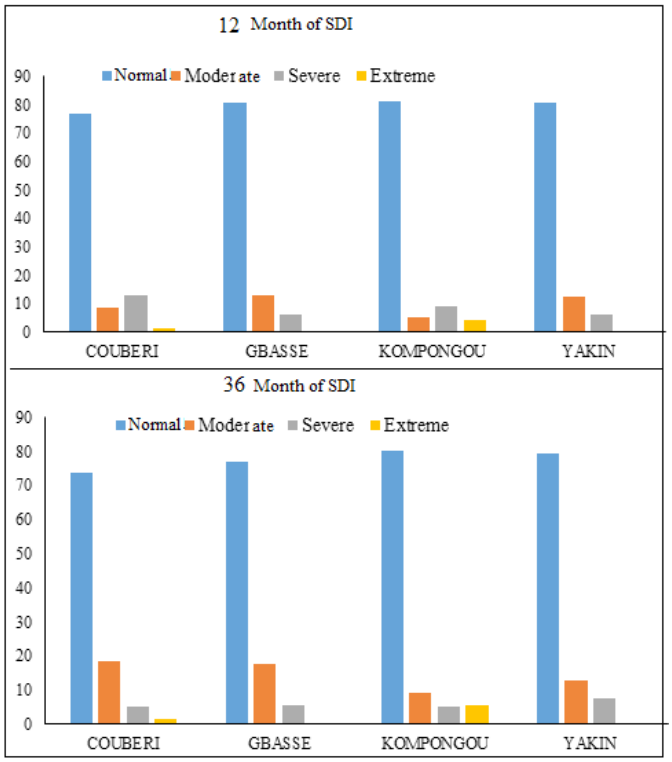

Figure 9. Occurrence of drought classes at each hydrological station.

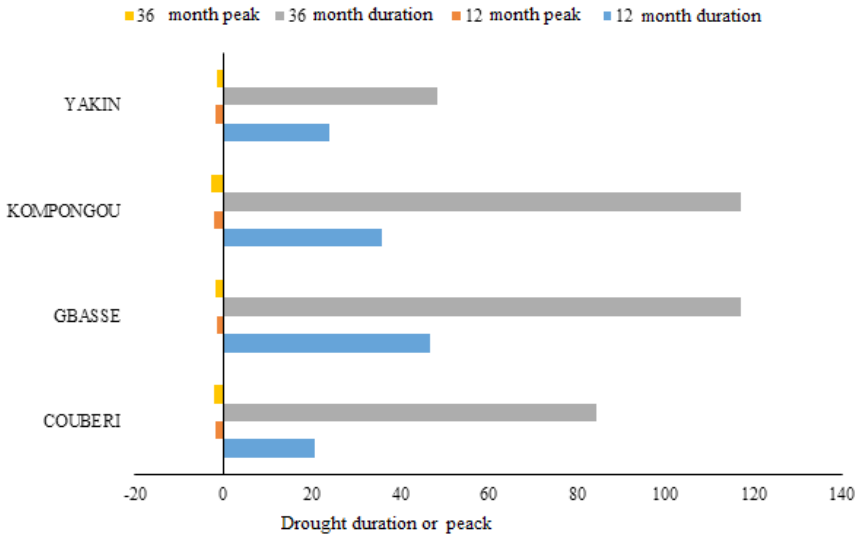

Figure 10. Drought duration and peaks by hydrological station.

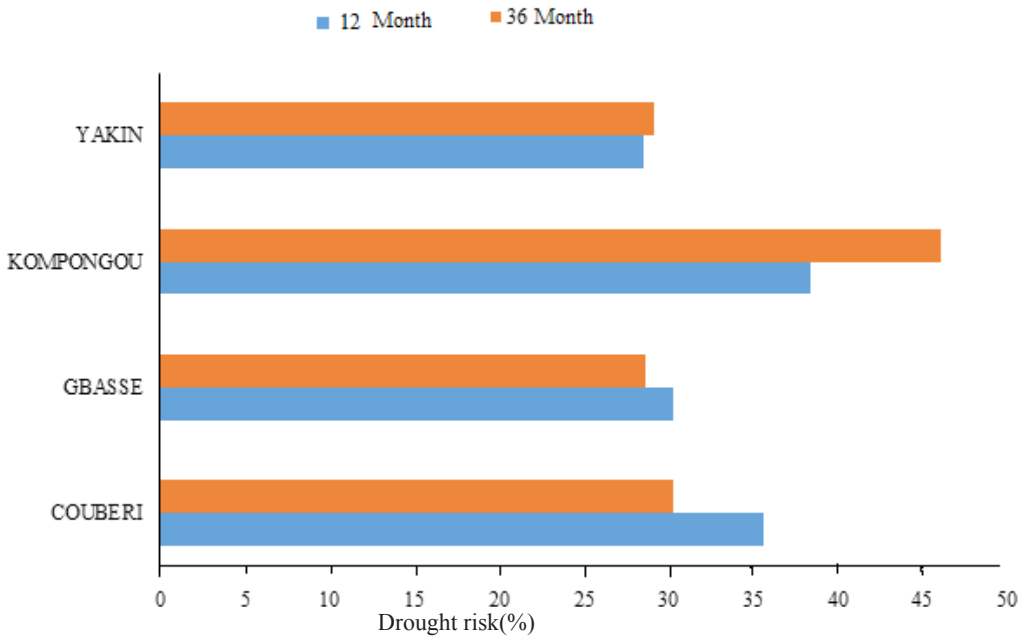

Figure 11. Drought risk by hydrological station.

3.4 Analysis of Projected Hydrological Droughts (2021-2050)

Both scenarios (RCP4.5 and RCP8.5) of the two models (HIRAHM and REMO) show at Couberi for the medium term, increasing time trends in normalized flow indices except for HIRHAM's RCP4.5 for the SDI-36month (Figures 12 and 13). These increases are very small (1/100000 per year) (Figures 12 and 13). At Gbassè, Kompongou and Yakin, the scenarios also show medium-term trends of increasing indices, except for HIRHAM's RCP4.5, which shows decreases for both indices at these stations (Figures 12 and 13). For all of these stations and for the 12 and 36 month SDI, the variations are very small (1/100,000 per year) (12 and 13). Except for Gbassè, where these trends were downward in the past, the other stations showed upward trends with variations that are in the same order.

On average for all hydrological stations during the period 2021-2050 and for the SDI-12 months, we note for the RCP4.5 of the HIRHAM, 80%, 11%, 7% and 1% respectively of near-normal, moderate, severe and extreme droughts. While with the RCP8.5 of the same model the values are respectively 77%, 14%, 8% and 1%. On the other hand, with the REMO model, the RCP4.5 gives 79%, 14%, 5% and 2% of near-normal, moderate, severe and extreme droughts respectively, while its RCP8.5 gives 74%, 21%, 4% and 1% respectively (Figure 14). During the reference period, 78%, 13%, 6% and 3% of near-normal, moderate, severe and extreme droughts were recorded for the 12-month IDS, respectively. At 36 months of the IDS and in the near future, the HIRHAM RCP4.5 shows 77%, 10%, 9% and 4% respectively of near-normal, moderate, severe and extreme droughts against 80%, 11%, 5% and 3% respectively for the RCP8.5 of the same model. The REMO model presents through the RCP4.5 respectively 78%, 10%, 7% and 5% of droughts close to normal, moderate, severe and extreme while through its RCP8.5 we note respectively 81%, 11%, 4% and 4% (Figure 15). In the past, 76%, 16%, 5% and 3% of droughts were near-normal, moderate, severe and extreme respectively. For all models and SDI steps, near-normal drought prevails in about 75% of the drought cases (Figures 14 and 15). In the past, 76%, 16%, 5%, and 3% of near-normal, moderate, severe, and extreme droughts were observed for the SDI-36 months, respectively.

For the drought duration in the medium term (2021-2050), for the 12-month SDI, with RCP4.5 of the HIRHAM model, average drought duration of 24 months, 19 months, 21 months and 22 months are recorded with respective peaks of –1.72, –1.65, –1.76 and –1.77 at Couberi, Gbassè, Kompongou and Yakin respectively (Figure 16). With RCP8.5 of the same model, these duration are respectively 18 months, 11 months, 12 months and 10 months associated with peaks of –1.67, –1.58, –1.57 and –1.64 (Figure 16). On the other hand, with REMO's RCP4.5, the duration for the near future are 31 months, 24 months, 24 months and 23 months with peaks of –1.76, –1.61, –1.66 and –1.7 respectively for the Couberi, Gbassè, Kompongou and Yakin stations, compared to duration of 22 months, 23 months, 18 months and 15 months and peaks of –1.43, –1.41, –1.48 and –1.4 for the RCP8.5 of the same model (Figure 16). During the baseline peri-

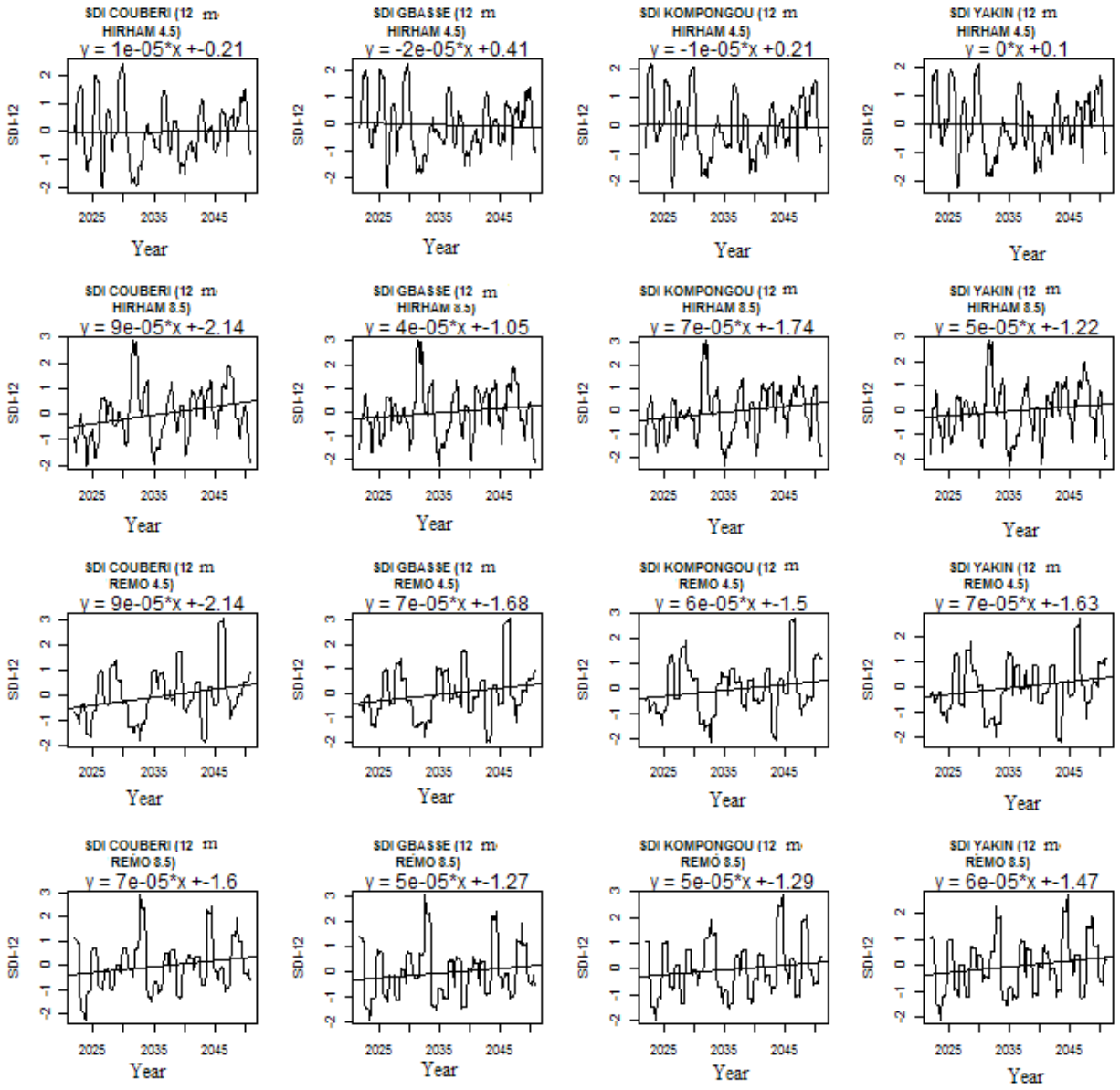

Figure 12. Projected 12-month SDI trends by hydrologic station (2021-2050).

od, drought duration of 21 months, 47 months, 36 months and 24 months was recorded at Couberi, Gbassè, Kompongou and Yakin respectively with peaks of –1.63, –1.57, –2.12 and –1.64. At 36 months from the SDI, the RCP4.5 of the HIRHAM model shows for the near future, drought duration of 45 months, 46 months, 56 months and 45 months respectively in Couberi, Gbassè, Kompongou and Yakin with respective peaks of –2.3, –2.2, –2.2 and –2.2 while its RCP8.5 shows respective duration of 33 months, 31 months, 42 months and 33 months with peaks of –1.75, –1.71, –1.8 and –1.7 (Figure 17). For the RCP4.5 of the REMO model, at 36 months from the SDI and in the near future, we have drought duration of 46 months, 34 months, 42 months and 31 months with respective peaks of –2, –1.6, –2 and –1.8 at Couberi, Gbassè, Kompongou and Yakin. With its RCP8.5, these stations have duration of 37 months, 51 months, 26 months and 21 months respectively with peaks of –1.7, –1.8, –1.6 and –1.7 (Figure 17). During the historical period, drought duration of 85 months, 117 months, 117 months and 48 months were observed at Couberi, Gbassè, Kompongou and Yakin respectively, with peaks of –2.17, –1.75, –2.75 and –1.59.

The two scenarios (RCP4.5 and RCP8.5) of the two models (HIRHAM and REMO) present on average 34% and 36% risk of hydrological drought for the study basin with SDI-12 and SDI-36 months respectively. In the past, these risks were estimated at 33% and 34% months respectively.

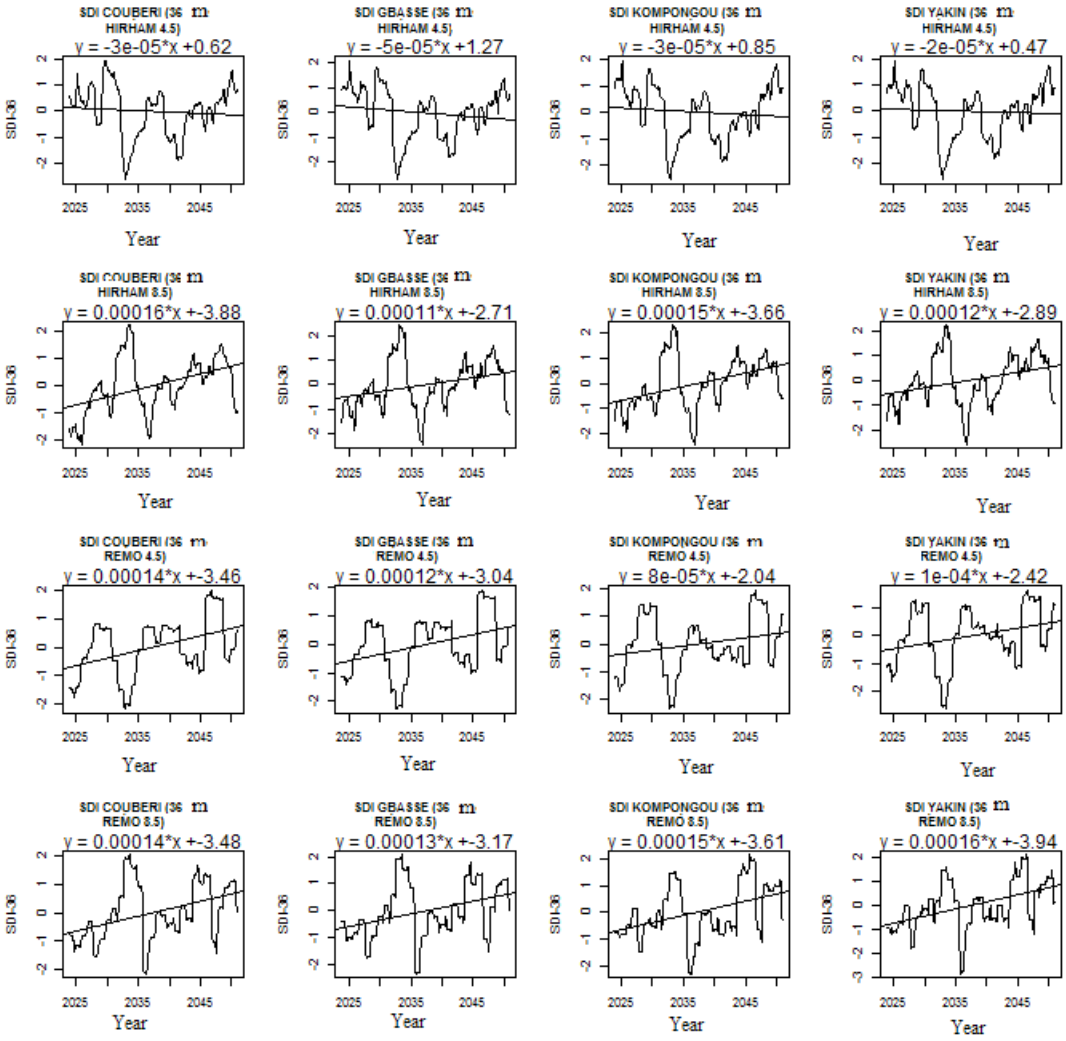

Figure 13. Projected 36-month SDI trends by hydrologic station (2021-2050).

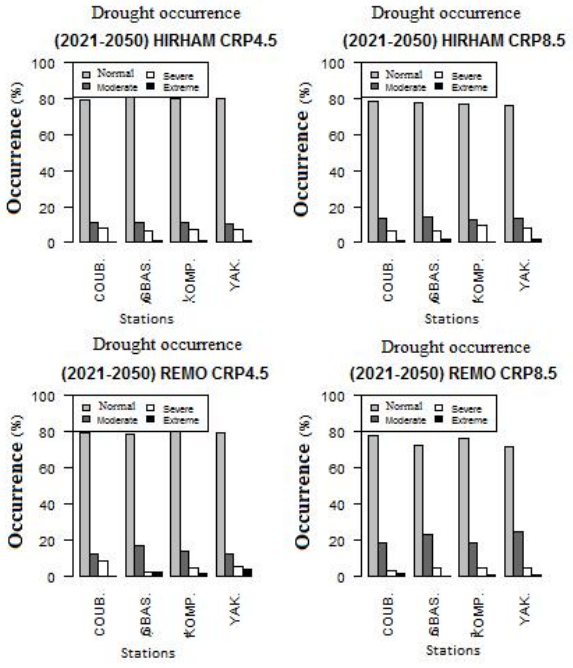

Figure 14. Projected drought class occurrences for each hydrologic station for the 12-month SDI (2021-2050).

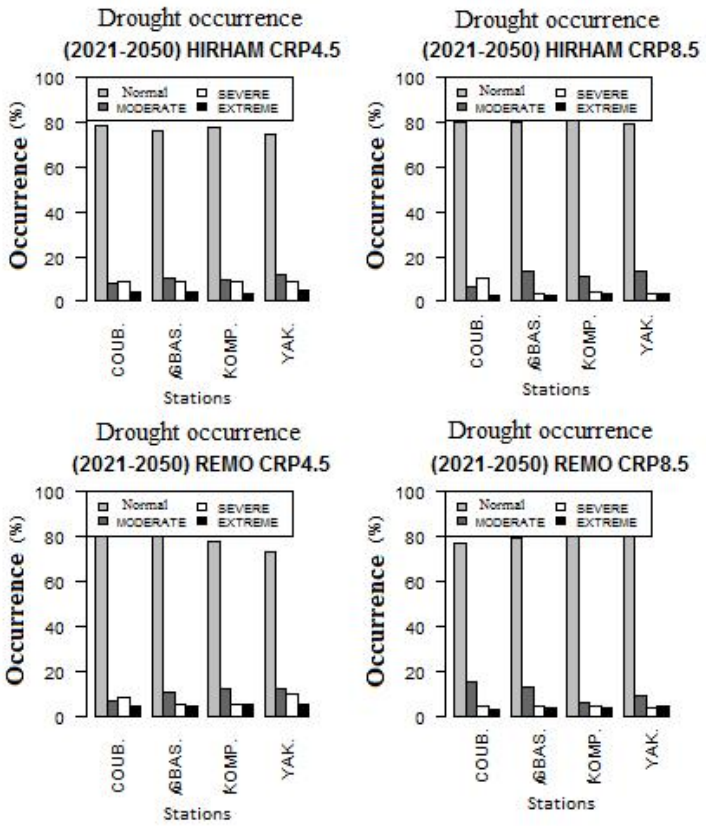

Figure 15. Projected drought class occurrences for each hydrologic station for the 36-month SDI (2021-2050).

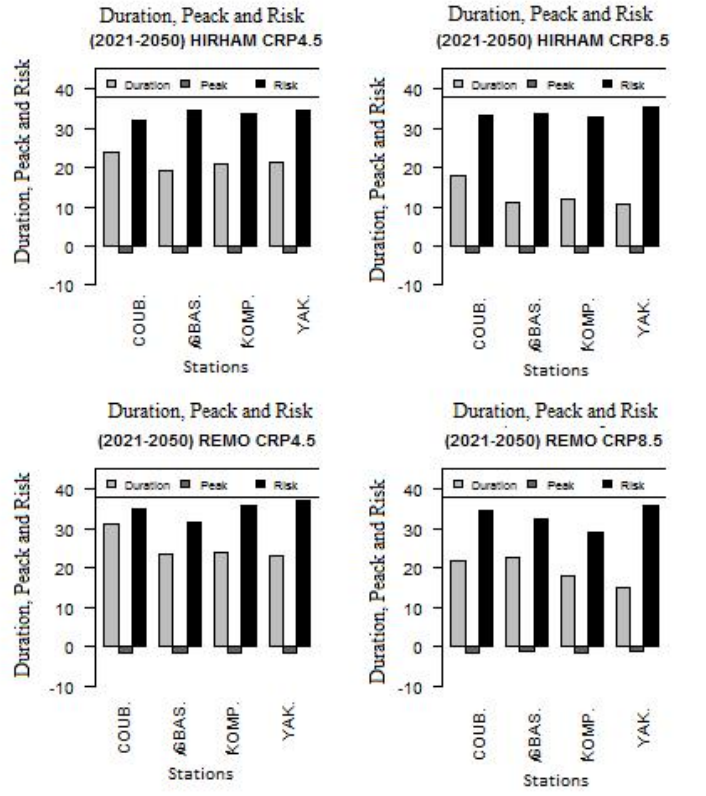

Figure 16. Projected duration, peaks, and risks for all hydrologic stations at the 12-month IDS scale (2021-2050).

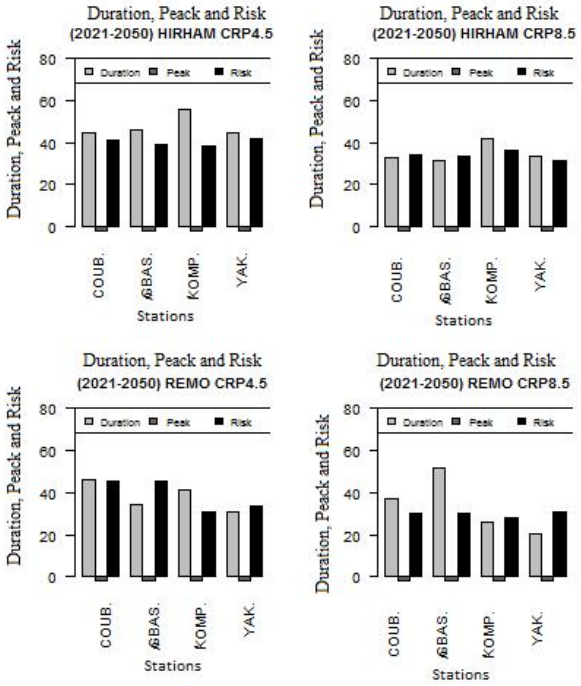

Figure 17. Projected duration, peaks, and risks for all hydrologic stations at the 36-month IDS scale (2021-2050).

3.5 Evaluation of Changes

In the study basin, in the medium term and for the SDI-12 months, we note on average through Figure 18 the decrease in moderate and extreme droughts and the increase in near-normal and severe droughts compared to the reference period according to HIRHAM's RCP4.5. In fact, we record –1.8%, –1.6%, 2.1% and 1.3% respectively for these drought classes. With the HIRHAM RCP8.5, we note the decrease in near-normal and extreme droughts and the increase in moderate and severe droughts compared to the reference period (Figure 18). The rates for these drought types are –0.77%, –1.45%, 0.5% and 1.69% respectively. REMO's RCP4.5, in the medium term and for the SDI-12 months, shows deviations of 1.35, 0.64, –1.14 and –0.85 respectively for near-normal, moderate, severe and extreme droughts compared to the baseline period (Figure 18). During the same period and for the same SDI step, REMO's RCP8.5 shows for near-normal, moderate, severe and extreme droughts respective deviations of –3.57%, 7.95%, –2.15% and –2.22% from the baseline period (Figure 18).

In the medium term and for the SDI-36 months, there is a decrease in moderate droughts and an increase in near-normal, severe and extreme droughts compared to the reference period according to HIRHAM RCP4.5 (Figure 18). For these drought classes, there are deviations of –0.67%, –5.79%, 3.97% and 1.15% respectively. With the HIRHAM RCP8.5, we observe a decrease in moderate and severe droughts and an increase in near-normal and extreme droughts compared to the reference period (Figure 18). For these drought types, the rates are –4.53%, –0.07%, 4.01% and 0.58%, respectively. REMO's RCP4.5, in the medium term and for the SDI-36 months shows deviations of 1.76%, –5.19%, 1.97% and 1.46% respectively for near-normal, moderate, severe and extreme droughts compared to the baseline period (Figure 18). During the same period and for the same IDS step, REMO's RCP8.5 shows for near-normal, moderate, severe and extreme droughts respective deviations of 5.25%, –4.96%, –0.61% and 0.32% from the baseline period (Figure 18).

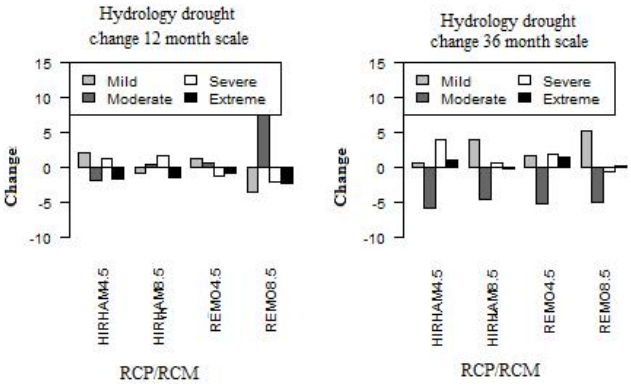

Figure 18. Change in drought types between the baseline and projection periods (12 and 36 month IDS scale).

At the 12-month step of the SDI, we note decreases

in drought duration with the HIRHAM RCP8.5 at all stations, while peaks increase at Kompongou and Yakin and decrease at Couberi and Gbassè (Figure 19). These decreases in duration are 1.95 months, 7.28 months, 6.25 months and 19.06 months respectively at Couberi, Gbassè, Kompongou and Yakin relative to the baseline period with respective peak deviations of –0.08, –0.03, 0.49 and 0.9 relative to the baseline period (Figure 19). For RCP4.5 of the same model, we note increases of 4 months, 0.7 months and 2.75 months respectively at Couberi, Gbassè and Kompongou with respective peak deviations of –0.13, –0.1 and 0.3 and a decrease of 8 months at Yakin with a peak deviation of –0.04 with respect to the baseline period (Figure 19). REMO's RCP4.5 shows increases of 11.58 months, 5 months and 6 months respectively in Couberi, Gbassè and Kompongou with respective peak differences of –0.16, –0.06 and 0.39 compared to the reference period and a decrease of 6.5 months in Yakin with a peak difference of 0.04 (Figure 19). In contrast, its RCP8.5 shows a decrease of 14.5 months at Yakin with a peak difference of 0.31 and increases of 1.85 months, 4.1 months and 0 month respectively at Couberi, Gbassè and Kompongou with respective peak differences of 0.16, 0.14 and 0.57 from the baseline period (Figure 19).

In the medium term and at 36 months from the SDI, we note increases in drought duration and decreases in peaks with HIRHAM's RCP4.5 at Gbassè, Kompongou and Yakin, while the opposite is noted at Couberi (Figure 20). These increases in duration are 46 months, 56 months, and 4.8 months respectively, associated with decreases in duration gaps of 2.23, 2.2, and 0.43 respectively at Gbassè, Kompongou, and Yakin compared to the baseline period, compared to a duration gap of –38.5 months and a peak gap of 0.35 at Couberi (Figure 20). For RCP8.5 of the same model, we note drought duration deviations of –50.33 months, 31.25 months, 41.66 months and –6.42 months respectively at Couberi, Gbassè, Kompongou and Yakin with respective peak deviations of 0.85, –1.72, –1.8 and 0.07 compared to the baseline period (Figure 20). REMO's RCP4.5 shows differences in drought duration of –31 months, 34.33 months, 41.5 months and 8.67 months respectively at Couberi, Gbassè, Kompongou and Yakin

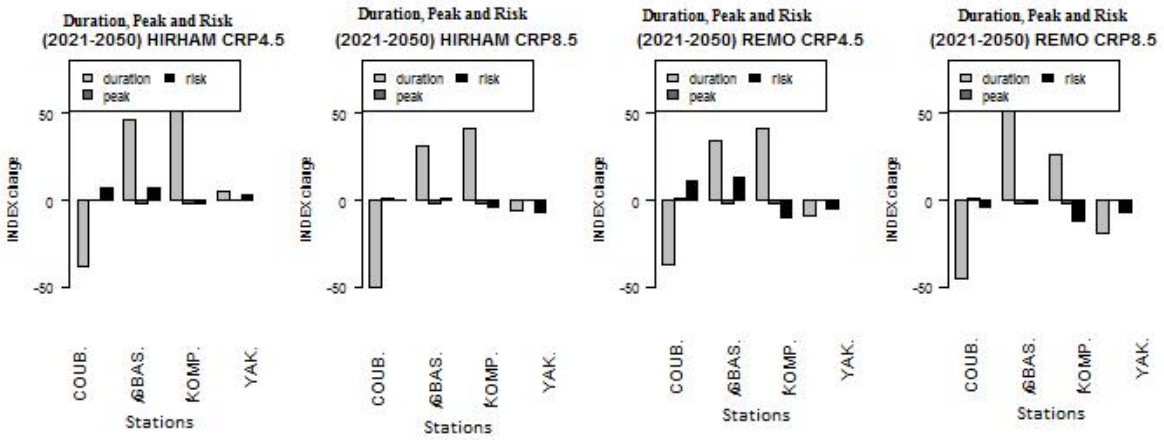

Figure 19. Changes in drought duration, peak and risk (12-month scale).

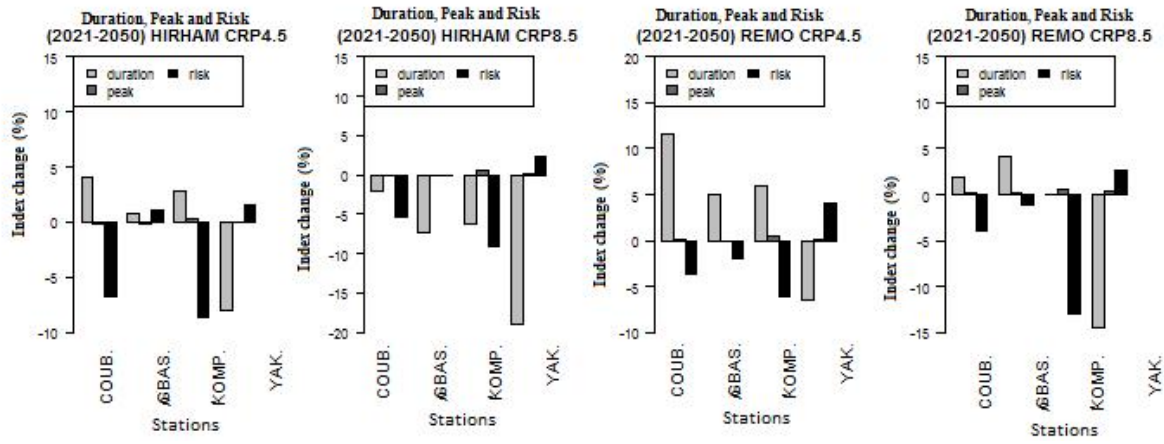

Figure 20. Changes in drought duration, peaks and risks (36-month scale).

with respective peak differences of 0.63, –1.57, –2.03 and –0.03 compared to the reference period. In contrast, its RCP8.5 shows drought duration differences of –45.66, 52, 26 and –18.92 associated with peak differences of 0.89, –1.84, –1.64 and 0.04 respectively at Couberi, Gbassè, Kompongou and Yakin relative to the baseline period (Figure 20).

Drought risk decreases by about 3.01% and 0.62% respectively for the SDI-12 and 36 months under the average of the two model scenarios during the medium term compared to the baseline period (Figures 19 and 20). It should be noted that these obtained changes are not significant as proven with the Student's test (p-Value > 0.05) applied to the indices at 95% confidence level. Whatever the model and the station considered, the Student's p_Value is greater than 0.05 (Figure 21).

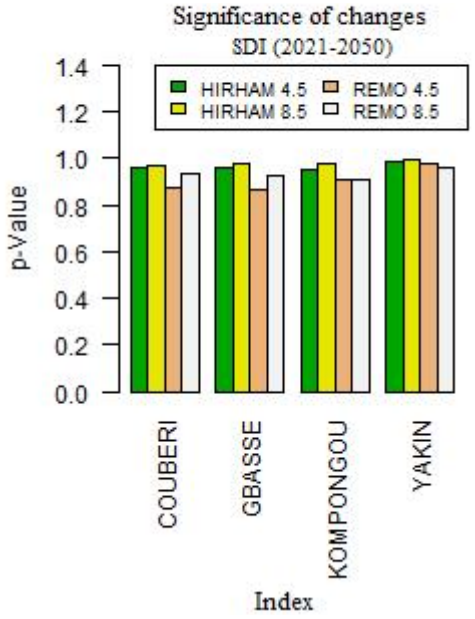

Figure 21. Significance of SDI changes.

4. Discussion

The calculated SDI indices show increasing trends on average for all the model scenarios used. These increases are insignificant (on the order of 0.00001 per year). Therefore, the trends in runoff over the basin will be slightly increasing. This reflects that the wet conditions observed during the baseline period will continue for the next 30 years. Badou [19] and Obada [29] described many changes for the rivers in the Benin River basin as is also the case with Zhao [33] for North America. Also, Koudamiloro [34], also show that the Oueme to Bétérou watershed in Benin is characterized by droughts to varying degrees. Indeed, hydrological droughts are likely to increase by about 0.0003% over the future period. These variations in droughts will be accompanied by an increase in their duration and a decrease in their magnitudes (peaks) as shown by all the climate models used. These results corroborate those obtained with several models of the CORDEX program used for many regions of the Arctic, Antarctic and Sahara by Spinoni [35].

On average, there is a slight increase in drought classes. These increases in drought will be followed by increases in drought duration and decreases in drought intensity (peak). These results are obtained in other regions of the world such as Senegal where runoff is expected to increase in the south and decrease in the north according to Moustapha [36]. Over the Kentucky basin, Somsubhra [37] showed decreases for hydrological drought intensities and increases in their duration. Zhao [33], on the other hand, predict drought duration of future periods to be longer than the historical period. For Zhao [38], future changes in extreme hydrological droughts are very dramatic and will be more severe than meteorological droughts. For all the SDI indices, we notice that the number of dry months increases with the index window, these results affirm those of Ghenim and Megnounif [39] for Northwest Algeria through the SPI and SSFI indices.

5. Conclusions

The calculated SDI indices show overall increasing trends during the historical period as well as in the projections. These increases are not significant and evolve in the same direction as precipitation, leading to a slight increase in runoff in the basin. The duration of droughts is also expected to increase, followed by a decrease in their intensity (peak). The basin will therefore experience more dry months but with low incidence. It is also important to note that the changes obtained are not significant at the Student's t test at the 95% level.

Conflict of Interest

There is no conflict of interest.

References

[1] Soubeyroux, J.M., Vidal, P.P., Baillon, M., et al., 2010. Characterization and forecasting of droughts and low water levels in France from the Saffron-Isba-Moscow hydrometeorological chain. The White Coal. 5,10. (In French)

[2] Serhat, S., Necla, T., Alper, A., et al., 2013. Trends in turkey climate indices from 1960 to 2010, 6th Atmospheric Science Symposium, Turkey. pp. 24-26.

[3] Zengchao, H., Amir, A., Navid, N., et al., 2014. Global integrated drought monitoring and prediction

system, scientific data. Subject Categories. Water resources. Hydrology. pp. 10.

[4] Giguère, M., Gosselin, P., 2006. Water and Health: A review of current climate change adaptation initiatives in Quebec. pp. 28. (In French)

[5] Gnanglè, C.P., Romain, G.K., Achille, E.A., et al., 2011. Past climate trends, modeling, perceptions and local adaptations in Benin. Climatology. 8, 14. (In French)

[6] Heim, R.R.Jr., Brewer, M.J., 2012. The global drought monitor portal: The foundation for a global drought information system. Earth Interactions. 16, 1-28.

[7] Layelmam, M., 2008. Calculation of drought indicators from NOAA/AVHRR images, Drought Early Warning System Project in three countries on the southern shore of the Mediterranean: Algeria, Morocco, and Tunisia LIFE05 TCY/TN/000150. pp. 38. (In French)

[8] FAO, 1998. Crop Evaporation - Guidelines for computing crop water requirements. Irrigation and Drainage paper; Rome (Italy). 56, http://www.fao.org/docrep/X0490E/X0490E00.htm.

[9] McKee, T.B., Doesken, N.J., Kleist, J., 1993. The relationship of drought frequency and duration at time scales. Eighth Conference on Applied Climatology, American Meteorological Society. Anaheim CA. pp. 179-186.

[10] OMM, 2006. Drought monitoring, progress and future challenges. (In French)

[11] Spinoni, J., Naumann, G., Carrao, H., et al., 2013. World drought frequency, duration, and severity for 1951-2010. International Journal of Climatology. 34, 2792-2804.

[12] Oguntundé, G.P., Lischeid, G., Abiodun, J.B. et al., 2016. Analysis of long-term dry and wet conditions over Nigeria, Journal international de climatologie. 37(9).

[13] Ozer, P., Ousmane, L.M., Adamou, D.T., et al., 2017. Recent evolution of rainfall extremes in Niger (1950-2014). Geo-Eco-Trop., 41, 3, n.s., 375-383. Special issue, 10. (In French)

[14] Batablinle, L., Lawin, A.E., Celestin, M., 2019. Future extremes temperature and rainfall : trends and changes assessment over the mono river basin in west Africa, XXXII AIC International Colloquium, Thessaloniki - Greece. pp. 9-14.

[15] Kodja, D.J., Batablinle, L., Akognongbe, A., et al., 2019. Rainfall and temperature changes in Oueme watershed by 2080 in west Africa, XXXII AIC International Colloquium, Thessaloniki - Greece.

[16] Mahé, G., Lienou, G., Bamba, F., et al., 2011. The Niger River and climate change over the last 100 years, Hydro-climatology: Variability and Change. Proceedings of symposium J-H02 held during IUGG2011 in Melbourne, Australia. pp. 7. (In French)

[17] Ozer, P., Hountondji, Y.C., Niang, A.J., et al., 2010. Desertification in the Sahel: history and perspectives. Bulletin of the Geographical Society of Liege. 54, 69-84. (In French)

[18] Vissin, E.W., 2007. Impact de la variabilité climatique et de la dynamique des états de surface sur les écoulements du bassin béninois du fleuve Niger, PhD thesis. pp. 310. (In French)

[19] Badou, F.D., 2016. Multi-model evaluation of blue and green water availability under climate change in four-non Sahelian basins of the Niger river basin, PhD thesis, University of Abomey-Calavi (UAC), National Water Institute (INE). pp. 155. (In French)

[20] Christensen, J.H., Hewitson, B., Busuioc, A., et al., 2006. Regional Climate Projections. In: Climate Change 2007: The physical Sciences Basis. Contribution of Working Group I to the Fourth Assessment Report of the Intergovernmental Panel on Climate Change, Solomon S, Qin D, Manning M, Chen Z, Marquis M, Averyt KB, Tignor M and HL Miller (eds.) Cambridge University Press: Cambridge, New York. pp. 847-940. https://www.ipcc-wg1.unibe.ch/publications/wg1-ar4/ar4-wg1-chapter11.pdf.

[21] Jacob, D., Bärring, L., Christensen, O.B., et al., 2007. An inter-comparison of regional climate models for Europe: design of the experiments and model performance. Climatic Change. 81, 31-52.

[22] Nalbantis, I., Tsakiris, G., 2008. Assessment of hydrological drought revisited. Water Resources Management. 23(5), 881-897.

[23] Graham, L.P., Andreasson, J., Carlsson, B., 2007. Assessing climate change impacts on hydrology from an ensemble of regional climate models, model scales and linking methods—A case study on the Lule River basin. Climatic Change. 81(S1), 293-307.

[24] Moore, K., Pierson, D., Pettersso, K., et al., 2008. Effects of warmer world scenarios on hydrologic inputs to Lake Mälaren, Sweden and implications for nutrient loads. Hydrobiologia. 599, 191-199.

[25] Sperna, F.C., Van Beek, L.P.H., Kwadijk, J.C.J., et al., 2010. The ability of a GCM-forced hydrological model to reproduce global discharge variability. Hydrology and Earth System Sciences. 14(8), 1595-1621.

[26] Lafon, T., Dadson, S., Buys, G., et al., 2013. Bias cor-

rection of daily precipitation simulated by a regional climate model: a comparison of methods. International Journal of Climatology. 33(6), 1367-1381.

[27] Allen, R.G., Pereira, L., Raes, D., et al., 1998. Crop evapotranspiration - Guidelines for computing crop waters requirements - FAO irrigation and drainge paper 56; chapters 1, 2, 3 & 4, annex 3 & 5. (https://www.fao.org/docrep/x0490E/x0490e00.htm)

[28] Gaba, O.U.C., Biao, I.E., Alamou, A.E., et al., 2015. An Ensemble Approach Modelling to Assess Water Resources in the Mékrou Basin, Benin. Hydrology. 3(2), 22-32.
DOI: https://doi.org/10.11648/j.hyd.20150302.11

[29] Obada, E., 2017. Approche de quantification des changements récents et futurs de quelques paramètres hydro-climatiques dans le bassin de la Mékrou (Bénin), Université d'Abomey-Calavi (Bénin), PhD Thesis. pp. 212. (In French)

[30] Afouda, A., Lawin, E., Lebel, Th., 2004. A stochastic Streamflow Model based on Minimum Energy Expenditure Concept. In contempory Problems in Mathematical Physics: Proceeding 3rd Intern. Workshop. Word Scientific Publishing Co. Ltd. pp. 153-169.

[31] Alamou, E., 2011. Application of the Least Action Principle to Rainfall-Flow Modelling, PhD thesis, University of Abomey Calavi, 231 pages & Appendices. (In French)

[32] Afouda, A., Alamou, E., 2010. Hydrological model based on the principle of least action (MODHYPMA). Annals of Agronomic Sciences of Benin. (In French)

[33] Zhao, C., Brissette, F., Chen, J., et al., 2019. Frequency change of future extreme summer meteorological and hydrological droughts over North America. Journal of Hydrology. pp. 11.

[34] Koudamiloro, O., Vissin, E.W., Sintondji, L.O., et al., 2015. Socio-economic and environmental effects of hydroclimatic hazards in the Oueme River watershed at the outlet of Bétérou in Benin (West Africa), XXVIIIth Colloquium of the International Association of Climatology, Liège. pp. 6. (In French)

[35] Spinoni, J., Paulo, B., Edoardo, B., et al., 2020. Future Global Meteorological Drought Hot Spots: A Study Based on CORDEX Data. Journal of Climate. pp. 27.

[36] Moustapha, T., Mouhamadou, B.S., Ismaïla, D., et al., 2017. Projected impact of climate change in the hydroclimatology of Senegal with a focus over the Lake of Guiers for the twenty-first century. Theoretical & Applied Climatology. 129, 655-665.
DOI: https://doi.org/10.1007/s00704-016-1805-y

[37] Somsubhra, C., Dwayne, R.E., Yao, Y., et al., 2017. An Assessment of Climate Change Impacts on Future Water Availability and Droughts in the Kentucky River Basin. Environment Process. pp. 30.

[38] Zhao, C., Brissette, F., Chen, J., et al., 2020. Evolution of future extreme drought frequency in two climate model large ensembles, EGU General Assembly 2020, Online. EGU2020-11449.
DOI: https://doi.org/10.5194/egusphere-egu2020-11449

[39] Ghenim, A.N., Megnounif, A., 2011. Characterization of the drought by the SPI and SSFI indices (northwest Algeria), Scientific and Technical Review, LJEE. 18, 20. (In French)

BILINGUAL PUBLISHING CO.
Pioneer of Global Academics Since 1984

Journal of Atmospheric Science Research
https://ojs.bilpublishing.com/index.php/jasr

ARTICLE

Wave Dynamics of the Average Annual Temperature Surface Air Layer New Delhi for 1931-2021

Peter Mazurkin *

Volga State University of Technology, Yoshkar-Ola, the Republic of Mari El, Russia

ARTICLE INFO

Article history
Received: 8 April 2022
Revised: 6 May2022
Accepted: 10 May 2022
Published: 17 May 2022

Keywords:
New Delhi
Temperature 1931-2021
Critical wavelet
Forecasts

ABSTRACT

The identification method revealed asymmetric fluctuations in the dynamics of the average annual temperature in New Delhi from 1931 to 2021, that is, for 90 years. An analysis of the wave patterns of climate until 2110 was carried out. Geotechnology of the Himalayan passage was proposed to reduce heat waves in India and China. Formulas containing four and 18 fluctuations were adopted for forecasting. Models give an increase in the heat wave from 2021, which is the fourth component. As a result, the landscape of the Himalayan mountains and the deserts of Thar and Takla Makan create a regional climate system that is original for the land of the Earth. In this system, oscillatory temperature adaptation in the future will be several times greater than the global warming rate predicted in the IPCC CMIP5 report. Between 2001 and 2019 the largest temperature increase wave maximum was observed in New Delhi at 0.65 °C in 2012-2013. In the sixth phase from 2036 to 2049, an ecological catastrophe will break out in New Delhi. According to calculations, the maximum value of the average annual temperature in New Delhi was 25.82 °C in 2017. Since then, the cooling has continued for four years, which will continue until 2028. The temperature will drop to 22.54 °C due to a change in solar activity by 3.28 °C. Then by 2044, the average annual temperature in New Delhi will increase to 31.03 °C, or the increment will be 31.03 – 22.54 = 8.49 °C. In 2035, the climate in New Delhi will become hotter compared to 2021. The increase in the heat wave is noticeable. From 1931 to 2049 there will be six half-periods of cooling and warming: 1) 23; 2) 23; 3) 20; 4) 18; 5) 15; 6) 13 years old. The most dangerous is the sixth stage. It is proposed at the fifth stage for 15 years until 2037 in northern India to the Takla Makan desert in China to build a passage up to 350 km long, 10 km-20 km wide and at least 4.5 km high.

*Corresponding Author:
Peter Mazurkin,
Volga State University of Technology, Yoshkar-Ola, the Republic of Mari El, Russia;
Email: kaf_po@mail.ru

DOI: https://doi.org/10.30564/jasr.v5i2.4639

1. Introduction

In ancient times, most of India was covered with swamps and impenetrable tropical forests teeming with predators - the jungle. The farmers of India since ancient times waged a real war with the forests. They had to win back plots for crops [1].

The report of the McKinsey institute "What threatens India with global warming" notes that climate change and global warming can deal a severe blow to the Indian economy before the end of this decade. These findings are reported on March 9 by The Times of India. By 2050, parts of India and Pakistan are projected to experience such heatwaves with a probability greater than 60% per year. The seriousness of the problem is so great, the newspaper notes, that as one of the adaptive measures MGI proposes to consider the organization of mass "climatic migration".

The Indian Meteorological Department (IMD) annual climate report for the country states that not only was 2021 the fifth warmest year since 1901, but the last decade, 2012 - 2021, was also the warmest on record. In addition, 11 of the 15 warmest years on record were between 2007 and 2021. Rising average temperatures can have a cascading effect on extreme weather events [2].

New Delhi (Figure 1): It's only March, but intense heat has already gripped much of India. And it's clear that this early summer in India is proof that this is the era of climate change, and it could have major implications for water security, the Center for Science and the Environment said.

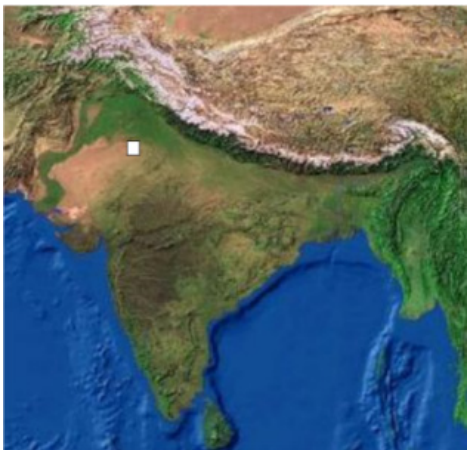

Figure 1. New Delhi weather station (marked with a white square)

Heat waves associated with abnormally high temperatures, which can also be fatal to humans and animals, are also on the rise throughout the country, while there is a downward trend in the frequency of occurrence of cold waves [3].

The climate of India is very diverse. Four types can be distinguished: dry tropical, humid tropical, subequatorial monsoon and high mountain. And at a time when the beach season begins in the south, real winter sets in the mountains, and the temperature drops below zero. There are areas where it rains almost all year round, while in others the plants suffer from drought. How can this be explained? In the north, the country is fenced off from the cold Asian winds by the Himalayas, and in the northwest, a large territory is occupied by the Thar Desert, which attracts warm, humid monsoons. They determine the peculiarities of the Indian climate [4].

Time series of global or regional surface air temperatures are of fundamental importance for climate change studies [5]. Monthly and annual temperature differences and their changes were considered, for example, in on the Tibetan plateau and its environs for 1963–2015 [6].

The sun heats the earth unevenly. In this case, the equator receives more heat, the poles less. This temperature gradient is one of the main forces that drives the ocean and atmosphere. In the tropics, the climate system of our planet receives energy, and in temperate and polar latitudes it gives it away. The main transfer of heat from the equator to the pole is carried out in the atmosphere. The ocean is the slow component of the climate system. It does not respond as sharply to external influences as the atmosphere does. In heat transfer, the ocean acts as a battery. Taking heat from the sun and heating up, it then shares it with the air [7].

The climate is mainly influenced by solar activity [8].

There are reasons to believe that global warming has almost ended and a slow decrease should be expected in the period up to 2040, especially in the Northern Hemisphere over land [9].

The purpose of the article is to identify asymmetric wavelets of the New Delhi average annual temperature dynamics from 1931 to 2021, that is, for 90 years, to analyze the wave patterns of climate fluctuations until 2110 by the identification method [10-12] in India and China.

2. Materials and Methods

For the possibility of modeling the dynamics of the average annual temperature of India by a set of wave equations, the initial time $\tau_0 = 0$ is taken for 1931.

Table 1 gives a fragment of the data array of the average annual temperature of the surface air layer at a height of 2 m according to measurements at the meteorological station in New Delhi. A series of surface mean annual temperatures for New Delhi was taken from the site http://www.pogodaiklimat.ru/history/42182.htm (Accessed 22.04.2022).

Table 1. New Delhi temperature

Year	Time τ, year	Temperature t, °C
1931	0	25.0
1932	1	25.1
1933	2	23.9
1934	3	24.7
1935	4	24.7
…	…	…
2017	86	25.9
2018	87	25.6
2019	88	25.1
2020	89	24.8
2021	90	24.9

It contains a total of 91 temperature values without gaps. Then the representativeness of the dynamic range is 100%. However, modeling is difficult due to the short time series, since it would be better to have data for New Delhi from 1831.

The dynamic series is approximately the same, so the trend was taken as an arithmetic mean of temperature. With a very low adequacy of less than 0.3, a trend appears in the form of the Mandelbrot law in the physics of exponential growth. The same Laplace law in mathematics, Zipf-Pearl in biology and Pareto in econometrics. In what follows, this law gives an additional critical wavelet.

Oscillations (asymmetric wavelet signals) are generally written by the wave formula [10-12] of the form.

$$y_i = A_i \cos(\pi x / p_i - a_{8i}),\ A_i = a_{1i} x^{a_{2i}} \exp(-a_{3i} x^{a_{4i}}),\ p_i = a_{5i} + a_{6i} x^{a_{7i}}, \quad (1)$$

where y is the indicator (dependent factor), i is the number of the component of the model (1), m is the number of members in the model (1), x is the explanatory variable (influencing factor), $a_1 \ldots a_8$ are the parameters of the model (1) that take numerical values during structural and parametric identification in program environment CurveExpert-1.40 (URL: http://www.curveexpert.net/) according to statistical data, A_i is the amplitude (half) of the wavelet (axis y), P_i is the half-period of oscillation (axis x).

3. Results and Discussion

The time series of New Delhi's mean annual temperature from 1931 to 2021 turned out to be relatively complex, but at the same time informative in comparison with other cities in Europe and Asia. The first forecasting scenario up to 2110 was carried out according to the model (1) containing four components. Then, with additional asymmetric wavelets, model (1) included 18 components.

Temperature is a physical quantity that is a measure of the average kinetic energy of the translational movement of molecules, in our case, air molecules in the surface layer at a height of 2 m above the land surface in the city of New Delhi. Therefore, the average annual temperature is a continuous physical quantity, the range of values of which should not be subjected to any transformations. Grouping by 10, 20 and other time intervals is not allowed to bring under linear models.

3.1 Wavelets of Dynamics of Mean Annual Temperature

3.1.1 Features of CurveExpert-1.40 Software Environment

The method for identifying asymmetric wavelets (1) was performed sequentially. At the same time, the arithmetic mean value of the average annual temperature in New Delhi for 91 years (Figure 2), equal to 25.14 °C, was taken as the beginning of the simulation. The standard deviation is only 0.4610 °C. the correlation coefficient as a measure of adequacy is 0.

The first wobble is an infinite-dimensional wavelet, meaning it starts much earlier than 1931 and will continue well beyond 2021. A distinctive feature is the continuous decrease in the amplitude of the fluctuation, which will favorably affect the regional climate. However, the climatic danger is represented by a decrease in the half-period of oscillations over the years, that is, the climatic system of the region becomes more frequent.

The second oscillation refers to finite-dimensional wavelets that have boundaries on the x-axis. It ended in 1964. Therefore, this wavelet does not affect the time after 2021.

The third oscillation is also an infinite-dimensional wavelet, however, unlike the first oscillation, it has an amplitude increasing according to the Mandelbrot law. It's a small consolation that the half-cycle of the oscillation is slowly decreasing.

All four of these components were identified together.

3.1.2 The Four Components of a Pattern

Table 2 shows the parameters of the model (1), and Figure 3 shows a graph of the general pattern.

The correlation coefficient of 0.5688 relates the composite regularity in terms of the level of adequacy to the average strength of the factor connection. Then other wave components will appear, so the adequacy will increase significantly.

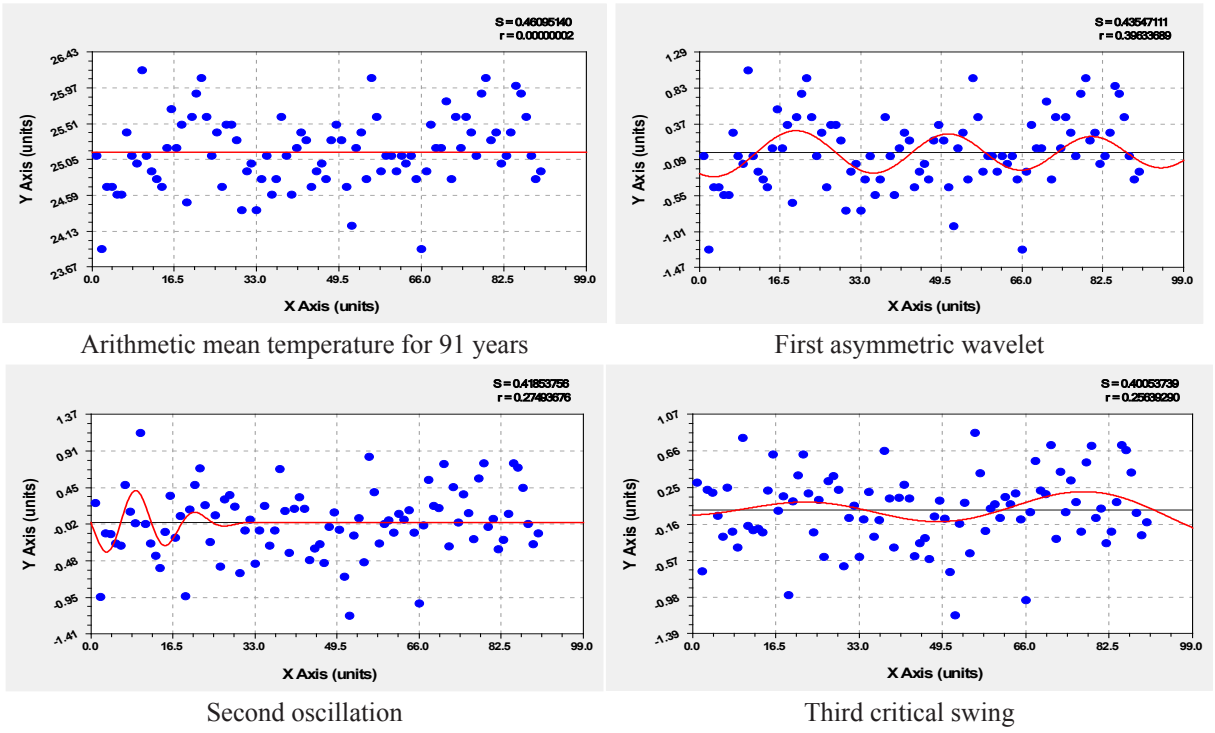

Figure 2. Graphs of the dynamics of the average annual temperature of New Delhi for the years 1931-2021 (in the upper right corner: S – standard deviation; r – correlation coefficient)

Table 2. Parameters of the dynamics of average annual temperatures in New Delhi for 1931-2021.

i	Asymmetric wavelet $y_i = a_{1i}x^{a_{2i}}\exp(-a_{3i}x^{a_{4i}})\cos(\pi x(a_{5i}+a_{6i}x^{a_{7i}})-a_{8i})$								Coef. correl. r
	Amplitude (half) oscillation				Half cycle oscillation			Shift	
	a_{1i}	a_{2i}	a_{3i}	a_{4i}	a_{5i}	a_{6i}	a_{7i}	a_{8i}	
1	25.10299	0	0	0	0	0	0	0	0.5688
2	0.50146	0	0.022460	1	–55.63167	60.36572	0.045774	1.27271	
3	0.097658	0.25091	9.67534e-6	2.39781	8.13641	0	0	–3.28657	
4	0.0023103	0	–0.070187	1	31.42437	–0.093036	1	4.07201	

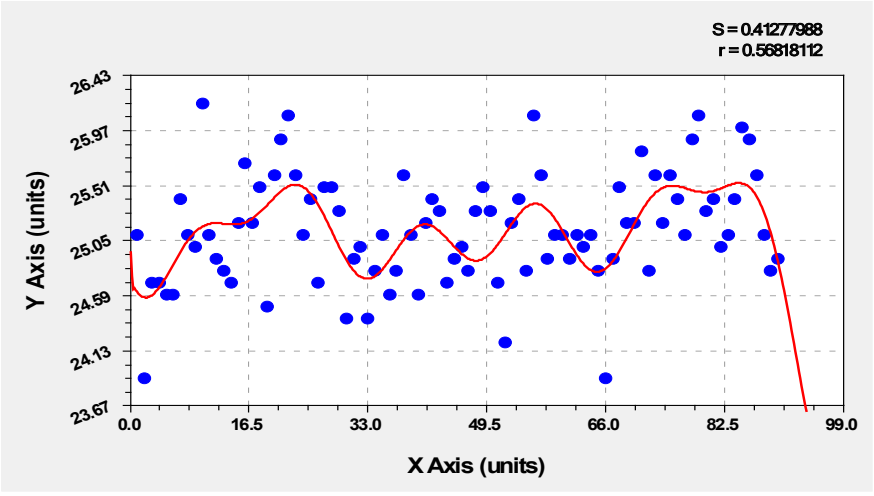

Figure 3. Plot of New Delhi's four-component annual average temperature formula

3.1.3 Error Distribution of the Four-component Model

The number of points n (pieces) distributed in intervals of 1 °C of the relative error $[\Delta]$ (°C) of the model (1) with the parameters from Table 2 is given in Table 3.

Table 3. Distribution of the relative error of the model from Table 2

Interval $[\Delta]$, °C	Quantity n, pcs.	Interval $[\Delta]$, °C	Quantity n, pcs.	Interval $[\Delta]$, °C	Quantity n, pcs.
4	1	1	25	–2	16
3	6	0	2	–3	5
2	16	–1	17	–4	3

From Table 3 it can be seen that the error of the four-term model from Table 2 changes between intervals of ± 4 °C.

Then the error changes according to the Gauss law (Figure 4) with the subtraction of the asymmetric wavelet in the form of a two-term equation.

$$n = 31.99860\exp(-0.20820([\Delta]+0.010940)^2) - \\ -3.73495\cdot10^{-6}([\Delta]+5)^{29.06657}\exp(-6.17339([\Delta]+5)) \\ \cos(\pi([\Delta]+5)/2.36884-0.17169) \quad (2)$$

The normal distribution law, together with the wavelet, barks a very high level of adequacy with a correlation coefficient of 0.9982.

3.1.4 A Look into the Future

In the Excel software environment, using the formulas from Table 2, the graphs shown in Figure 5 were obtained for different forecast horizons.

On the forecast horizon until 2104, the temperature will reach about 450 °C. Then, apparently, starting from India, the same climate will be established on Earth as in the atmosphere of the planet Venus. But before that, in the beginning, in the period 2093 to 2100, a global cooling is likely to be expected. The forecast horizon up to 2084 gives that the climate in New Delhi will be similar to that in the Gobi Desert. Since 1973, a Sahara desert climate has been expected in India. After 2060, the whole territory of India will become like in the Thar Desert.

Thus, an indicative forecast is possible until 2050.

3.1.5 Forecast until 2050

A four-component model makes it possible to make a plausible forecast only 30 years ahead, that is, until 2050 (Figure 6).

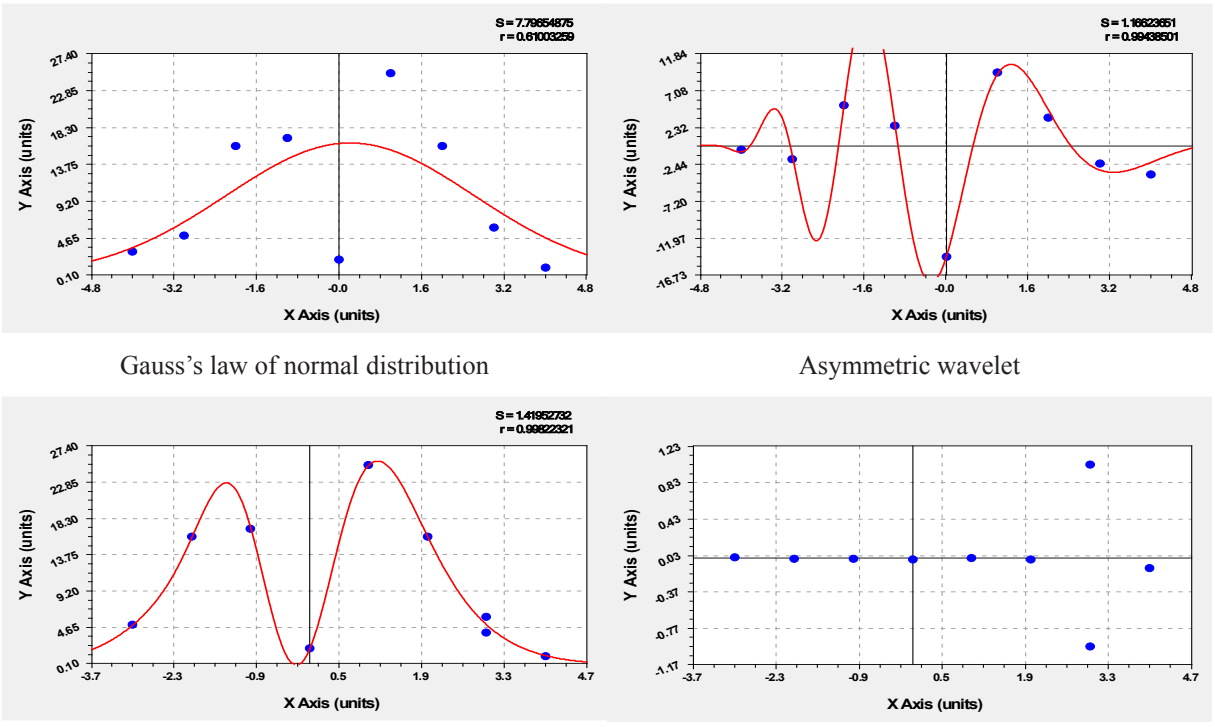

Gauss's law of normal distribution | Asymmetric wavelet

Gauss law and wavelet | Residues after formula (2)

Figure 4. Graphs of the relative error of the four-component model

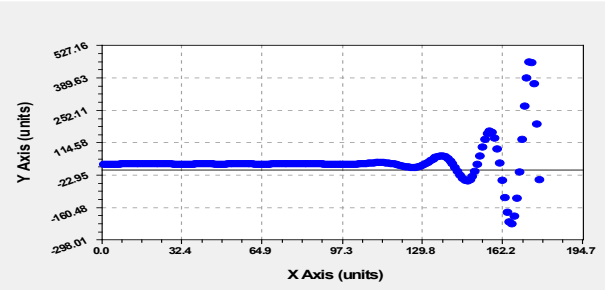

Forecast until 2104 (analogue - Venus)

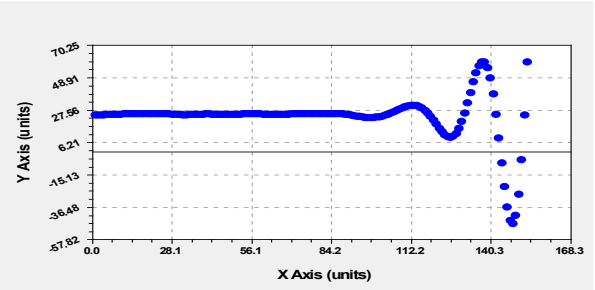

Forecast to 2084 (Gobi Desert)

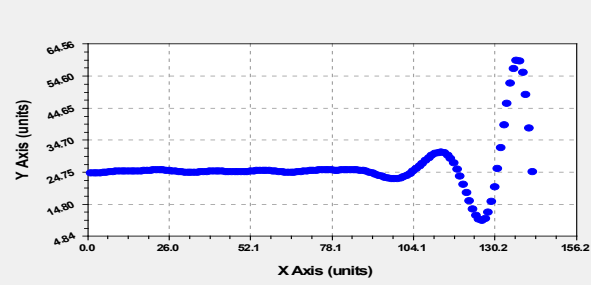

Forecast to 2073 (Sahara desert)

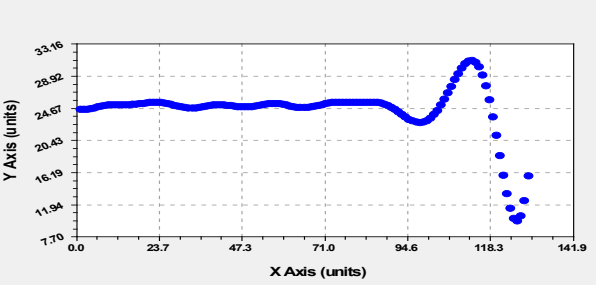

Forecast to 2060 (Thar Desert India)

Figure 5. Graphs of forecasts of average annual temperature in New Delhi

The maximum average annual temperature of 25.53 °C was in New Delhi in 2016. Then there will be a drop in temperature, due to the influence of the Sun [8], to 22.84 °C in 2030. After that, by 2044 there will be a sharp rise in the average annual temperature to 31.04 °C.

3.1.6 Critical Swing

Note that the forecast for 18 components gives almost similar results. Therefore, the critical oscillation, accelerating in amplitude, is among the two wavelets from Table 2. From it, we notice that the fourth component has an increasing amplitude. The rate of increase in the average annual temperature in New Delhi, this heat wave is shown in Figure 7.

The critical wobble or heat wave indicates that New Delhi's maximum annual mean temperature increase from 1931 to 2050 will be 6.06 °C in 2044. The average annual temperature will also reach a maximum of 31.04 °C. If nothing is done, then there will be an ecological disaster in India. Cardinal climate technologies need to start from 2022 to 2037, that is, in just 15 years.

Next, consider the stages of the heat wave for the period from 1931 to 2021 (Figure 8).

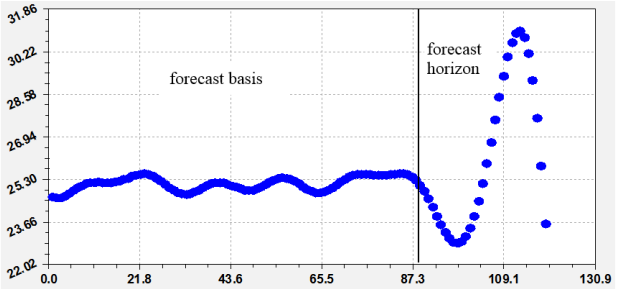

Figure 6. Average annual temperature forecast for New Delhi until 2050

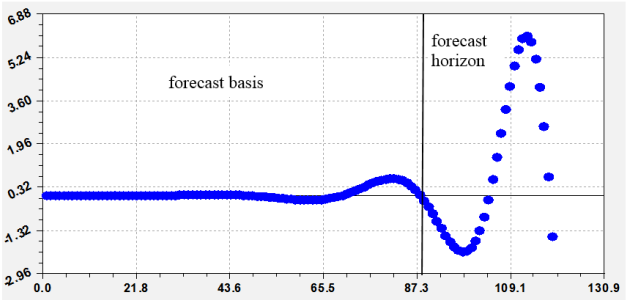

Figure 7. Critical fluctuation in the average annual temperature in New Delhi until 2050

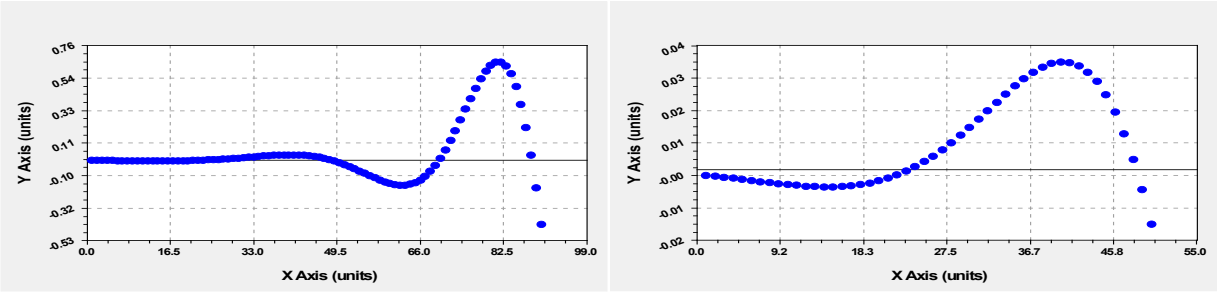

Critical wave until 2021 Critical wave before 1981

Figure 8. Critical Line Plots at the Forecast Base

The first stage was in 1931-1954, when the heat wave in New Delhi had negative values of the average annual temperature of the surface air layer. Then it turns out that at the first stage the fluctuation was aimed at reducing regional warming. However, this decrease was very small.

Second stage 1955-1978 is characterized by a burst of warming with a maximum temperature increment in 1971 of 0.034 °C. At the third stage, the heat wave again became negative in the period 1980-2000 with a minimum temperature of –0.07 °C in 1993. In the period of 2001-2019 (fourth stage), the largest maximum wave of the average annual temperature in New Delhi was observed at 0.65 °C in 2012-2013. And finally, the fifth stage will be in 2020-2035 (coinciding with the forecast of solar activity [11]) with another cooling down to a minimum of –2.14 °C in 2029.

At the sixth stage from 2036 to 2049, if India and China do not make joint efforts in the geological technology called "Himalayan Passage", an ecological disaster will break out in New Delhi with a maximum increase in the average annual temperature of 6.06 °C in 2044. The temperature in 2044 is expected to be 31.04 °C. This will be higher than the level of 2021 on 31.04 – 24.9 = 6.14 °C.

The increase in the heat wave is noticeable. From 1931 to 2049 in the dynamics of the average annual temperature in New Delhi, there will be six half-periods of cooling and warming: 1) 23 years; 2) 23 years old; 3) 20 years; 4) 18 years old; 5) 15 years and 6) 13 years. The most environmentally dangerous is the sixth stage.

3.2. General Formula (1) with 18 Components

3.2.1 Features CurveExpert-1.40

Subsequently, the identification method was used to increase the asymmetric components up to 18 (Table 4). The first four components were placed together in the CurveExpert-1.40 software environment (Table 2), and the remaining components were identified separately. This technique allows you to achieve a level of adequacy in terms of the correlation coefficient up to 1.

Each component is a quantum of climate behavior at a given point on the Earth. The high quantum certainty of the mean annual temperature makes it possible to decompose the dynamic series into behavioral quanta to a level where the modeling error becomes even less than the measurement error of ± 0.05 °C.

In many examples, it was noted that with an increase in the number of components, the sensitivity of forecasting increases sharply. Therefore, models with several components, simultaneously identified in the CurveExpert-1.40 software environment, are sufficient for orientation. The possibilities of forecasting decrease with an increase in the number of wavelets in the general model due to the fact that in the near future new fluctuations appear that can drastically change the forecast trends. For verification, it is enough to wait one year to get the actual temperature. Then the predictive model is re-identified. This is how the forecasts are refined by the iterative forecasting mode every year.

3.2.2 Infinite-dimensional and Finite-dimensional Wavelets

All wavelets are divided into two groups: a) infinite-dimensional wavelets, when the amplitude of formula (1) has the form of a modified Mandelbrot law (or simply Mandelbrot law) under the condition a_{2i}=0; b) finite-dimensional wavelets, when the amplitude takes the form of a biotechnical law, provided that in this case there are boundaries of the beginning a_{2i}>0 and end of the wave.

When a_{2i}<0 the first component of the biotechnical law turns into a power law $y_1 = ax^{-b}$, which has no physical meaning. Therefore, the identification formula $A = ax^{-b}\exp(-cx^d)$ is converted into a modified Mandelbrot's law $A = a\exp(-cx^d)$. This means that the finite-dimensional wavelet becomes infinite-dimensional, having no boundary on the x-axis.

New Delhi is characterized by the fact that the first

Table 4. Parameters of the dynamics of average annual temperatures in New Delhi for 1931-2021

i	Asymmetric wavelet $y_i = a_{1i}x^{a_{2i}}\exp(-a_{3i}x^{a_{4i}})\cos(\pi x/(a_{5i}+a_{6i}x^{a_{7i}})-a_{8i})$								Coef. correl. r
	Amplitude (half) oscillation				Half cycle oscillation			Shift	
	a_{1i}	a_{2i}	a_{3i}	a_{4i}	a_{5i}	a_{6i}	a_{7i}	a_{8i}	
5	0.00054435	4.22926	0.49910	0.82454	3.50187	–0.014887	0.98802	–3.44314	0.3967
6	0.00078737	1.81738	0.00071581	1.88069	1.80573	0	0	–1.90137	0.4433
7	–0.017298	1.98575	0.14897	1	1.67777	–0.013562	1	–1.56286	0.4101
8	4292.4895	1.72566	4.85364	1.04222	0.66531	0	0	–0.004365	0.2973
9	4.01010e–6	4.23534	0.53036	0.60570	4.26620	–0.013578	0.93421	–2.62647	0.4756
10	3.09870e-9	5.70583	0.11295	0.97011	3.56199	–0.0080408	1.02558	–1.67364	0.2145
11	7.49041e-13	15.85123	4.68050	0.52311	1.55376	0	0	1.01110	0.2960
12	–2.2294e-18	11.92441	0.17376	1	1.23694	0	0	–5.64086	0.2260
13	–7.4047e-11	5.82239	0.016214	1.75224	3.78946	0	0	–1.16050	0.5241
14	–6.7307e-16	34.07655	4.79541	0.98230	9.55288	–0.58031	1.06987	–4.32146	0.2406
15	–0.043993	0.37746	0.039086	0.92935	1.9311	0	0	0.83091	0.2020
16	–0.032169	0.52255	0.023195	0.89865	4.67504	0.00010175	1.65349	–2.48032	0.4187
17	0.0067699	1.18317	0.041962	1.03570	6.40214	5.33348e-5	1.78867	–2.34360	0.2745
18	3.9665e-19	13.17326	0.21263	1.00114	1.31855	0.00066014	0.96384	5.52885	0.7574

component receives the arithmetic mean value. It becomes an infinite-dimensional wavelet that goes on infinitely and therefore has no boundaries on the x-axis. Similarly, the second and fourth wavelets are infinite-dimensional wavelets. All other 15 components belong to the group of finite-dimensional wavelets. The latter are divided into two subgroups: 1) their boundaries are within (Figure 8) the basis of the forecast (wavelets 3, 5, 7, 8, 11, 14, 17); 2) the right border is located outside the right border of the forecast base, that is, in the interval of the forecast horizon (Figure 9, Figure 10), at least even at its beginning (wavelets 6, 9, 10, 12, 13, 15, 16, 18). The predictive model will include three infinite-dimensional wavelets and, additionally, the second subgroup of finite-dimensional wavelets.

In Figure 8, there is an eighth wavelet that allows you to jump from the abs-ciss axis before 1931. The remaining finite-dimensional wavelets with left and right boundaries on the x-axis are located at the base of the forecast, that is, in the time interval from 1931 to 2021. As a result, they do not participate in the predictive model and therefore do not affect the future. However, when building a general graph, they allow you to visually show the change in the average annual temperature in New Delhi. Retrospective historical research is needed to explain these fluctuations.

As can be seen from the graphs in Figure 9, the length of oscillations is different.

As can be seen from the graphs in Figures 10 and 11, all graphs affect the forecast in the near future, but some of them penetrate far into the future. At the end of the dynamic series, new fluctuations may occur, which will then continue into the future. It is this circumstance that does not allow us to make working forecasts.

As a result, the average annual temperature has two contradictory properties.

Firstly, the dynamic series allows decomposing up to the measurement error into a large number of asymmetric wavelets. Then it turns out that the average annual temperature gets a quantum certainty due to the fact that each wavelet in isolation represents a separate quantum of the behavior of the climate system in New Delhi. Note that other meteorological parameters do not have quantum certainty.

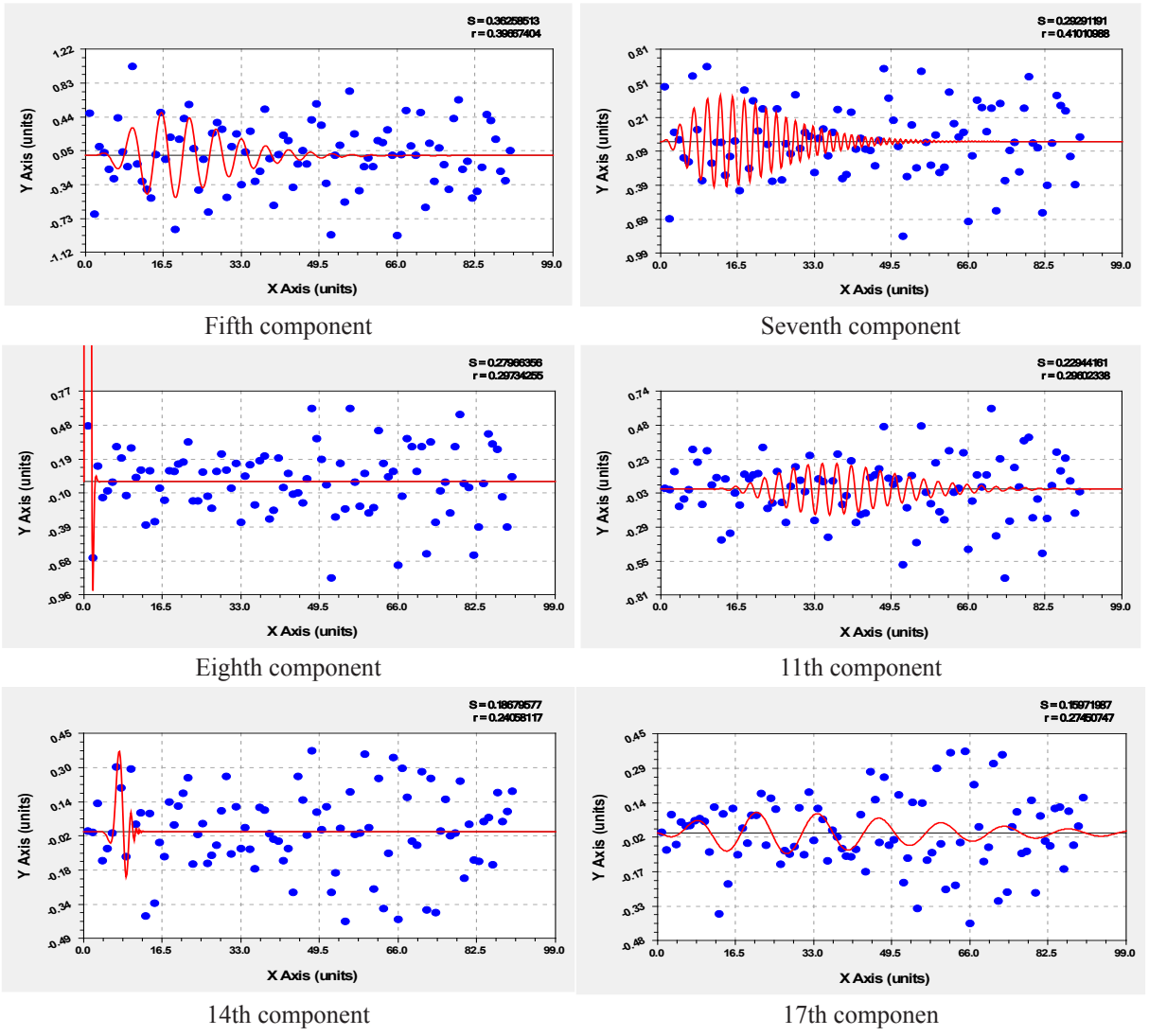

Figure 9. New Delhi annual mean temperature charts at the base of the forecast

Secondly, with an increase in the number of components in the general model (1), the predictive ability is gradually lost. It turns out that even the next year, the calculated average annual temperature may not coincide with the actual temperature. In this regard, it turns out to be sufficient for a look into the future, the model by the parameters in Table 2. And for New Delhi, the fourth component becomes the decisive wavelet, which becomes the critical wavelet or the decisive heat wave.

Everything in nature is subject to vibrational adaptation. The air is so changeable that there are many fluctuations on the surface of the Earth, first of all, the air temperature. Why can a dynamic series be decomposed into a large number of oscillations? Other meteorological parameters are not amenable to wavelet analysis. We don't know yet. Also, New Delhi is a unique geographic point on Earth, the dynamics of the average annual temperature in which is clearly determined by a heat wave in the form of a critical fluctuation.

3.2.3 Model Error Distribution

With an increase in the number of wavelets in model (1), the relative modeling error decreases. The number of points n, equal to 91, is distributed without gaps in the dynamic range. Due to the small error of modeling by the general equation (1) with 18 components, the temperature interval was taken equal to 0.5 °C. Then the permissible relative error [Δ] (°C) of model (1) with parameters from Tables 2 and 4 is given in Table 5.

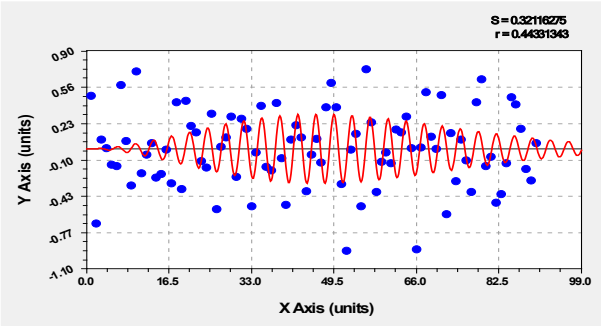

Sixth component (1)

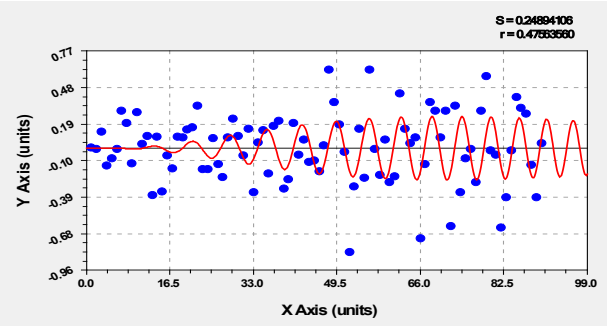

Ninth component

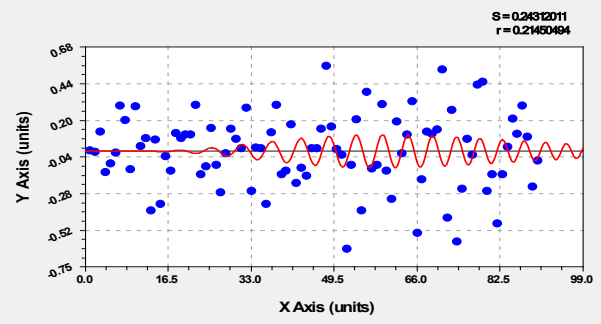

10th component

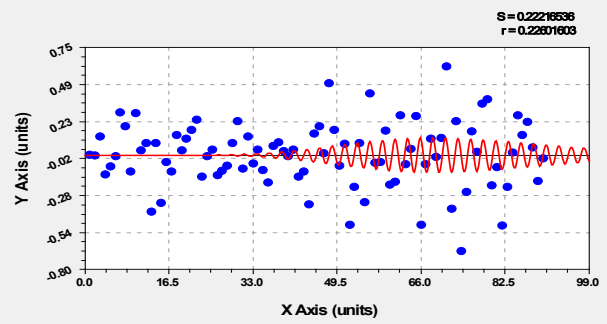

12th component

Figure 10. New Delhi annual average temperature plots after moving from the base of the forecast

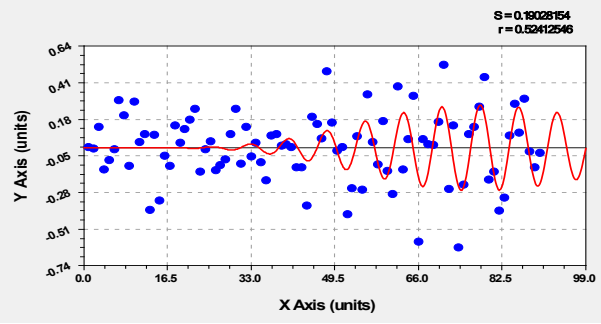

13th component

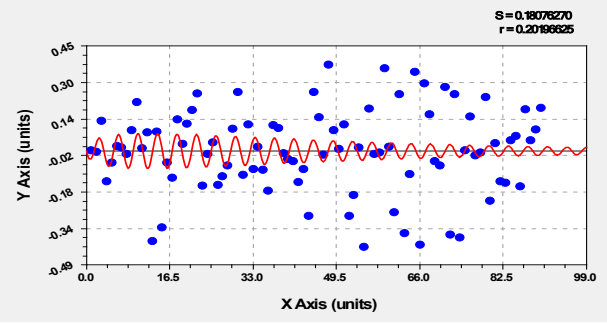

15th component

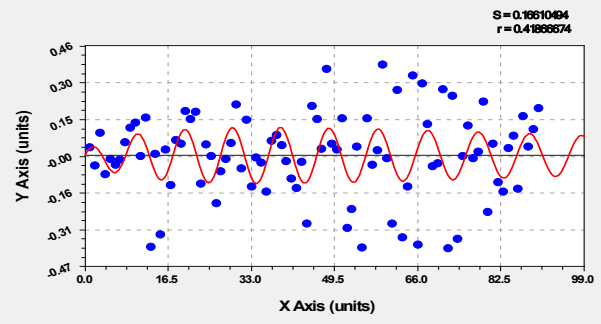

16th component

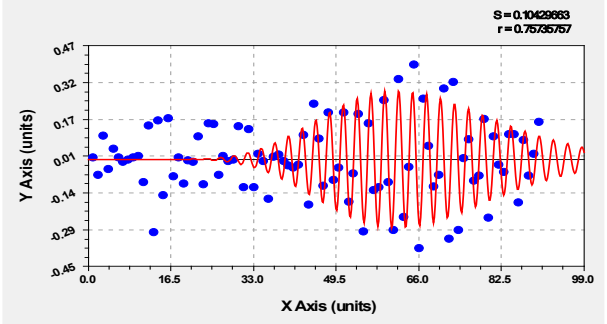

18th component

Figure 11. Additional temperature plots for New Delhi after forecast base

The relative error is in the range from 2 °C to –2.5 °C.

Then the error changes according to the Gauss law (Figure 12) in the form of the equation.

$$n = 21.57717 \exp(-0.45215([\Delta] - 0.036538)^2) \quad (3)$$

The normal distribution law is observed with an adequacy of 0.9612.

3.2.4 Looking Ahead to 2050

In the Excel software environment, using the formulas from Tables 2 and 4, the graph shown in Figure 12 was obtained.

Table 6 shows the actual and estimated average annual temperatures in New Delhi from 2010 to 2021. According to the calculated values in Figure 13, a small wave of oscillatory climate adaptation is noticeable.

The hottest year in New Delhi was in 2010. The actual temperature was 26.1 °C, and the calculated one was 26.029 °C. The remainder after calculations using 18 wavelets is 26.1 – 26.029 = 0.071 °C. then the relative error is 100 × 0.071 / 26.1 = 0.27%. In 2021, the relative modulo error is only 0.07%. At the same time, the actual temperature has been decreasing since 2016 (calculated since 2017).

In Tables 2 and 4, the parameters of the model (1) are given with five significant figures. However, in the calculations we used all 11 significant figures. For example, the fourth component is written as an expression:

User-Defined Model: y=a*exp(b*x)*cos(pi*x/(c+d*x)–e)
Coefficient Data:
a = 6.24682600130E–002
b = 1.54780416027E–002
c = 2.31517776521E+001
d = 4.18674722591E–002
e = 2.78089604956E+000

According to calculations, the maximum value of the average annual temperature in New Delhi is 25.82 °C in 2017. Since then, the cooling has been going on for four years, which will continue until 2028. The temperature will drop to 22.54 °C due to the change in solar activity [11]

Table 5. Distribution of the relative error of the model from Tables 2 and 4

Interval [Δ], °C	Quantity *n*, pcs.	Interval [Δ], °C	Quantity *n*, pcs.	Interval [Δ], °C	Quantity *n*, pcs.
2	3	0.5	22	–1.5	9
1.5	10	–0.5	19	–2	4
1	11	–1	11	–2.5	2

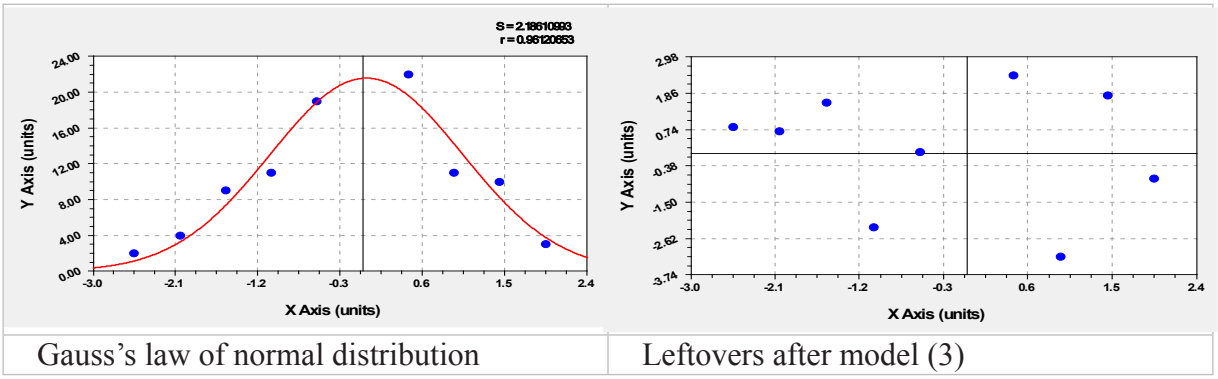

Figure 12. Relative error distribution plot for 18 wavelets

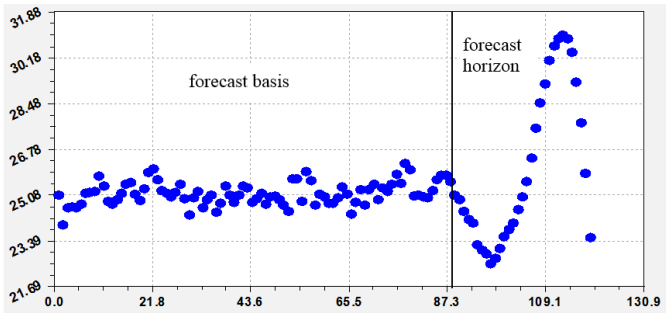

Figure 13. New Delhi 2050 Forecast Graph for the 18-Component Model

Table 6. Average annual temperature in New Delhi since 2010

Year	Time τ, year	Fact t_f, °C	Design temperature		
			t, °C	ε, °C	Δ, %
2010	79	**26.1**	**26.029**	0.071	0.27
2011	80	25.3	25.068	0.232	0.92
2012	81	25.4	25.091	0.309	1.22
2013	82	25.0	25.026	–0.026	–0.10
2014	83	25.1	25.004	0.096	0.38
2015	84	25.4	25.266	0.134	0.53
2016	85	**26.0**	25.657	0.343	1.32
2017	86	25.9	**25.818**	0.082	0.32
2018	87	25.6	25.814	–0.214	–0.84
2019	88	25.1	25.592	–0.492	–1**.96**
2020	89	24.8	25.092	–0.292	–1.18
2021	90	24.9	24.916	–0.016	–0.07

by 25.82 – 22.54 = 3.28 °C. Then by 2044, the average annual temperature in New Delhi will increase to 31.03 °C, or the increment will be 31.03 – 22.54 = 8.49 °C. In 2035, the climate in New Delhi will become hotter than in 2021.

3.2.5 Fractal Distribution of Wavelets

Each fluctuation is a quantum of behavior, in our case, of the New Delhi regional climate system in terms of the average annual temperature of the surface air layer at a height of 2 m from the surface.

Then the sequence of 18 wavelets must itself be distributed fractally according to the modified Mandelbrot law (Table 7, Figure 13).

For the fractal distribution, the standard deviation is taken, the value of which is shown on the graphs in the upper right corner.

Table 7. Relative errors of the calculated values of the standard deviation

Rank R	Coef. correl. r	Standard Deviation σ_f	Estimated standard deviation		
			σ	Remainder ε	Error Δ,%
0	0	0.4610	0.4608	0.0002	0.05
1	0.3963	0.4355	0.4443	–0.0088	–2.02
2	0.3971	0.4185	0.4232	–0.0047	–1.11
3	0.4772	0.4005	0.4006	–0.0001	–0.01
4	**0.5682**	0.4128	0.3775	0.0353	8.55
5	0.3967	0.3626	0.3546	0.0080	2.22
6	0.4433	0.3212	0.3320	–0.0108	–3.37
7	0.4101	0.2929	0.3101	–0.0172	–5.88
8	0.2973	0.296	0.2890	0.0070	2.35
9	0.4756	0.2489	0.2688	–0.0199	–8.01
10	0.2145	0.2431	0.2496	–0.0065	–2.66
11	0.2960	0.2294	0.2313	–0.0019	–0.83
12	0.2260	0.2222	0.2140	0.0082	3.68
13	0.5241	0.1903	0.1978	–0.0075	–3.92
14	0.2406	0.1868	0.1825	0.0043	2.32
15	0.2020	0.1806	0.1681	0.0125	6.90
16	0.4187	0.1661	0.1547	0.0114	6.84
17	0.2745	0.1597	0.1422	0.0175	10.94
18	0.7524	0.1043	0.1306	–0.0263	–25.21

Regardless of the appearance in the CurveExpert-1.40 software environment, the fractal sequence is expressed by the formula.

$$\sigma = 0.46078 \exp(-0.036403 R^{1.22643}) \quad (4)$$

where σ is the standard deviation (root-mean-square error), R is the rank of the asymmetric wavelet, starting from the arithmetic mean (it is a special case of the wavelet).

In Table 7, the arithmetic mean formula gets the zero rank. Code 1 refers to the Mandelbrot law, and rank 2 refers to the sum of the arithmetic mean and the first asymmetric wavelet. Rank 3 is given to a three-component model, while rank 4 is given to a model from Table 2 containing four components.

According to the remainders of formula (4) from Figure 14, it can be seen that an oscillation is additionally possible, which will reduce the relative error at the end of the fractal series of all 18 asymmetric wavelets.

Formula (4) receives adequacy in the form of a correlation coefficient of 0.9911.

3.3 Passage for the Winds in the Himalayas

In India, experts are thinking about how to resettle the population from the growing Thar Desert to other regions of the country. However, instead of this pessimistic alternative, we propose a radical change in the landscape in northern India and southwestern China (Figure 15). The passage is shown as a double line. The maximum length of the passage will be 350 km with a width of 10 km-20 km.

The idea is to connect a 10 km-20 km wide passage between the Thar desert and the Takla Makan desert. For 15 years until 2037, such a volume of earthworks can be mastered by explosive methods.

The wind passage may have two entrances to the foothills from India.

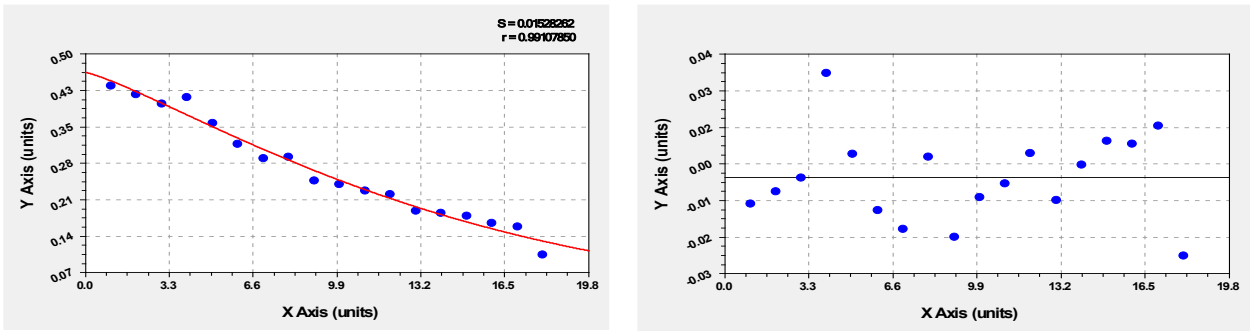

Modified Mandelbrot's Law — Leftovers after model (4)

Figure 14. Graph of the fractal distribution of the standard deviation for 18 wavelets

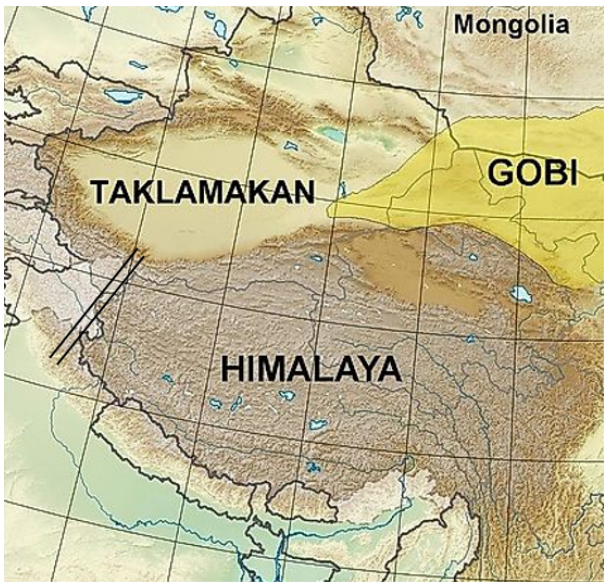

Figure 15. Himalayan Passage for Winds (shown by double line)

After the construction of the passage is completed, the wind with rains will be transferred to the Takla-Makan desert and the steppe with rich herbs will come to life there. At the same time, the intensity of rains will decrease in India. And from the north side, along the passage through the Himalayas, cold winds will blow, cool both deserts.

Now the monsoons bring rain and heat to the country. In India, there is the rainiest place on Earth - Cherrapunji, where more than 12,000 millimeters of precipitation falls annually. And in the north-west of the country, in the Thar Desert, there is not a drop of rain for about 10 months [4]. An ecological passage in the Himalayas will be able to reduce the maximum rainfall to 8-9 meters and part of the monsoons will move towards the Takla-Makan desert. The new direction of the monsoons will noticeably cool the climate of the Thar Desert.

For 4000 years of the life of the population in India, the Himalayan mountains have grown by 400 m (every year by 10 mm). Over the increased mountains it is difficult for birds to fly. I saw the film, how the geese waited in the northern part of the Himalayas, so that strong winds appeared in the direction of the south across the mountains. Birds will use the man-made passage for flights. The climate will change and rich steppe grasses will appear in the Thar and Takla Makan deserts.

For India and China, such passage construction will be a planetary undertaking.

4. Conclusions

The Himalayas are rising 10 mm per year. For 4 thousand years of the existence of civilizations on the island of Hindustan, the mountains have risen by at least 400 m. As a result, the heat is increasing, which can only be reduced by geotechnological measures to reduce the height of the ridges by 4.5 km and create a wide passage 10 km-20 km wide. This will allow the north winds to penetrate into India, and the monsoons to reach the territory of China. The construction of the passage must be completed by 2037.

The wave patterns of the average annual temperature of New Delhi from 1931 to 2021, revealed by the identification method, made it possible to answer that models with four and 18 asymmetric wavelets have been giving a continuous increase in the heat wave since 2021. As a result, the landscape of the Himalayan mountains and the deserts of Thar and Takla Makan create a regional climate system that is original for the land of the Earth. In this system, the oscillatory adaptation of the mean annual temperature in the future will be several times higher than the rate of global warming predicted in the IPCC CMIP5 report.

On the forecast horizon until 2104, the temperature will reach about 450 °C. Then, apparently, starting from India, the same climate will be established on Earth as in the atmosphere of the planet Venus. But before that, in the beginning, in the period 2093 to 2100, a global cooling is likely to be expected. The forecast horizon up to 2084 gives that the climate in New Delhi will be similar to that in the Gobi Desert. Since 1973, a Sahara desert climate has been expected in India. After 2060, the whole territory of India will become like in the Thar Desert.

Thus, an indicative forecast is possible until 2050.

The critical wobble or heat wave indicates that New Delhi's maximum annual mean temperature increase from 1931 to 2050 will be 6.06 °C in 2044. The average annual temperature will also reach a maximum of 31.04 °C. If nothing is done, then there will be an ecological disaster in India.

In dynamics, the first stage of the heat wave according to the fourth component of the model was in 1931-1954, when the critical fluctuation in New Delhi had negative values of the average annual temperature of the surface air layer. Then it turns out that at the first stage, the fluctuation was aimed at reducing regional warming.

Second stage 1955-1978 is characterized by a burst of warming with a maximum temperature increment in 1971 of 0.034 °C. At the third stage, the heat wave again became negative in the period 1980-2000 with a minimum temperature of –0.07 °C in 1993. In the period of 2001-2019 (the fourth stage), the largest maximum of the temperature increment wave in New Delhi was observed in 0.65 °C in 2012-2013. And finally, the fifth stage will be in 2020-2035 (coinciding with the forecast of solar activity) with another cooling down to a minimum of –2.14 °C in 2029.

At the sixth stage from 2036 to 2049, if India and China do not make joint efforts in the geological technology called "Himalayan Passage", an ecological disaster will break out in New Delhi with a maximum increase in the average annual temperature of 6.06 °C in 2044. The temperature in 2044 is expected to be 31.04 °C. This will be higher than the level of 2021 on 31.04 – 24.9 = 6.14 °C.

An increase in the frequency of the thermal wave is noticeable. From 1931 to 2049 in the dynamics of the average annual temperature in New Delhi, there will be six half-periods of cooling and warming: 1) 23 years; 2) 23 years old; 3) 20 years; 4) 18 years old; 5) 15 years and 6) 13 years. The most dangerous in ecological terms is the sixth stage.

According to calculations, the maximum value of the average annual temperature in New Delhi is 25.82 °C in 2017. Since then, the cooling has been going on for four years, which will continue until 2028. The temperature

will drop to 22.54 °C due to the change in solar activity [8] by 25.82 – 22.54 = 3.28 °C. Then by 2044, the average annual temperature in New Delhi will increase to 31.03 °C, or the increment will be 31.03 – 22.54 = 8.49 °C. In 2035, the climate in New Delhi will become hotter than in 2021.

Conflict of Interest

There is no conflict of interest.

Funding

This research received no external funding.

References

[1] Ancient India. URL: https://history.wikireading.ru/314323 (Accessed 04/22/2022).

[2] India getting warmer, hotter: 2021 fifth warmest year since 1901, says IMD.URL: https://www.business-standard.com/article/current-affairs/india-getting-warmer-hotter-2021-fifth-warmest-year-since-1901-says-imd-122011401133_1.html (Accessed 04/22/2022).

[3] Extreme heat in India. URL: https://www.drishtiias.com/daily-updates/daily-news-editorials/heat-extremes-in-india (Accessed 04/22/2022).

[4] Climate of India. URL: https://fb.ru/article/146454/klimat-indii-osobennosti-klimata-indii (Accessed 04/22/2022).

[5] Li, G.X., Zhou, G., 2016. Comparisons of time series of annual mean surface air temperature for china since the 1900s: observations, model simulations, and extended reanalysis.
DOI: https://doi.org/10.1175/bams-d-16-0092.1

[6] Ding, J., Cuo, L., Zhang, Y.X., et al., 2018. Monthly and annual temperature extremes and their changes on the Tibetan Plateau and its surroundings during 1963-2015. https://www.ncbi.nlm.nih.gov/pmc/articles/PMC6082912/.

[7] Chernokulsky, A. Will Europe freeze without the Gulf Stream? URL: https://zen.yandex.ru/media/nplus1/zamerznet-li-evropa-bez-golfstrima-62028bab5eaa831b62461219?&utm_campaign=dbr& (Accessed 03/13/2022). (In Russian)

[8] Zharkova, V. The solar magnet field and the terrestrial climate. URL: https://watchers.news/2018/11/11/valentina-zharkova-solar-magnet-field-and-terrestrial-climate-presentation/ (Accessed 01.03.2019).

[9] Zherebcov, G.A., Kovalenko, V.A., Molodyh, S.I., et al., 2013. Vlijanie solnechnoj aktivnosti na temperaturu troposfery i poverhnosti okeana [Influence of solar activity on tropospheric and ocean surface temperatures]. Izvestija Irkutskogo gosudarstvennogo universiteta. Serija Nauki o Zemle. 6(1), 61-79. (In Russian).

[10] Mazurkin, P.M., 2021. Quantum Biophysics of the Atmosphere: Factor Analysis of the Annual Dynamics of Maximum, Minimum and Average Temperatures from 1879 to 2017 to Hadley English Temperature Center (Hadcet). Journal of Environmental & Earth Sciences. 3(1).
DOI: https://doi.org/10.30564/jees.v3i1.2489

[11] Mazurkin, P.M., Kudryashova, A.I., 2019. Quantum meteorology. International Multidisciplinary Scientific GeoConference Surveying Geology and Mining Ecology Management, SGEM. (5.1), 619-627.
DOI: https://doi.org/10.5593/sgem2019/5.1/S20.077

[12] Mazurkin, P.M., Kudryashova, A.I., 2019. Urban phytometeorology: influence of the sum of temperatures on the ontogeny of drooping birch leaves. Geographical Bulletin. 4(51), 45-58. (In Russian).
DOI: https://doi.org/10.17072/2079-7877-2019-4-45-58

BILINGUAL
PUBLISHING CO.
Pioneer of Global Academics Since 1984

Tel:+65 65881289
E-mail: contact@bilpublishing.com
Website:ojs.bilpublishing.com

2630-5119 02
9 772630 511225